

# A Spectroscopic Survey of the Youngest Field Stars in the Solar Neighborhood

## II. The optically faint sample <sup>\*,\*\*</sup>

A. Frasca<sup>1</sup>, P. Guillout<sup>2</sup>, A. Klutsch<sup>1</sup>, R. Freire Ferrero<sup>2\*\*\*</sup>, E. Marilli<sup>1</sup>, K. Biazzo<sup>1</sup>, D. Gandolfi<sup>3</sup>, and D. Montes<sup>4</sup>

<sup>1</sup> INAF - Osservatorio Astrofisico di Catania, via S. Sofia, 78, 95123 Catania, Italy

<sup>2</sup> Université de Strasbourg, CNRS, Observatoire astronomique de Strasbourg, UMR 7550, F-67000 Strasbourg, France

<sup>3</sup> Dipartimento di Fisica, Università di Torino, via P. Giuria, 1, 10125 Torino, Italy

<sup>4</sup> Departamento de Astrofísica y Ciencias de la Atmósfera, Universidad Complutense de Madrid, 28040 Madrid, Spain

Received / accepted

### ABSTRACT

**Context.** Star formation in the solar neighborhood is mainly traced by young stars in open clusters, associations and in the field, which can be identified, e.g., by their X-ray emission. The determination of stellar parameters for the optical counterparts of X-ray sources is crucial for a full characterization of these stars.

**Aims.** This work extends the spectroscopic study of the *RasTyc* sample, obtained by the cross-correlation of the TYCHO and ROSAT All-Sky Survey catalogs, to stars fainter than  $V = 9.5$  mag and it is aimed to the identification of sparse populations of young stars in the solar neighborhood.

**Methods.** We acquired 625 high-resolution spectra for 443 presumably young stars with four different instruments in the Northern hemisphere. The radial and rotational velocity ( $v \sin i$ ) of our targets are measured by means of the cross-correlation technique, which is also helpful to discover single-lined (SB1), double-lined spectroscopic binaries (SB2), and multiple systems. We use the code ROTFIT for performing an MK spectral classification and for determining the atmospheric parameters ( $T_{\text{eff}}$ ,  $\log g$ ,  $[\text{Fe}/\text{H}]$ ) and  $v \sin i$  of the single stars and SB1 systems. For these objects, the spectral subtraction of slowly rotating templates is used to measure the equivalent widths of the  $\text{H}\alpha$  and  $\text{Li}\text{I}6708\text{\AA}$  lines, which enables us to derive their chromospheric activity level and lithium abundance. We make use of *Gaia* DR1 parallaxes and proper motions for locating the targets in the HR diagram and for computing the space velocity components of the youngest objects.

**Results.** We find a remarkable fraction (at least 35 %) of binaries and multiple systems. On the basis of the lithium abundance, the sample of single stars and SB1 systems appears to be mostly ( $\sim 60\%$ ) composed of stars younger than the members of the UMa cluster. The remaining sources are in the age range between the UMa and Hyades clusters ( $\sim 20\%$ ) or older ( $\sim 20\%$ ). In total, we identify 42 very young (*PMS-like*) stars, which lie above or very close to the Pleiades upper envelope of the lithium abundance. A significant fraction ( $\sim 12\%$ ) of evolved stars (giants and subgiants) is also present in our sample. Some of them ( $\sim 36\%$ ) are also lithium rich ( $A(\text{Li}) > 1.4$ ).

**Key words.** stars: fundamental parameters – stars: chromospheres – stars: pre-main sequence – binaries: spectroscopic – techniques: spectroscopic – X-rays: stars

---

Send offprint requests to: A. Frasca

e-mail: [antonio.frasca@oact.inaf.it](mailto:antonio.frasca@oact.inaf.it)

\* Based on observations collected at the Italian *Telescopio Nazionale Galileo* (TNG) operated by the *Fundación Galileo Galilei – INAF* (Canary Islands, Spain), at the *Observatoire de Haute Provence* (OHP, France), and the *Osservatorio Astrofisico di Catania* (OAC, Italy)

\*\* Tables A.1, A.2, A.3, and A.4 are available at the CDS via anonymous ftp to [cdsarc.u-strasbg.fr](http://cdsarc.u-strasbg.fr) (130.79.128.5) or via <http://cdsarc.u-strasbg.fr/viz-bin/qcat?J/A+A//?/>.

### 1. Introduction

It has been shown that open clusters (OCs) cannot account for the total star formation in the Galaxy, but, at most, for about 50%, the remaining occurring in OB associations (see, e.g., Piskunov et al. 2008; Zinnecker 2008). Although at the end of their parent cloud collapse newly-formed stars are located in the same region of space, many

---

\*\*\* Rubens Freire Ferrero passed away on September 10, 2015.

events tend to carry them away from each other. After being mixed with the stellar population of the galactic plane, young stars are hardly distinguishable from older ones. Indeed, their magnitudes and colors are similar to the latter ones and there is no gas left from the parent cloud that can help to identify them. Other properties related to their young age, such as their kinematics, magnetic activity, infrared (IR) excess, and the presence of lithium in their atmospheres, must be used to spot them among the older population.

The most favorite scenario for the recent history of star formation in the solar neighborhood is that of a large structure in which giant molecular clouds generated massive stars about 50 Myr ago. The latter, exploding as supernovae, triggered star formation in a ring-like structure, the Gould Belt (see, e.g., Comerón & Torra 1994; Bally 2008, and references therein), and cleaned the region around the Sun from the residual gas, generating the local bubble (see, e.g., Bonchukov 1984; Gehrels & Chen 1993). Many OB associations and star forming regions (SFRs) within 500–600 pc are known to be part of the Gould Belt (Elias et al. 2009; Bobylev 2014).

Most studies on young low-mass stars in the solar vicinity were focused on SFRs or young OCs that represent homogeneous samples in terms of age and chemical composition. However, sparse populations of late-type young stars apparently unrelated to known SFRs and young OCs have been discovered (e.g., Guillout et al. 1998a, and references therein). Different scenarios, like ejection from their birth sites by close encounters (Sterzik et al. 1995) or by a very fast dispersion of small clouds (Feigelson 1996), have been proposed to explain these sources scattered over the sky. Depending on their sky position, they could also be related to star formation in the Gould Belt (e.g., Biazzo et al. 2012a, and references therein).

To pick up isolated young stars scattered over the whole sky, Guillout et al. (1999) cross-correlated the ROSAT All-Sky Survey (RASS, Voges et al. 1999) and the TYCHO (or Hipparcos) catalogs (ESA 1997). This selection produced the so-called *RasTyc* and *RasHip* samples, containing about 14 000 and 6200 active stars, respectively. These samples are very suitable for the study of the large-scale distribution of X-ray active stars in the solar neighborhood and led to the discovery of the late-type stellar population of the Gould Belt (Guillout et al. 1998a,b). A similar approach was followed by Haakonsen & Rutledge (2009) who made a statistical cross-association of the ROSAT bright source catalog with the 2MASS point source catalog (Cutri et al. 2003). However, complementary optical data are absolutely needed for a full and safe exploitation of the huge scientific potential of the *RasTyc* and *RasHip* samples, and to search for young field stars unrelated to the main nearby SFRs and young associations.

To this aim we started a large program for following up spectroscopically a significant fraction of the *RasTyc* sample observable from the Northern hemisphere. The results

of the optically bright ( $V_T \leq 9.5$  mag) subsample were presented in Guillout et al. (2009, hereafter Paper I). In that paper, we analyzed high resolution spectra of 426 stars with no previous spectroscopic data and found that this sample is mainly composed of stars with ages between 100 and 600 Myr, with a minor contribution from an older population (1–2 Gyr). A significant fraction of binaries and lithium-rich giants ( $\approx 30\%$ ), which can be considered as contaminants, was also found. Based on their high lithium abundance, seven very young ( $age \leq 30$  Myr) stars, that appear to be unrelated to any known SFR, were also uncovered. Some of them are good post-T Tau candidates and five are likely members of Pleiades or Castor stellar kinematic groups.

In the present paper we extend this study to the optically faint ( $V > 9.5$  mag) *RasTyc* sources. The inclusion of optically fainter sources in the total sample of investigated *RasTyc* stars improves the statistics and allows us to reach a larger distance or intrinsically fainter objects.

A first result of the optically faint sample was the discovery of four lithium-rich stars packed within a few degrees on the sky in front of an area void of interstellar matter in the Cepheus complex. They form a homogeneous moving group, with a likely age of 10–30 Myr. We published a preview of the results for these four stars in Guillout et al. (2010), but we include them in the present paper where additional spectra have been also analyzed.

The paper is organized as follows. In Sect. 2 we present the data set, with a brief description of the observations and spectra reduction. In Sect. 3 we describe the analysis aimed at measuring radial and rotational velocities (Sects. 3.1 and 3.2), atmospheric parameters (Sect. 3.3), chromospheric emission fluxes and lithium equivalent widths (Sect. 3.4). The results are presented in Sect. 4, where the properties and evolutionary status of the targets are discussed on the basis of their position on the Hertzsprung-Russell diagram (Sect. 4.2), the abundance of lithium and  $H\alpha$  emission (Sects. 4.3 and 4.6), kinematics (Sect. 4.8), and spectral energy distribution (Sect. 4.7). The main conclusions are summarized in Sect. 5. Individual notes on the youngest stars in our sample can be found in Appendix B.

## 2. Observations and reduction

We use the *RasTyc* catalog (Guillout et al. 1999) to obtain a statistically significant sample of the youngest field stars in the solar neighborhood. We adopted the criteria described in Paper I to select the optically fainter sources to be investigated spectroscopically for this study. We briefly recall them for the reader's convenience:

- declination  $\delta \geq 0^\circ$  to observe the targets with telescopes located in the Northern hemisphere;
- right ascension between 15h and 8h;
- $0.6 \leq (B - V)_T \leq 1.3$ , which is the range in which the lithium  $\lambda 6707.8$  Å line can be used as an age indicator;

- ROSAT PSPC count rate greater than or equal to  $0.03 \text{ ctss}^{-1}$  to avoid RASS scanning bias (see Guillout et al. 1999);
- $V_T \leq 10.5$  mag, since the Tycho catalog is largely incomplete above this limit.

As we observed many targets from La Palma, the first selection criterion has been slightly relaxed, so that this sample contains also some objects with negative declination ( $\delta \geq -15^\circ$ ). This allowed us to compare our results with those of the SACY survey (Torres et al. 2006) of Southern stellar X-ray sources.

We made a detailed search of previous data and works dealing with these sources in the Simbad and Vizier astronomical databases. We did not observe the stars whose physical parameters were already derived in the literature from high resolution spectra. However, a few stars with published high-resolution spectra are present in our list either because they were purposely selected for doing a comparison with the results of previous surveys or because their data were published after the approval of our observation proposals. Moreover, when two stars of similar brightness are located near the X-ray source within the typical ROSAT positional accuracy of  $30''$  (Voges et al. 1999), we decided to observe both of them.

We observed 134 optically faint stars from November 2001 to August 2005 with the spectrograph AURELIE at the 1.52-m telescope at the Observatoire de Haute Provence (OHP, France; see Paper I for details) and 178 stars with SARG, the high-resolution spectrograph at the 3.5-m TNG telescope (Canary Islands, Spain), in 2007<sup>1</sup>. We chose the SARG setup with the yellow grism and the slit width of  $0''.8$ , which provides a resolving power of  $R = \lambda/\Delta\lambda \simeq 57\,000$  and a spectral coverage in the range  $4600$ – $7900 \text{ \AA}$ . Exposure times ranged from 4 to 35 minutes, according to the star magnitude, and allowed us to reach a signal-to-noise (S/N) ratio from 50 to 110, depending also on the seeing and sky conditions. Ten stars were observed in August 2009 and June 2011 with SARG and the red grism, which covers the wavelength range  $5500$ – $11\,000 \text{ \AA}^2$ . We adopted the same slit as for the previous spectra.

Moreover, 140 spectra of 120 *RasTyc* stars were acquired in 2000 and 2001 with the ELODIE échelle spectrograph ( $R \simeq 42\,000$ ) at the 1.93-m OHP telescope. Sixty-four of these targets with  $V \leq 9.5$  mag were included in the bright *RasTyc* survey (Paper I). The atmospheric parameters reported in that work have been derived with the TGMET online analysis software (Katz et al. 1998) running at the 1.93-m OHP telescope. However, in the present paper we analyze in a homogeneous way both the optically bright and faint ELODIE targets that are all included in this study and listed in Tables A.1–A.4. Likewise, a few sources (about 25 in total) brighter than  $V = 9.5$  mag without previous spectroscopic information or with incomplete data in Paper I were also observed with the other spectrographs and included in the present work.

<sup>1</sup> Proposals TAC67-AOT15/07A and TAC35-AOT16/07B.

<sup>2</sup> Proposals TAC71-AOT20/09B and TAC34-AOT23/11A.

Further observations of 30 sources were conducted in 2008 and 2009 at the 0.91-m telescope of the *Osservatorio Astrofisico di Catania* (OAC, Italy) with the FRESCO spectrograph that covers the spectral range  $4250$ – $6850 \text{ \AA}$  with a resolution  $R \simeq 21\,000$ . The S/N ratio of these spectra is in the range 40–80.

In the present paper we use a total of 625 spectra of 443 different sources taken with the aforementioned instruments, while more than 1660 spectra were acquired during about ten years for the full program (bright+faint samples). We present a concise log of the observations in Table 1.

We were not able to observe the full sample of faint *RasTyc* sources selected according to the above criteria and about 40 stars, i.e.  $\sim 10\%$  of the sample, remained unobserved. Although a few other very young stars could have been found among them, the lack of their data is not expected to significantly bias our results.

**Table 1.** Observing log for the full program (bright + faint sample).

Year	Period	Instrument	Resolution	Spectra
2000	Jul–Sep	ELODIE	42 000	83
2001	Aug	ELODIE	42 000	57
2001	Oct–Dec	AURELIE	38 000	290
2002	Jun–Nov	AURELIE	38 000	396
2003	Jan	AURELIE	38 000	207
2004	Jun–Sep	AURELIE	38 000	231
2005	Jul–Aug	AURELIE	38 000	126
2007	Sep–Oct	FRESCO	21 000	28
2007	Feb–Dec	SARG	57 000	184
2008	Mar–Jul	FRESCO	21 000	19
2009	Jun–Oct	FRESCO	21 000	35
2009	Aug	SARG	57 000	4
2011	Jun	SARG	57 000	6
Total				1666

Details on the reduction of spectra acquired at OHP can be found in Paper I.

The reduction of the SARG and FRESCO spectra was basically done inside the IRAF<sup>3</sup> package, following standard steps of overscan and bias subtraction, flat field division, and scattered light subtraction. The extraction of the spectra from the pre-reduced images was performed with the ECHELLE task of IRAF, which allowed us to subtract the sky spectrum, extracted at the two sides of the stellar one.

Due to the gap between the two CCDs of SARG, which causes the loss of more than one échelle order, the reduction of the “red” and “blue” chip has been done separately. Particular care has been paid to the correction for the fringes at red and near-IR wavelengths and to the

<sup>3</sup> IRAF is distributed by the National Optical Astronomy Observatory, which is operated by the Association of the Universities for Research in Astronomy, inc. (AURA) under cooperative agreement with the National Science Foundation.

merging of échelle orders, which was very important for the analysis of broad lines that are close to the edges of spectral orders, such as the hydrogen H $\alpha$  line. For these tasks we developed ad-hoc tools in IDL<sup>4</sup> environment. In particular, the fringe removal was accomplished by means of contemporaneous flat field spectra that were rectified by low-order polynomial fits to obtain the fringing pattern. We have optimized the fringe-correction procedure on spectra of hot and rapidly rotating stars.

Spectra of rapidly-rotating AB stars (templates for telluric subtraction) as well as of radial and rotational velocity standard stars were also acquired with all spectrographs and have been used for the data analysis.

The telluric water vapor lines at the H $\alpha$  and Na I D<sub>2</sub> wavelengths were subtracted using an interactive procedure described by Frasca et al. (2000) and adopting the well-exposed telluric templates acquired during the observing runs. The broad and shallow spectral lines of the latter have been removed by high-order polynomial fits.

### 3. Data analysis

We made an analysis of the spectra with different purposes: i) to measure the radial velocity (RV) and the projected rotational velocity ( $v \sin i$ ); ii) to determine the basic atmospheric parameters ( $T_{\text{eff}}$ ,  $\log g$ , and [Fe/H]); iii) to evaluate the photospheric lithium content; and iv) to define the level of chromospheric activity.

We used different techniques and reached different goals and accuracies for single stars, double-lined spectroscopic binaries (SB2), and triple (SB3) or multiple systems.

#### 3.1. Radial velocity

The measurement of RV for AURELIE and ELODIE spectra was already described in Paper I. It is based on the use of a numerical mask or a synthetic spectrum as RV template. For the ELODIE spectra this task is normally done by the on-line reduction pipeline just after the acquisition of the spectrum.

For the SARG and FRESCO échelle spectra, the RV was measured by means of the cross-correlation between the target spectrum and a template chosen among a list of spectra of RV standard stars (Table 2) that were observed with the same instrument and in the same seasons as our targets. All these stars are slow rotators and display a very low or negligible level of magnetic activity so that they were also used as non-active templates (Sect. 3.4). The cross-correlation functions (CCFs) were computed for all échelle orders but those with the lowest S/N ratio (usually for blue wavelengths). Very broad lines, such as Na I D<sub>2</sub> and H $\alpha$ , as well as strong telluric features were excluded from the CCF analysis. The latter was performed with an ad-hoc software developed by us in the IDL environment.

<sup>4</sup> IDL (Interactive Data Language) is a registered trademark of Harris Corporation.

The CCF peak has been fitted with a Gaussian to evaluate its centroid and full width at half maximum (FWHM). The RV error for each spectral order,  $\sigma_i$ , was estimated by the fitting procedure accounting for the CCF noise (far from the peak). For a few spectra, we compared the results of our code with those from the IRAF task FXCOR, finding similar results and errors.

The final RV is obtained as the weighted mean (weight  $w_i = 1/\sigma_i$ ) of the  $RV_i$  values measured in the individual orders. We adopted as RV uncertainty the standard error of the weighted mean,  $\sigma_{RV}$ . The RV values and errors for single stars or single-lined binaries (SB1) are reported in Table A.1. The targets observed more than once were classified as SB1 systems whenever the difference of two RV values is larger than the sum of the corresponding errors. A note about SB1 systems is added in Table A.4. We note that each target with a single RV measurement has been classified as a single star (S), although this does not exclude that it is indeed an SB1 system, or even an SB2 system observed close to the conjunction, when the lines of the individual components are fully blended.

This procedure was also used to measure the RV of the components of SB2 or multiple systems. We considered a secondary CCF peak as significant whenever it exceeded the  $5\sigma$  level, where  $\sigma$  is the CCF noise calculated far from the peaks.

**Table 2.** Radial/rotational velocity standard stars.

Name	Sp. Type	RV (km s <sup>-1</sup> )	$v \sin i^d$ (km s <sup>-1</sup> )	Notes
HD 187691	F8 V	-0.0 <sup>a</sup>	2.8	RV, $v \sin i$
HD 102870	F8 V	4.3 <sup>a</sup>	4.5	RV
HD 157214	G0 V	-79.2 <sup>b</sup>	1.6	$v \sin i$
HD 32923	G4 V	20.50 <sup>a</sup>	1.5	RV, $v \sin i$
HD 117176	G5 V	4.6 <sup>b,*</sup>	1.2	$v \sin i$
HD 10700	G8 V	-17.1 <sup>b</sup>	0.9	$v \sin i$
HD 145675	K0 V	-13.69 <sup>c,*</sup>	0.8	$v \sin i$
HD 221354	K1 V	-25.20 <sup>a</sup>	0.6	RV, $v \sin i$
HD 115404	K2 V	7.60 <sup>a</sup>	3.3	RV
HD 182572	G8 IV	-100.35 <sup>a</sup>	1.9	RV, $v \sin i$
HD 12929	K2 III	-14.6 <sup>a</sup>	1.6	RV
HD 161096	K2 III	-12.5 <sup>a</sup>	2.1	RV

<sup>a</sup> Udry et al. (1999). <sup>b</sup> Nordström et al. (2004). <sup>c</sup> Nidever et al. (2002). <sup>d</sup> Glebocki & Gnacinski (2005).

\* Exoplanet hosting star. RV variable.

#### 3.2. Projected rotational velocity

The  $v \sin i$  was measured in two different ways. The first is based on the FWHM of the CCF peak through calibrations FWHM– $v \sin i$  obtained for several standard stars among those listed in Table 2. For each standard star, the calibration relationship was defined by measuring the FWHM of the CCF peak obtained correlating the original

spectrum with the same spectrum after being artificially broadened by the convolution with a rotation profile of increasing  $v \sin i$  (from 0 to 150 km s $^{-1}$ ). We applied this method only to 21 échelle orders of the blue-chip SARG spectra covering the wavelength range from about 4900 to 6000 Å. We rejected the orders with very wide lines, which would make the results worse. The FWHM measured on the CCF of each échelle order of target spectra and RV standard stars was converted to  $v \sin i$  using these calibrations. We took the average of the values for each order and the standard deviation as  $v \sin i$  and error, respectively. The same procedure was applied to the FRESCO spectra, for which we used nine échelle orders in the range 5400–6400 Å, and to the single-order AURELIE spectra, for which synthetic templates were adopted (see Paper I). The measure of  $v \sin i$  on the ELODIE spectra was also performed with this method. We adopted the relation proposed by Queloz et al. (1998) to convert the  $\sigma$  of the Gaussian fitted to the CCF peak into  $v \sin i$ . In a few cases, it was necessary to perform a new cross-correlation analysis on the original ELODIE spectra for measuring RV and  $v \sin i$ , because the range of radial velocity encompassed by the CCF made on the fly during the observation was not sufficient. This was the case of a few very rapid rotators and SB2 systems.

This method was also used for measuring  $v \sin i$  for the components of SB2 and SB3 systems. We performed independent Gaussian fits to the CCF peaks of the system components whenever they are well separated, while a double (or multiple) Gaussian fit was applied in cases of blended CCFs. In the latter case the accuracy of  $v \sin i$  and RV determinations decreases with the increase of line blending and with the decrease in peak intensity. The RV and  $v \sin i$  of the individual components of SB2 and SB3 spectroscopic systems are listed in Table A.2 and A.3, respectively.

The other method for measuring  $v \sin i$ , which can be applied only to single stars or SB1 systems, is based on the minimization of the residuals *observed – template*, where the *template* is one of the spectra in Table 2 rotationally broadened from 0 to 150 km s $^{-1}$  with a step of 0.5 km s $^{-1}$ . This is the same algorithm used by ROTFIT for the determination of the atmospheric parameters (see Sect. 3.3 for further details) by adopting a wider list of reference stars. For very rapid rotators, we explored a wider range of  $v \sin i$  (from 0 to 500 km s $^{-1}$ ) with a larger sampling (5 km s $^{-1}$ ).

The values of  $v \sin i$  obtained for single or SB1 stars with both methods,  $v \sin i_{\text{CCF}}$  and  $v \sin i_{\text{ROTFIT}}$  are quoted, along with their errors, in Table A.1. They are clearly in very good agreement with each other, as shown in Fig. 1, where the two data sets follow a close one-to-one relationship. The average difference, calculated for values of  $v \sin i \leq 100$  km s $^{-1}$ , is only 0.38 km s $^{-1}$ , which is not significant, accounting for the measurement errors. The standard deviation of the residuals is 2.26 km s $^{-1}$ . We note that the scatter enhances for the stars rotating faster than about 30 km s $^{-1}$ , especially for the ELODIE data. This is

probably due to the fit of the CCF peak, whose shape is far from a Gaussian for high  $v \sin i$ , and to the Queloz et al. (1998) calibration relation adopted for the ELODIE spectra, which has a full validity for  $v \sin i$  up to 20 km s $^{-1}$ . A few discrepant values around 10 km s $^{-1}$  are visible for the FRESCO data. This is likely the result of the lower resolution of this instrument for which the minimum detectable  $v \sin i$  is about 5–7 km s $^{-1}$ . From the above arguments, we consider as most reliable the values derived with ROTFIT, which are used in the following.

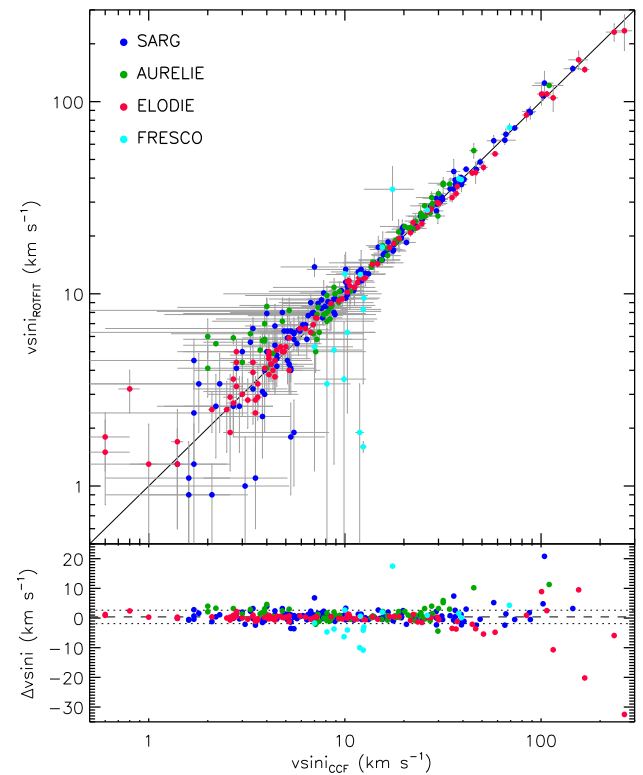


**Fig. 1.** *Top panel*) Comparison between the  $v \sin i$  values measured with ROTFIT and those derived from the FWHM of the cross-correlation peak (Table A.1). Dots with different colors have been used for the different instruments, as indicated in the legend. The continuous line is the one-to-one relationship. *Bottom panel*) The residuals from the one-to-one relationship, excluding the values with  $v \sin i \geq 100$  km s $^{-1}$ , have a mean of +0.38 km s $^{-1}$  (dashed line), and a standard deviation of 2.26 km s $^{-1}$  (dotted lines).

### 3.3. Atmospheric parameters and spectral classification

The MK spectral classification and the determination of the basic atmospheric parameters ( $T_{\text{eff}}$ ,  $\log g$ , and [Fe/H]) were performed by means of the code ROTFIT (Frasca et al. 2006). We adopted, as templates, a library of 270 high-resolution spectra of slowly-rotating stars with well known parameters (Soubiran et al. 2010) span-

ning a wide range of effective temperature, gravity, and iron abundance, which were retrieved from the ELODIE Archive (Moultaka et al. 2004).

The SARG spectra ( $R_{\text{SARG}} = 57\,000$ ) were degraded to the ELODIE resolution ( $R_{\text{ELODIE}} = 42\,000$ ) by means of the convolution with a Gaussian kernel of width  $W = \lambda\sqrt{1/R_{\text{ELODIE}}^2 - 1/R_{\text{SARG}}^2}$  Å. We applied ROTFIT only to the échelle orders with the best S/N ratio, which span from about 4500 to 6800 Å, both in the SARG and FRESCO spectra. To match the lower resolution of FRESCO spectra ( $R_{\text{FRESCO}} = 21\,000$ ) we degraded the resolution of the ELODIE templates by convolving them with a Gaussian kernel of width  $W = \lambda\sqrt{1/R_{\text{FRESCO}}^2 - 1/R_{\text{ELODIE}}^2}$  Å. The same was done for the AURELIE spectra, even though their resolution ( $R_{\text{AURELIE}} \simeq 40\,000$ ) is close to the ELODIE spectra.

All the selected échelle orders were analyzed independently. The cores of Balmer lines, which can be contaminated by chromospheric emission, the  $\text{Li I } \lambda 6707.8$  line, and the spectral regions severely affected by telluric line absorption or by CCD defects, were excluded from the analysis. The final stellar parameters are weighted averages of the results of each  $i$ -th échelle order, where the weight accounts for both the  $\chi^2$  of the fit (more weight is given to the most closely fitted or higher S/N orders) and the amount of information contained in each spectral order, which is expressed by the total line absorption,  $f_i = \int(F_\lambda/F_C - 1)d\lambda$ , where  $F_\lambda/F_C$  is the continuum-normalized spectrum in the  $i$ -th échelle order. The uncertainties of atmospheric parameters are the standard errors of the weighted means to which we added in quadrature the average uncertainties of the reference stars evaluated as  $\pm 50$  K,  $\pm 0.1$  dex, and  $\pm 0.1$  dex for  $T_{\text{eff}}$ ,  $\log g$ , and  $[\text{Fe}/\text{H}]$ , respectively.

As already explained in Sect. 3.1, ROTFIT provides us also with a measure of the star projected rotational velocity, because it iteratively broadens each template spectrum in a wide range of  $v \sin i$  and find the  $\chi^2$  minimum. However, the values of  $v \sin i$  reported in Table A.1 were obtained using as templates the few inactive and slowly rotating standard stars of Table 2, whose spectra were acquired with the same instrumentation as for the target ones. This enabled us to overcome any possible systematic error due to the different resolution.

Finally, the MK classification of the target star is also provided by the code. It is defined by the spectral type and the luminosity class of the reference star that more frequently matches the target spectrum in the different échelle orders.

In Table A.4, we list the stellar parameters, along with their errors ( $\sigma_{T_{\text{eff}}}$ ,  $\sigma_{\log g}$ , and  $\sigma_{[\text{Fe}/\text{H}]}$ ), and the MK classification for the single stars and SB1 binaries. The median errors of the atmospheric parameters are about 100 K, 0.16 dex, and 0.11 dex, for  $T_{\text{eff}}$ ,  $\log g$ , and  $[\text{Fe}/\text{H}]$ , respectively.

For double-lined spectroscopic binaries (SB2) and triple systems we do not determine the atmospheric parameters but we only provide the values of radial and ro-

tational velocities of their components measured thanks to the CCF analysis (cf. Sect. 3.1). The spectral classification and estimates of the atmospheric parameters of the components of SB2s via the COMPO2 code (see, e.g., Frasca et al. 2006) is deferred to a subsequent work devoted to systems with more observations, for which we will also discuss their orbital parameters. However, ten SB2 and one SB3 system for which one component is much brighter than the other have been also analyzed with ROTFIT.

### 3.4. Chromospheric activity and lithium equivalent width

As we did for the optically-bright sources (Paper I), we evaluated the level of chromospheric activity from the emission in the core of the Balmer  $\text{H}\alpha$  line for the single stars and SB1 systems. A rough age classification was performed based on the lithium abundance (see Sect. 4.3).

We measured both the lithium equivalent width and the chromospheric emission level with the “spectral subtraction” technique (see, e.g., Herbig 1985; Frasca & Catalano 1994; Montes et al. 1995). This technique is based on the subtraction of a template, which is the spectrum of a slowly rotating star rotationally broadened to the  $v \sin i$  of the target. We chose templates with the same spectral type as the target, with a negligible level of chromospheric activity, and without any detectable lithium absorption line. This method allows us to remove the  $\text{Fe I } \lambda 6707.4$  Å absorption line, which is normally blended with the lithium line, from the target spectrum. Likewise, the subtraction of the photospheric absorption profile of the non-active template allows us to measure the net chromospheric emission that fills in the  $\text{H}\alpha$  line core. Therefore, the equivalent width of the lithium line,  $W_{\text{Li}}$ , and the net equivalent width of the  $\text{H}\alpha$  line,  $W_{\text{H}\alpha}^{\text{em}}$ , were measured in the residual spectrum obtained by subtracting the non-active template. The values of  $W_{\text{Li}}$  and  $W_{\text{H}\alpha}^{\text{em}}$  have been obtained by integrating the residual emission (absorption for the lithium line) profile (see Fig. 2). The errors on the equivalent width of  $\text{H}\alpha$  and lithium lines,  $\sigma_{W_{\text{H}\alpha}^{\text{em}}}$  and  $\sigma_{W_{\text{Li}}}$ , were estimated as the product of the integration range and the mean error per spectral point, which results from the standard deviation of the flux values of the residual spectrum measured at the two sides of the line. The equivalent widths of  $\text{H}\alpha$  and lithium lines are reported in Table A.4 together with their errors.

We also evaluated the  $\text{H}\alpha$  surface flux (or radiative losses),  $F_{\text{H}\alpha}$ , and the ratio of the  $\text{H}\alpha$  and bolometric luminosity,  $R'_{\text{H}\alpha}$ <sup>5</sup>, that are calculated according to the following equations:

$$F_{\text{H}\alpha} = F_{6563} W_{\text{H}\alpha}^{\text{em}}, \quad (1)$$

<sup>5</sup> The prime in  $R'_{\text{H}\alpha}$  indicates that the photospheric contribution was subtracted as usual in the definition of activity indices.

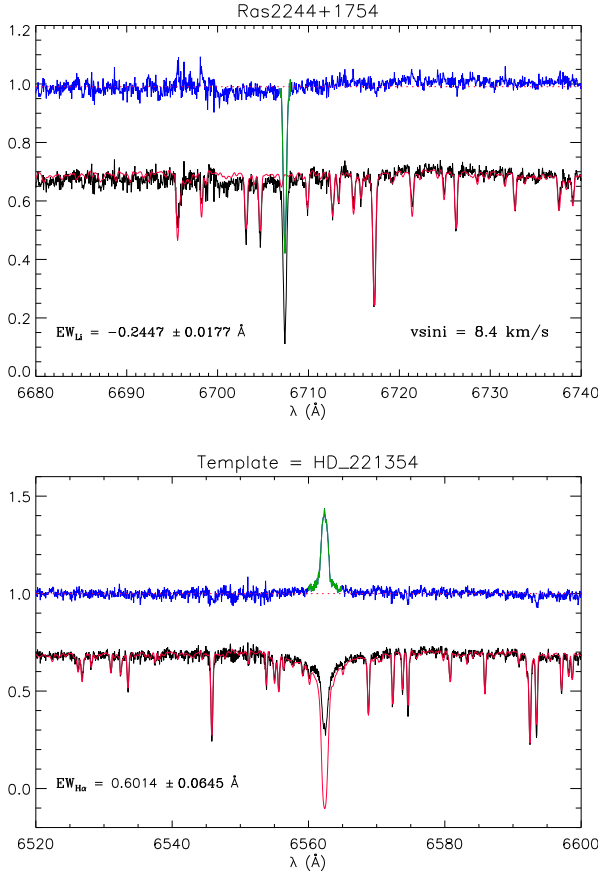


**Fig. 2.** Example of the subtraction technique applied to an active and lithium-rich star both in the lithium (*upper panel*) and H $\alpha$  spectral regions (*lower panel*). In both panels, the continuum of the residual spectrum (blue line) is set to 1, while the original spectrum (full black line) and the non-active template (thin red line) are shifted downwards by 0.3 in continuum units. The green lines indicate the residual absorption (for Li I) or emission (for H $\alpha$ ) profile that has been integrated to obtain the equivalent width.

$$R'_{\text{H}\alpha} = L_{\text{H}\alpha}/L_{\text{bol}} = F_{\text{H}\alpha}/(\sigma T_{\text{eff}}^4), \quad (2)$$

where  $F_{6563}$  is the continuum flux at the stellar surface at the H $\alpha$  wavelength, which has been evaluated from the NextGen synthetic low-resolution spectra (Hauschildt et al. 1999) at the stellar temperature and surface gravity of the target. We have evaluated the flux error considering the  $W_{\text{H}\alpha}^{\text{em}}$  error and the uncertainty in the continuum flux at the line center,  $F_{6563}$ , which is obtained propagating the  $T_{\text{eff}}$  and  $\log g$  errors.

Finally, as far as the lithium line is concerned, we estimate the threshold for lithium line detection as  $\approx 10$  mÅ, on the basis of typical  $W_{\text{Li}}$  errors and S/N ratios.

The  $T_{\text{eff}}$ – $\log g$  diagram of the single and SB1 sources is shown in Fig. 3, where the symbols are color coded according to the value of  $W_{\text{Li}}$  (Fig. 3a) and  $R'_{\text{H}\alpha}$  (Fig. 3b).

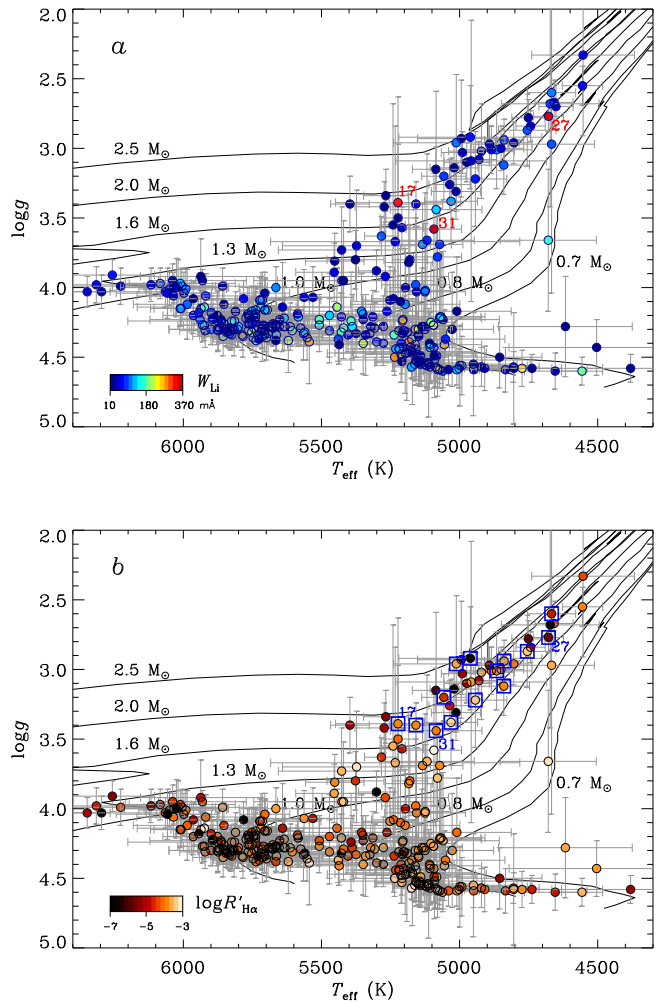


**Fig. 3.**  $T_{\text{eff}}$ – $\log g$  diagram for all the single stars and SB1 systems. The symbols are color coded by  $W_{\text{Li}}$  (*upper panel*) and  $R'_{\text{H}\alpha}$  (*lower panel*). The black lines are post-MS evolutionary tracks from Girardi et al. (2000) with a metallicity  $Z=0.019$ . In the *lower panel*, the lithium-rich giant candidates listed in Table 4 are enclosed in open squares. The two very lithium rich giants (#17 and #27) and the youngest PMS star (#31, see Sect. 4.3) are also marked.

## 4. Results

### 4.1. Binaries and multiple systems

Close binaries are expected to give a large contribution to X-ray selected or chromospherically-active stellar samples (see, e.g., Brandner et al. 1996). In fact, the tidal synchronization of the rotation of the components with the orbital period can greatly intensify the magnetic field, and hence the level of activity. Therefore, stellar samples like the *RasTyc* one allow us to detect close binaries, which can be followed up for the study of their properties. At the same time, they behave as contaminants when looking for young stars. Based on the CCF shape and the variation of the peak centroid, we found 12 SB3 (2.7%), 114 SB2 (25.7%),

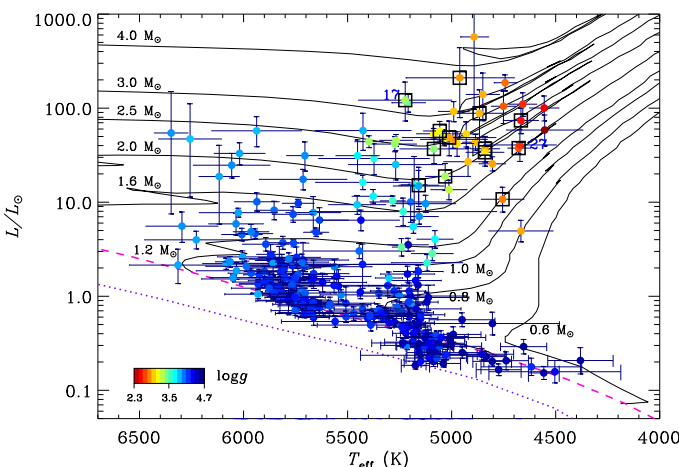


**Fig. 4.** Hertzsprung–Russell diagram of the single and SB1 sources with known parallaxes. The symbols are color coded by  $\log g$ . The evolutionary tracks of Girardi et al. (2000) are shown as solid lines with the labels representing their masses. The zero-age main sequence (ZAMS) with solar metallicity ( $Z = 0.019$ ) and with  $Z = 0.001$  by the same authors are also shown with a dashed and a dotted line, respectively. The lithium-rich giant candidates listed in Table 4 are enclosed in open squares. The two giants with the highest Li abundance are labeled as in Table 3.

and 38 SB1 (8.6 %) systems. We note that these numbers, especially that of SB1, must be considered as lower limits, since stars with only one observation or even with more spectra could be indeed SB1 systems observed in similar configurations or SB2 close to the conjunctions. Indeed, eight SB1 systems were discovered by the comparison of our single RV value with that reported in the SACY catalog (see Sect. 4.5). Altogether, the close binary systems account for more than 37 % of the whole sample. A similar contamination (31 %) was estimated for the bright sample in Paper I.

#### 4.2. Hertzsprung–Russell diagram

In Fig. 4, we report the position of the single and SB1 targets with known parallaxes in the Hertzsprung–Russell (HR) diagram, which are 263 out of a total of 328 such targets. We used the  $T_{\text{eff}}$  values derived with ROTFIT (Table A.4) and the  $V$  magnitudes from the TYCHO catalog that are listed in Table A.1. For most stars (243) the parallaxes are retrieved from the TGAS catalog in the first *Gaia* data release (Gaia Collaboration 2016), while for 22 objects with no entry in that catalog we adopted the values reported by van Leeuwen (2007). The  $V$  magnitudes were corrected for the interstellar extinction as in Paper I, i.e. assuming a mean extinction of  $A_V = 1.7 \text{ mag/kpc}$  on the galactic plane ( $|b| < 5^\circ$ ) and  $0.7 \text{ mag/kpc}$  out of the plane. To convert the  $V$  magnitudes to bolometric magnitudes we used the bolometric correction ( $BC$ ) derived by

interpolating the relation  $T_{\text{eff}}-BC$  of Pecaut & Mamajek (2013). In the same figure we overplot the post-main sequence evolutionary tracks by Girardi et al. (2000).

As apparent in Fig. 4, the values of  $\log g$  found from the analysis of the spectra are fully consistent with the evolutionary status of the targets, supporting the reliability of the atmospheric parameters derived by ROTFIT with these spectra.

#### 4.3. Lithium abundance and age

Lithium is burned at relatively low temperatures in stellar interiors ( $\sim 2.5 \times 10^6 \text{ K}$ ). As a consequence, it is progressively depleted from the stellar atmospheres of late-type stars when mixing mechanisms pull it deeply in their convective layers. Thus, its abundance can be used as an empirical indicator of age for stars cooler than about 6500 K. A simple and effective way to get an age estimate is a diagram showing the equivalent width of lithium as a function of the color index  $(B-V)_0$  together with the upper envelopes of young OCs that serve as boundaries to delimit the different age classes (Fig. 5). Although the stars are not very distant from the Sun, their colors are affected by reddening, which has been calculated from the magnitude extinction,  $A_V$  (see Sect. 4.2) according to standard extinction law  $E(B-V) = A_V/3.1$ .

We adopted, as in Paper I, the upper envelopes of the following clusters: the Hyades (Soderblom et al. 1990), the Pleiades (Soderblom et al. 1993c; Neuhäuser et al. 1997), and IC 2602 (Montes et al. 2001a), whose ages are of about 650 (White et al. 2007), 125 (White et al. 2007), and 30 Myr (Stauffer et al. 1997), respectively. As shown by Soderblom et al. (1993b), the lower envelope of the Pleiades behaves as an upper boundary for the members of the Ursa Major (UMa) cluster ( $\text{age} \approx 300 \text{ Myr}$ ). Therefore, we considered as pre-main sequence (PMS) or very young star candidates (*PMS-like*) those stars located above the Pleiades upper envelope (big dots in Fig. 5) or very close to it (triangles) and divided the remaining stars into *Pleiades-like*, *UMa-like*, *Hyades-like*, and *Old* classes according to their position in the diagram, the *Old* ones being those with a  $W_{\text{Li}} < 10 \text{ m}\AA$ . We remark that our selection criterion is not conservative, but it is inclusive; in fact we are not taking into account the errors on  $W_{\text{Li}}$  and  $(B-V)_0$ . On the other hand, the upper envelopes of OCs are not “knife edges” that can sharply separate classes of objects of different ages. That is why we used the suffix *like* in our classes. This also means, for example, that the *PMS-like* class can include stars that are indeed closer to the Pleiades age.

As a further test of our method to select young stars, we calculated the lithium abundance,  $A(\text{Li})$ , from our values of  $T_{\text{eff}}$ ,  $\log g$ , and  $W_{\text{Li}}$  by interpolating the curves of growth of Soderblom et al. (1993c). We adopted this calibration in order to treat our data homogeneously to Sestito & Randich (2005) for the stars in 22 galactic OCs. In Fig. 6 we display the lithium abundance as a function of

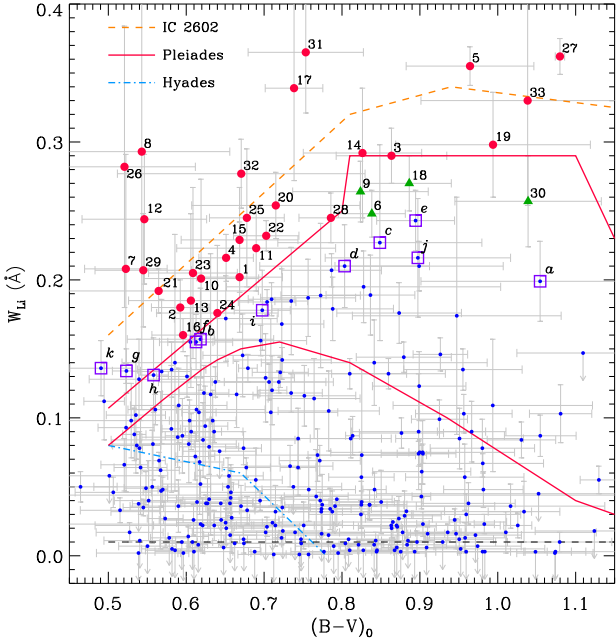


**Fig. 5.** Equivalent width of the  $\text{Li I} \lambda 6707.8$  line ( $W_{\text{Li}}$ ) plotted as a function of the dereddened Johnson  $(B - V)_0$  color index for the single or SB1 stars in our sample (Table A.4). The lines display the upper boundaries for Hyades (blue dash-dotted), Pleiades (red solid for both lower and upper boundary) and IC 2602 (orange dashed) clusters. The black dashed line marks the lower limit for positive detection of the  $\text{Li I} \lambda 6707.8$  line estimated by us ( $10 \text{ m}\text{\AA}$ ). Twenty-nine stars (red big dots) show lithium equivalent width in excess with respect to the lithium-richest Pleiades stars and ten of them fall above the upper envelope of the PMS cluster IC 2602. Four stars (green triangles) have  $W_{\text{Li}}$  just below the Pleiades upper envelope. The open squares enclose other eleven very young objects selected on the basis of their lithium abundance (see text and Fig. 6). All the lithium-rich stars are labeled according to Table 3.

$T_{\text{eff}}$  along with the upper envelopes of the distributions of some young OCs shown by Sestito & Randich (2005). We note that, contrary to the color indices, the effective temperature does not need to be corrected for interstellar reddening, avoiding to introduce further uncertainties. Apart from the large errors of  $A(\text{Li})$ , which take into account both the  $T_{\text{eff}}$  and  $W_{\text{Li}}$  errors<sup>6</sup>, Figure 6 clearly shows that all the 33 *PMS-like* stars already selected from the  $W_{\text{Li}}$  diagram (Fig. 5), with the exception of only two sources, are located on or above the Pleiades upper envelope. The two stars falling just below the Pleiades upper envelope are RasTyc 0316+5638 (#11) and RasTyc 2039+2644 (#22). However, considering the errors, they can be still

<sup>6</sup> We did not consider the errors of  $\log g$  for the evaluation of  $A(\text{Li})$  errors, because an error  $\sigma_{\log g} = 0.5$  dex translates into an uncertainty of only a 0.1 or 0.2 dex, at most, in  $A(\text{Li})$ , in the  $T_{\text{eff}}$  range of our targets.

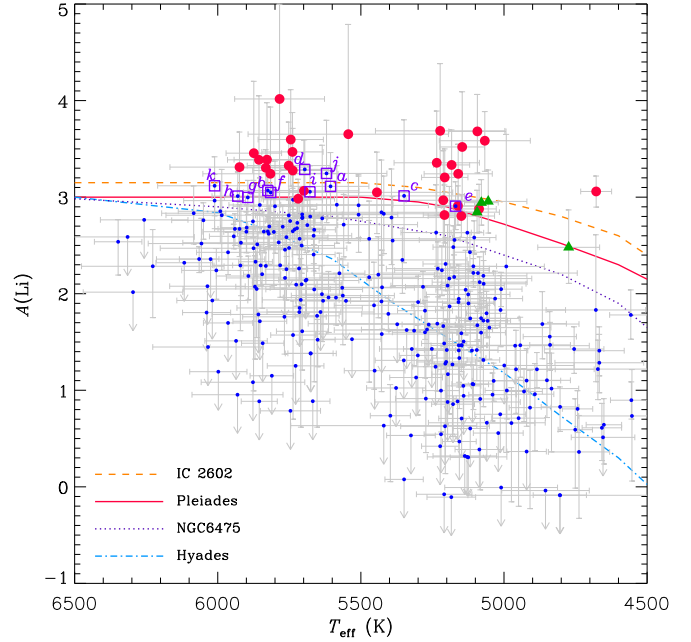


**Fig. 6.** Lithium abundance as a function of  $T_{\text{eff}}$  for the stars in Table A.4. The upper envelopes of  $A(\text{Li})$  for IC 2602, Pleiades, NGC 6475 ( $age \approx 300$  Myr), and Hyades clusters adapted from Sestito & Randich (2005) are overplotted. The meaning of the symbols is the same as in Fig. 5. Other eleven stars with high lithium content are found thanks to this diagram (open squares) and are labeled with letters from *a* to *k*, as in Table 3.

included in the *PMS-like* class. Moreover, the four stars that lie just below the upper envelope of the Pleiades at  $0.8 \leq (B - V)_0 \leq 1.1$  mag in Fig. 1 (green triangles) are located above or exactly superimposed to it in the  $T_{\text{eff}}-A(\text{Li})$  diagram (Fig. 6). In addition, eleven other stars that were not selected on the basis of  $W_{\text{Li}}$  show a high lithium abundance, above the Pleiades  $A(\text{Li})$  upper envelope. We have highlighted them with open squares and flagged with letters from *a* to *k* both in Figs. 5 and 6 as well as in Table 3. The inclusion of these targets leads the number of very young star candidates to 44.

In the end, the percentage of *PMS-like*, *Pleiades-like*, *UMa-like*, *Hyades-like*, and *Old* stars is about 14 %, 13 %, 34 %, 19 %, and 20 %, respectively, while for the bright sample (Paper I) they were about 3 %, 7 %, 39 %, 19 %, and 32 %. Considering the population of very young stars as defined in Paper I, i.e. *PMS-like*, *Pleiades-like* and *UMa-like* stars taken altogether, their percentage in the faint sample increases from 49 % to 61 %, while the fraction of the older population decreases of about 10 % accordingly. In particular, the fraction of the youngest stars (*PMS-like* and *Pleiades-like*) is almost three times higher in the faint sample than in the bright one.

In an X-ray flux-limited and optically magnitude-limited sample, the fraction of the various populations depends on the X-ray and optical horizons, i.e. the maxi-

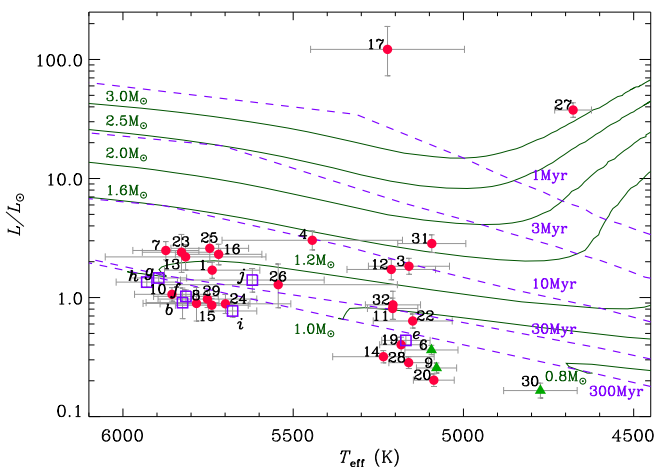


**Fig. 7.** Hertzsprung-Russell diagram of the *PMS-like* sources with known parallaxes. The symbols are as in Fig. 5. The pre-main sequence evolutionary tracks of Siess et al. (2000) are shown as solid lines with the labels representing their masses. The isochrones at ages of 1, 3, 10, 30, and 300 Myr are shown with dashed lines. The stars labeled as #17 and #27 lie above the 1-Myr isochrone and are likely lithium-rich giants.

mum distance at which we can detect stars in X-ray and at optical wavelengths, respectively. On the average, when the X-ray horizon is farther than the optical one and the last is increased by changing the limiting magnitude of the sample (fainter stars detected at larger distance), the fraction of young stars increases as well. This can be easily understood because young stars are brighter in X-ray and thus also detectable at larger distances compared to older stars. However, this applies only in general terms, because of the role of other stellar parameters in the X-ray luminosity, which depends, *inter alia*, on both age and mass, making the details more complicated. X-ray population models are absolutely needed for a meaningful interpretation of the observed properties (sky positions, distance distribution, magnitudes, colors, proper motions, etc.) of the *RasTyc* sample. This is out of the scope of the present work and will be the subject of a dedicated paper. We also note that the differences may also arise from the higher incidence of Gould Belt sources in the optically faint sample that reaches beyond the space volume sampled in Paper I.

Figure 7 shows the HR diagram for the *PMS-like* objects along with the PMS evolutionary tracks and isochrones by Siess et al. (2000). We note that stars #17 and #27 lie above the isochrone at 1 Myr and are likely lithium-rich giants, as also shown in Fig. 4 where they lie close to the post-main sequence tracks for stellar models with  $3.0 M_{\odot}$  and  $1.5 M_{\odot}$ , respectively. We have therefore disregarded them as PMS-like candidates (see also Table 3 and Appendix B).

#### 4.4. Evolved stars

Besides the two stars mentioned above, a considerable number of giants and subgiants is present among single stars and SB1 systems, as apparent from the  $T_{\text{eff}}-\log g$  diagram (Fig. 3) and the HR diagram (Fig. 4). Considering as ‘evolved stars’ those ones with  $\log g \leq 3.5$ , we got a sample of 39 out of 328 sources, i.e. 12% of the single+SB1 sources. Half of them also exhibit a remarkable chromospheric emission ( $\log R'_{\text{H}\alpha} \gtrsim -5$ , see Fig. 3b), which is normally paired to a rapid rotation ( $v \sin i \gtrsim 9 \text{ km s}^{-1}$ ). It is worth noticing that all the SB1 and possible SB2 systems (10 in total) among the 39 evolved stars also display a high chromospheric activity level. The remaining active giants could be either single stars that are rotating quite fast as a result of a particular evolutionary path or spectroscopic binaries that are still undetected.

Fourteen out of the 39 evolved stars are lithium-rich giant candidates ( $A(\text{Li}) > 1.4$ , e.g., Charbonnel & Balachandran 2000). Their properties are summarized in Table 4. Among them, only the bright source HD 214995 is already known as a Li-rich giant at the position of the red-giant bump (Charbonnel & Balachandran 2000). The other stars, excepting perhaps BD+48 3149 and HD 220338, are hotter than the boundary corresponding to the deepest penetration of the convective zone during the first dredge up (cf. Fig. 1 of Charbonnel & Balachandran 2000), which is around 4400–4600 K for the stars in our mass range. Therefore, these stars have started but not yet completed the standard first dredge-up dilution and should not be considered as abnormally lithium rich. They would exhibit a lithium abundance close to its initial value. As suggested by Fekel & Balachandran (1993), angular momentum may be dredged-up from the stellar interior along with Li-rich material during this phase, giving rise to a faster rotation and, consequently, to a higher activity level. This can explain the higher incidence (more than 35%) of lithium-rich giant candidates in our X-ray selected sample compared to the typical fraction of 1% found in several spectroscopic surveys of giant stars (e.g., de la Reza et al. 2012, and references therein). This is also in line with the high percentage (about 50%) of Li-rich candidates among fast rotating K giants (with  $v \sin i \gtrsim 8 \text{ km s}^{-1}$ ) reported by Drake et al. (2002). It is worth noticing that most of the stars listed in Table 4 are indeed rotating faster than  $8 \text{ km s}^{-1}$ .

The source TYC 3501-626-1 could be an SB2 system with a faint component, on the basis of the CCF. It has a high chromospheric activity level  $\log R'_{\text{H}\alpha} = -3.55$  and has been reported as a rotationally variable source ( $P_{\text{rot}} \simeq 7.93$  days) by Kiraga & Stepien (2013). The presence of the faint secondary component could have affected the determination of the atmospheric parameters of this star; therefore we cannot exclude that it is a binary system containing young Li-rich stars. In addition, seven of the stars in Table 4, namely TYC 4319-714-1, TYC 4364-1262-1, BD+06 3372a, BD+02 3384, BD-

045118, HD 205173, and HD 220338, are also classified as rotationally variable sources by Kiraga & Stepien (2013) and Watson et al. (2015), who report photometric periods of 34.5, 35.6, 6.5, 20.4, 39.8, 101.8, and 15.4 days, respectively. With the exception of TYC 4364-1262-1 and HD 220338, which have been detected by us as SB1 systems (see Tables A.1 and A.4), these stars have been observed only once and are therefore preliminarily classified as single stars. We cannot exclude that they are single-lined binaries similar to some long-period RS CVn systems, which also show a fast rotation and lithium enrichment (e.g., Pallavicini et al. 1992; Barrado y Navascués et al. 1998).

#### 4.5. Comparison with the SACY survey

As anticipated in Sect. 2, a similar high-resolution spectroscopic survey of optical counterparts of Southern X-ray sources (SACY) was carried out by Torres et al. (2006). They cross-correlated the RASS catalog with Hipparcos and Tycho-2 catalogs to build their sample of stellar X-ray sources and considered only stars with  $(B - V) \geq 0.6$ , as we have done in Paper I and in the present work. Unlike us, they observed stars at all right ascensions, but excluded all Hipparcos stars having  $M_V < 2.0$  mag to reduce the sample contamination by evolved stars as much as possible. Moreover, they excluded all the already known giants and active binaries of the RS CVn and W UMa classes. This explains the higher incidence of such objects in our survey with respect to SACY.

As we have observed a few stars with a low or negative declination (mainly with SARG@TNG), we have some sources in common with the SACY survey. In Table 5 we compare the parameters derived by us for the single stars and SB1 systems with those in the SACY survey. The SACY catalog (Torres et al. 2006) lists the spectral type, RV,  $W_{\text{Li}}$  for 16 of such sources and  $v \sin i$  for eight of them. For three other stars da Silva et al. (2009) report  $W_{\text{Li}}$ ,  $v \sin i$ , and  $T_{\text{eff}}$  (instead of spectral type), while Elliott et al. (2014) quote their RV values. As shown in Table 5, there is a general good agreement between  $T_{\text{eff}}$  values (within 150 K), spectral types (within 1–2 spectral subclasses),  $v \sin i$  (within 10 %), and  $W_{\text{Li}}$  (within 10 %) with only three exceptions. For RasTyc 2155-0947 there is a large discrepancy between spectral types. It is an eclipsing binary system according to the ASAS data analysed by Kiraga (2012). The presence of a secondary component could have affected the spectra giving rise to this large discrepancy. We found a very different spectral type also for RasTyc 2256+0235. It is classified by Kiraga (2012) as a rotationally variable star with a very short period,  $P_{\text{rot}} = 0.8389$  days. Different  $T_{\text{eff}}$  determinations are available in the literature, including that of 5316 K (Muñoz Bermejo et al. 2013) based on the same ELODIE spectrum taken by us. This determination is midway between  $T_{\text{eff}} \simeq 4900$  K corresponding to

the SACY K1 IV spectral type (according to the relation of Pecaut & Mamajek 2013) and our value of 5665 K. The distortion of spectral lines and CCF that is likely due to starspots can be responsible for that discrepancy. RasTyc 2352-1143 shows instead a remarkable difference of  $v \sin i$  values, which is still larger if compared to the value of  $8.2 \text{ km s}^{-1}$  reported by Jenkins et al. (2011), who also quote a value of  $\text{RV} = -13.4 \pm 1.9 \text{ km s}^{-1}$ . This star has been recently discovered to be a close visual binary with a separation of only 0''.22 (Horch et al. 2011).

As regards the RV, we note that ten objects have very discrepant values and should be considered as SB1 systems. For eight of them we could collect only one spectrum; therefore, without literature data, we would have preliminarily classified them as single stars.

#### 4.6. Chromospheric activity

The H $\alpha$  fluxes and  $R'_{\text{H}\alpha}$  indices, plotted against  $T_{\text{eff}}$ , are shown in Fig. 8, where the boundary between accreting objects and chromospherically active stars, as defined by Frasca et al. (2015), is also shown.

Our targets display a wide range in  $R'_{\text{H}\alpha}$  with only a few of them close to the saturation of magnetic activity, i.e. with  $\log(F_{\text{H}\alpha}) \geq 6.3$  (e.g., Martínez-Arnáiz et al. 2011, and references therein) or  $\log(R'_{\text{H}\alpha}) < -4.0$  (e.g., Soderblom et al. 1993a). We note that there is no object above the activity/accretion boundary, but only the target with the highest H $\alpha$  flux, namely #31 (V395 Cep), is nearly superimposed to it. This star is classified by Kun et al. (2009) as a classical T Tau star (CTTS) belonging to the L1261 cloud. Indeed, the H $\alpha$  emission profile displayed by the SARG spectrum is broad and double-peaked, with a central absorption, i.e. it is typical for a CTTS. Moreover, the full width at 10% of the line peak ( $10\%W_{\text{H}\alpha}$ ) is about  $480 \text{ km s}^{-1}$ , suggesting an accreting object according to the White & Basri (2003) criterion,  $10\%W_{\text{H}\alpha} \geq 270 \text{ km s}^{-1}$ . From the H $\alpha$  luminosity, we have also estimated the mass accretion rate as  $M_{\text{acc}} \simeq 3.6 \times 10^{-9} M_{\odot}/\text{yr}$ , following the prescriptions of Biazzo et al. (2012b). This value confirms #31 as a CTTS that displays a significant accretion (e.g., Alcalá et al. 2017). This object is also a class II source, as testified by the large IR excess (see Fig. 9).

The other two stars close to the boundary are #2 (TYC 4496-780-1) and #26 (TYC 1154-1546-1). The former belongs to a small group of young stars discovered by Guillout et al. (2010) in the surroundings of the Cepheus flare region (e.g., Tachihara et al. 2005, and references therein). It is the only object that displays a substantial IR excess among those in Guillout et al. (2010). Furthermore, its H $\alpha$  profile is similar to that of a CTTS, with a double-peaked shape and  $10\%W_{\text{H}\alpha} \simeq 510 \text{ km s}^{-1}$ . However, this star is a close visual binary (e.g., Fabricius et al. 2002) that deserves a deeper analysis, which is deferred to a subsequent work. The second one (#26) is an ultrafast rotator ( $v \sin i \simeq 234 \text{ km s}^{-1}$ ) with a broad and shallow H $\alpha$

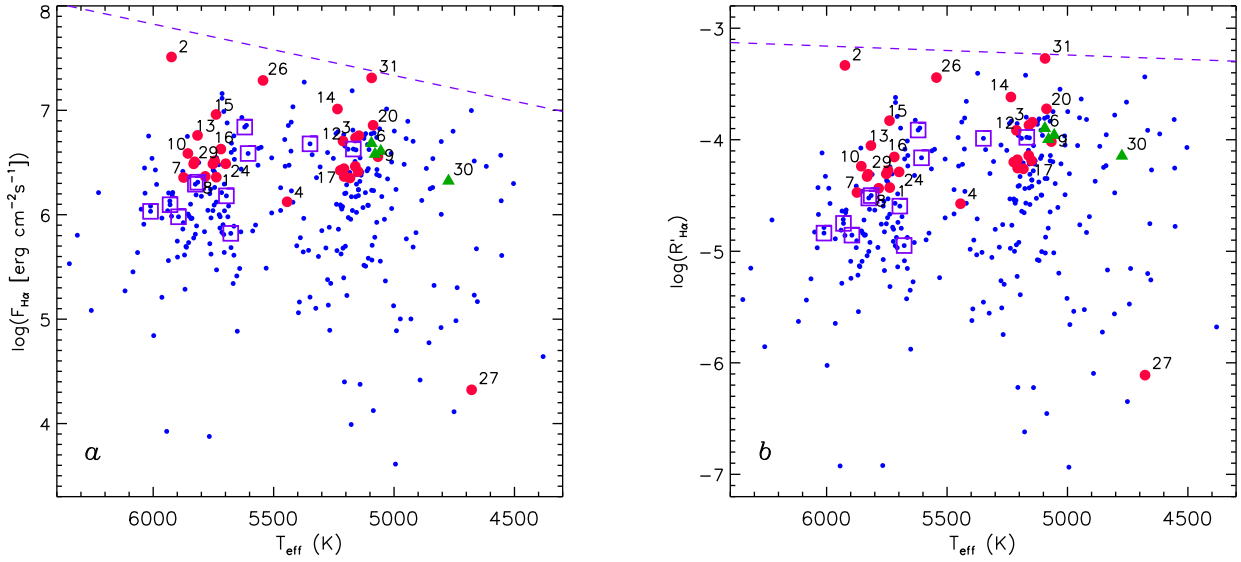


**Fig. 8.** H $\alpha$  flux (a) and  $R'_{\text{H}\alpha}$  (b) as a function of  $T_{\text{eff}}$ . The symbols are as in Fig. 5. The lithium-rich stars that are not too crowded are labeled according to Table 3. The dashed straight line is the boundary between chromospheric activity (below it) and emission due to accretion as derived by Frasca et al. (2015).

profile filled in by emission. This object is likely a zero-age main sequence (ZAMS) star, as also suggested by the HR diagram (Fig. 7) and by the lack of IR excess (see Fig. 9).

One of the candidate lithium-rich giants, namely #27 (HD 214995) shows a very low H $\alpha$  emission ( $\log(R'_{\text{H}\alpha}) = -6.11$ ), while the other one (#17=HD 234808) has  $\log(R'_{\text{H}\alpha}) = -4.20$ , which is similar to the values of other very young stars in our sample. We note that the former star does not display IR excess, while star #17 shows far-infrared excess (see Sect. 4.7).

#### 4.7. Spectral energy distributions of the very young sources

We analyzed the spectral energy distribution (SED) of the very young and *PMS-like* candidates to check the consistency between the photometry and the stellar parameters derived from our spectra. This analysis also allows us to detect IR excesses and to classify the sources in the Lada (1987) scheme.

We constructed the SED of the *RasTyc* sources using the optical and near-infrared (NIR) photometric data available in the literature. In particular, we used *BVR* photometry from the NOMAD catalog (Zacharias et al. 2004), where the magnitudes in the Johnson *B* and *V* bands are obtained by transformations from TYCHO  $B_{\text{T}}-V_{\text{T}}$  system and the *R* magnitude is normally taken from the USNO-B1.0 catalog (Monet et al. 2003). Whenever available (in a few cases), a more precise simultaneous photometry in the optical bands was adopted instead (e.g., Guillout et al. 2010; Frasca et al. 2011; Fröhlich et al. 2012). For all the sources we retrieved *I* magnitudes from the TASS catalog (Droege et al. 2006)

and completed the optical/NIR SED with the 2MASS *JHK<sub>s</sub>* photometry (Cutri et al. 2003; Skrutskie et al. 2006). The mid-infrared (MIR) photometry was retrieved from the AllWISE Data release (Wright et al. 2010; Cutri et al. 2013) and, for a few sources, from AKARI (Ishihara et al. 2010) and IRAS (e.g., Helou & Walker 1995; Abrahamyan et al. 2015).

We adopted the grid of NextGen low-resolution synthetic spectra, with  $\log g$  in the range 3.5–5.0 and solar metallicity by Hauschildt et al. (1999), to fit the optical-NIR portion (from *B* to *J* band) of the SEDs, as done by Frasca et al. (2009). In the fitting procedure we fixed  $T_{\text{eff}}$  and  $\log g$  of each target to the values found with the code ROTFIT (Table 3) and let the angular stellar diameter and the extinction  $A_V$  vary until a minimum  $\chi^2$  was reached. For the stars with known distance, this also provides us with a measure of the stellar radius. We always found low values of  $A_V$ , ranging from 0.0 to 0.6 mag, in agreement with the estimates made in Sect. 4.2.

We found a relevant MIR excess only for two stars, RasTyc 0013+7702 and RasTyc 2320+7414 (V395 Cep), which behave as class II IR sources. This classification agrees with their H $\alpha$  profiles, which are typical of CTTS. In addition, another star in Cepheus, namely RasTyc 0000+7940 (#1) displays a small MIR excess (class III), in line with its weak-line T Tauri star (WTTS) nature.

#### 4.8. Kinematics of the very young sources

The availability of accurate radial velocities and the *Gaia* DR1 TGAS parallaxes and proper motions (Gaia Collaboration 2016) allowed us to calculate the

galactic space-velocity components for most of the sources investigated in the present paper. We used the outline of Johnson & Soderblom (1987) to compute the velocity components,  $U_{\odot}$ ,  $V_{\odot}$ , and  $W_{\odot}$  and their uncertainties, which we report in a heliocentric, left-handed coordinate system, where  $U_{\odot}$  is directed towards the galactic anti-center.

Space-velocity components are of great importance to assign membership to a known stellar kinematic group (SKG). We show in Fig. 10 the  $(U_{\odot}, V_{\odot})$  and  $(V_{\odot}, W_{\odot})$  diagrams for the *PMS-like* stars, along with the average position of the five major young SKGs discussed in Montes et al. (2001b), namely the IC 2391 supercluster ( $\sim 50$  Myr), the Local association or Pleiades group ( $\sim 20$ – $150$  Myr Asiain et al. 1999; Montes et al. 2001b), the Castor group ( $\sim 200$  Myr), the Ursa Major (UMa) group ( $\sim 300$  Myr), and the Hyades supercluster ( $\sim 600$  Myr). Additional SKGs and loose associations, such as TW Hya (3–15 Myr),  $\beta$  Pic (10–24 Myr), Octans (20–40 Myr), AB Dor (50–150 Myr), and Coma Ber ( $\sim 400$  Myr) have been also considered (e.g., Zuckerman et al. 2001, 2004, 2013; Riedel et al. 2017, and references therein). The locus of the young-disc population (YD; age  $\leq 2$  Gyr) as defined by Eggen (1996, and references therein) is shown as well.

We note that the two lithium-rich giant candidates, #17 and #27, lie outside the YD locus, which confirms their nature of evolved stars.

Most of the *PMS-like* sources have  $U_{\odot}$ ,  $V_{\odot}$ , and  $W_{\odot}$  compatible with the Pleiades and/or Castor and/or TW Hya SKGs, which are the youngest SKGs considered in this study. However, #12, #16, #24, and #29, are located far outside of the YD locus in the  $(U_{\odot}, V_{\odot})$  plane. With the exception of #16, for which we measured the same RV in the two spectra within the errors, the other three sources have been observed only once. Therefore we cannot exclude that they are SB1 systems observed far from the conjunctions, so that their barycentric RV could be very different from the value measured by us. This would lead to wrong space velocity components.

Some notes about the possible association to the aforementioned SKGs are given in Appendix B.

## 5. Summary

We have presented the results of a high-resolution spectroscopic survey of optical counterparts of X-ray sources. Our targets were selected from the *RasTyc* sample (Guillout et al. 1999), which is obtained by the cross-correlation of the TYCHO and RASS catalogs. In particular, we have measured radial (RV) and projected rotational velocities ( $v \sin i$ ) for 443 stars, most of which are optically faint *RasTyc* sources ( $V \geq 9.5$  mag). We found 114 double-lined spectroscopic binaries (SB2) and 12 triple systems among these sources.

For the remaining targets, including 38 single-lined binaries (SB1), we were also able to determine the atmospheric parameters ( $T_{\text{eff}}$ ,  $\log g$ , and  $[\text{Fe}/\text{H}]$ ), lithium

abundance, and the level of chromospheric activity as measured by the ratio of  $H\alpha$  and bolometric luminosity. The trigonometric parallax from the TGAS catalog (Gaia Collaboration 2016) or from the catalog of van Leeuwen (2007) is also available for 263 of the stars with measured parameters. The position of these stars in the HR diagram is in very good agreement with the gravities derived with our analysis code (ROTFIT).

The equivalent width of the  $\text{Li I} \lambda 6707.8$  and the lithium abundance allowed us to perform an age classification of our targets that were divided in five classes, *PMS-like* (14 %), *Pleiades-like* (13 %), *UMa-like* (34 %), *Hyades-like* (19 %), and *Old* stars (20 %). The higher percentage of *PMS-like* and *Pleiades-like* stars found in comparison with the bright *RasTyc* sample is likely the result of the greater distances reached in the present work for objects optically fainter. Indeed, at larger distances, the X-ray brighter sources (younger stars) are more easily detected compared to less active (older) stars.

We have investigated in more detail the 44 *PMS-like* candidates and found that two of them must be rejected from this class, because their position in the HR diagram, their spectral classification, and their space velocity components suggest they are lithium-rich giants. The remaining *PMS-like* sources display a rather high level of chromospheric activity,  $\log(R'_{H\alpha}) > -5.0$  and, with few exceptions, are located in the domain of the  $(V_{\odot}, U_{\odot})$  plane occupied by young-disk stars. The two objects with the highest values of  $R'_{H\alpha}$  (#2 and #31) are very close to the dividing line between chromospheric sources and accreting stars defined by Frasca et al. (2015). They both display a broad and double-peaked  $H\alpha$  profile that is typical of CTTS, as well as a remarkable IR excess in their SEDs.

Another important outcome of this survey is the presence of a significant fraction of giant and subgiant stars ( $\sim 12$  %). Half of them also display a high activity level, comparable to that of some *PMS-like* sources, and a rather rapid rotation, which could be the result of a particular evolutionary path or the effect of an undetected binarity (spin-orbit synchronization). Some of these evolved stars ( $\sim 36$  %) are also rich in lithium ( $A(\text{Li}) > 1.4$ ).

**Acknowledgements.** This paper is dedicated to the memory of our colleague and friend Rubens Freire Ferrero. We thank the anonymous referee for useful suggestions. We are grateful to the TNG staff and, particularly, to Aldo F. Fiorenzano and Antonio Magazzù for conducting the service observations with SARG. We also thank the night assistants of the OHP and OAC observatories for their support and help with the observations. Support from the Italian *Ministero dell'Istruzione, Università e Ricerca* (MIUR) is also acknowledged. D.M. acknowledges financial support from the Universidad Complutense de Madrid (UCM) and the Spanish Ministry of Economy and Competitiveness (MINECO) from project AYA2016-79425-C3-1-P. This research made use of SIMBAD and VIZIER databases, operated at the CDS, Strasbourg, France. This publication uses ROSAT data. This publication makes use of data products from the Wide-field

Infrared Survey Explorer, which is a joint project of the University of California, Los Angeles, and the Jet Propulsion Laboratory/California Institute of Technology, funded by the National Aeronautics and Space Administration. This work has made use of data from the European Space Agency (ESA) mission *Gaia* (<https://www.cosmos.esa.int/gaia>), processed by the *Gaia* Data Processing and Analysis Consortium (DPAC, <https://www.cosmos.esa.int/web/gaia/dpac/consortium>). Funding for the DPAC has been provided by national institutions, in particular the institutions participating in the *Gaia* Multilateral Agreement.

## References

- Abrahamyan, H. V., Mickaelian, A. M., & Knyazyan, A. V. 2015, *Astronomy and Computing*, 10, 99
- Alcalá, J. M., Nanara, C. F., Natta, A., et al. 2017, *A&A*, 600, A20
- Ammons, S.M., Robinson, S.E., Strader, J., et al. 2006, *ApJ*, 638, 1004
- Appenzeller, I., Thiering, I., Zickgraf, F.-J., et al. 1998, *ApJS*, 117, 319
- Asiain, R., Figueras, F., & Torra, J. 1999, *A&A*, 350, 434
- Bally, J. 2008, in *Handbook of Star Forming Regions*, Vol. I, ed. B. Reipurth, ASP Monograph Publications, 459
- Barrado y Navascués, D., De Castro, E., Fernández-Figueroa, M. J., Cornide, M., & García López, R. J. 1998, *A&A*, 337, 739
- Biazzo, K., Alcalá, J. M., Covino, E., et al. 2012a, *A&A*, 542, A115
- Biazzo, K., Alcalá, J. M., Covino, E., et al. 2012b, *A&A*, 547, A104
- Binks, A. S., Jeffris, R. D., & Maxted, P. F. L. 2015, *MNRAS*, 452, 173
- Bobylev, V.V., 2014, *Astrophysics*, 57, 583
- Boller, T., Freyberg, M. J., Truemper, J., et al. 2016, *A&A*, 588, A103
- Bonchikarev, N. G. 1984, *Ap&SS*, 138, 229
- Brandner, W., Alcalá, J. M., Kunkel, M., Moneti, A., & Zinnecker, H. 1996, *A&A*, 307, 121
- Cameron, A. G. W., & Fowler, W. A. 1971, *ApJ*, 164, 111
- Charbonnel, C. & Balachandran, S. C. 2000, *A&A*, 359, 563
- Christian, D. J., & Mathioudakis, M. 2002, *AJ*, 123, 2796
- Comerón, F., & Torra, J. 1997, *A&A*, 281, 35
- Cutri, R. M., Skrutskie, M. F., Van Dyk, S., et al. 2003, *2MASS All-Sky Catalog of Point Sources*, University of Massachusetts and Infrared Processing and Analysis Center (IPAC/California Institute of Technology)
- Cutri, R. M., et al. 2013, *AllWISE Data Release*, IPAC/Caltech University of Massachusetts and Infrared Processing and Analysis Center (IPAC/California Institute of Technology)
- da Silva, L., Torres, C. A. O., de La Reza, R., et al. 2009, *A&A*, 508, 833
- de la Reza, R., Drake, N. A., & da Silva, L. 1996, *ApJ*, 456, 115
- de la Reza, R., & Drake, N. A. 2012, *ASP Conf. Ser.*, 464, 51
- Desidera, S., Covino, E., Messina, S., et al. 2105, *A&A*, 573, A126
- Dias, W. S., Monteiro, H., Caetano, T. C., et al. 2014, *A&A*, 564, A79
- Dragomir, D., Roy, P., & Rutledge, R. E. 2007, *AJ*, 133, 2495
- Drake, N. A., de la Reza, R., da Silva, L., & Lambert, D. L. 2002, *AJ*, 123, 2703
- Droege, T. F., Richmond, M. W., Sallman, M. P., & Creager, R. P. 2006, *PASP*, 118, 1666
- Eggen, O. J. 1996, *AJ*, 112, 1595
- Elias, F., Alfaro, E. J., & Cabrera-Caño, J. 2009, *MNRAS*, 397, 2
- Elliott P., Bayo, A., Melo, C. H. F., et al. 2014, *A&A*, 568, A26
- Elliott P., Huelamo N., Bouy, H., et al. 2015, *A&A*, 580, A88
- Fabricius, C., Høg, E.; Makarov, V. V., et al. 2002, *A&A*, 384, 180
- Fekel, F. C. 1997, *PASP*, 109, 514
- Fekel, F. C., & Balachandran, S. 1993, *ApJ*, 403, 708
- Feigelson, E. D. 1996, *ApJ*, 468, 306
- Folsom C. P., Petit, P., Bouvier, J., et al. 2016, *MNRAS*, 457, 580
- Frasca, A., & Catalano, S. 1994, *A&A*, 284, 883
- Frasca, A., Freire Ferrero, R., Marilli, E., & Catalano, S. 2000, *A&A*, 364, 179
- Frasca, A., Guillout, P., Marilli, E., et al. 2006, *A&A*, 454, 301
- Frasca, A., Covino, E., Spezzi, L., et al. 2009, *A&A*, 508, 1313
- Frasca, A., Biazzo, K., Kővári, Zs., Marilli, E., & Çakırlı, Ö. 2010, *A&A*, 518, 48
- Frasca, A., Fröhlich, H.-E., Bonanno, A., et al. 2011, *A&A*, 523, A81
- Frasca, A., Biazzo, K., Lanzafame, A. C., et al. 2015, *A&A*, 575, A4
- Fröhlich, H.-E. 2007, *Astron. Nachr.*, 238, 1037
- Fröhlich, H.-E., Frasca, A., Catanzaro, G., et al. 2011, *A&A*, 543, A146
- Jeffries, R. D. 1995, *MNRAS*, 273, 559
- Gaia Collaboration, Brown, A. G. A., Vallenari, A., Prusti, T. et al. 2016, *A&A*, 595, A2
- Galicher R., Marois C., Macintosh B., et al. 2016, *A&A*, 594, A63
- Gehrels, N., & Chen, W. 1993, *Nature*, 361, 706
- Gillet, D., Burnage, R., Kohler, D. et al. 1994, *A&AS*, 108, 181
- Girardi, L., Bressan, A., Bertelli, G., & Chiosi, C. 2000, *A&AS*, 141, 371
- Glebocki, R., & Gnacinski, P. 2005, *The Catalogue of Rotational Velocities of Stars*, ESA, SP-560, 571
- Guillout, P., Sterzik, M. F., Schmitt, J. H. M. M. et al. 1998a, *A&A*, 334, 540
- Guillout, P., Sterzik, M. F., Schmitt, J. H. M. M. et al. 1998b, *A&A*, 337, 113
- Guillout, P., Schmitt, J. H. M. M., Egret, D., et al. 1999, *A&A*, 351, 1003

- Guillout, P., & Motch, C. 2003, *Astron. Nachr.*, 324, 81
- Guillout, P., Hérent, O., & Motch, C. 2006, in: A. Wilson (ed.), *The X-ray Universe 2005*, ESA SP-604, 89
- Guillout, P., Klutsch, A., Frasca, A., et al. 2009, *A&A*, 504, 829 (Paper I)
- Guillout, P., Frasca, A., Klutsch, A., Marilli, E., & Montes, D. 2010, *A&A*, 520, 94
- Gray, D. F. 1992, The Observation and Analysis of Stellar Photospheres, 2<sup>nd</sup> ed. (Cambridge University Press)
- Haakonsen, C. B., & Rutledge, R. E. 2009, *ApJS*, 184, 138
- Hauschildt, P. H., Allard, F., & Baron, E. 1999, *ApJ*, 512, 377
- Helou, G., & Walker, D. W. 1995, *yCat*, 7073, 0
- Henden, A. A., Levine, S., Terrell, D., & Welch, D. L. 2015, APASS - The Latest Data Release. American Astron. Soc. meeting, 225, 336
- Henden, A. A., Guarro-Flo, J., & Garcia-Melendo, E. 1999, *Inf. Bull. Var. Stars*, 4807
- Herbig, G. H. 1977, *ApJ*, 214, 747
- Herbig, G. H. 1985, *ApJ*, 289, 269
- Herbig, G. H., Bell, K. R. 1988, *Lick Observatory Bull.* No. 1111
- Hoogerwerf, R. 2000, *MNRAS*, 313, 43
- Høg, E., Fabricius, C., Makarov, V.V., et al. 2000, *A&A*, 355, L27
- Horch, E. P., Van Belle, G. T., Davidson, J. W. Jr., et al. 2015, *AJ*, 150, 151
- Ishihara, D., Onaka, T., Kataza, H., et al. 2010, *A&A*, 514, A1
- Jeffries, R. D. 1995, *MNRAS*, 273, 559
- Jenkins, J. S., Murgas, F., Rojo, P., et al. 2011, *A&A*, 531, A8
- Johnson, D. R. H. & Soderblom, D. R. 1987, *AJ*, 93, 864
- Katz, D., Soubiran, C., Cayrel, R., Adda, M., & Cautain, R. 1998, *A&A*, 338, 151
- Kharchenko, N. V., Piskunov, A. E., Roeser, S., Schilbach, E., & Scholz, R.-D. 2004, *Astron. Nachr.*, 325, 740
- Kiraga, M. 2012, *Acta Astron.*, 62, 67
- Kiraga, M., & Stepień K. 2013, *Acta Astron.*, 63, 53
- Klutsch, A., Frasca, A., Guillout, P., et al. 2008, *A&A*, 490, 737
- Kun, M., Balog, Z., Kenyon, S. J., Mamajek, E. E., & Gutermuth, R. A. 2009, *ApJS*, 185, 451
- Kunder, A., Kordopatis, G., Steinmetz, M., et al. 2017, *AJ*, 153, 75
- Lada, C. J. 1987, in Star forming regions, IAU Symp., 115, 1
- Li, J. Z. 2004, *Chinese J. Astron. Astrophys.*, 4, 258
- Li, J. Z., Hu, J. Y. 1998, *A&AS*, 132, 173
- López-Santiago, J., Montes, D., Gálvez-Ortiz, M. C., et al. 2010, *A&A*, 514, 97
- Luck, R. E., & Heiter U. 2007, *AJ*, 133, 2464
- Luhman, K. L., Stauffer, J. R., & Mamajek, E. E. 2005, *ApJ*, 628, L69
- Makarov, V. V. 2006, *AJ*, 131, 2967
- Marilli, E., Catalano, S., & Frasca, A. 1997, *Mem. Soc. Astron. Ital.*, 68, 895
- Martínez-Arnáiz, R., López-Santiago, J., Crespo-Chacón, I., & Montes, D. 2011, *MNRAS*, 414, 2629
- Mason, B.D., Wycoff, G.L., Hartkopf, W.I., Douglass, G.G., & Worley, C.E. 2001, *AJ*, 122, 3466
- Messina, S., Desidera, S., Turatto, M., Lanzafame, A. C., & Guinan, E. F. 2010, *A&A*, 520, 15
- Metchev, S. A., & Hillenbrand, L. A. 2009, *ApJS*, 181, 62
- Moultaka, J., Illovaisky, S. A., Prugniel, P., & Soubiran, C. 2004, *PASP*, 116, 693
- Monet, D. G., Levine, S. E., Canzian, B., et al. 2003, *AJ*, 125, 984
- Montes, D., Fernández-Figueroa, M. J., De Castro, E., & Cornide, M. 1995, *A&AS*, 109, 135
- Montes, D., López-Santiago, J., Fernández-Figueroa, M. J., & Gálvez, M. C. 2001a, *A&A*, 379, 976
- Montes, D., López-Santiago, J., Gálvez, M. C., et al. 2001b, *MNRAS*, 328, 45
- Motch, C., Guillout, P., Haberl, F., et al. 1997, *A&A* 318, 111
- Motch, C., Guillout, P., Haberl, F., et al. 1998, *A&AS*, 132, 341
- Muñoz Bermejo, J., Asensio Ramos, A., & Allende Prieto, C. 2013, *A&A*, 553, A95
- Neuhäuser, R., Torres, G., Sterzik, M. F., & Randich, S. 1997, *A&A*, 325, 647
- Nidever, D. L., Marcy, G. W., Butler, R. P., Fischer, D. A., & Vogt, S. S. 2002, *ApJS*, 141, 503
- Nordström, B., Mayor, M., Andersen, J., et al. 2004, *A&A*, 418, 989
- Norton, A. J., Wheatley, P. J., West, R. G., et al. 2008, *A&A*, 467, 785
- Pallavicini, R., Randich, S., & Giampapa, M. S. 1992, *A&A*, 253, 185
- The Hipparcos and TYCHO Catalogues, 1997, ESA SP-1200
- Pecaut, M. J., & Mamajek, E. E. 2013, *ApJS*, 208, 9
- Pigulski, A., Pojman'ski, G., Pilecki, B. & Szczygiel, D. M. 2009, *Acta Astron.*, 59, 33
- Piskunov, A. E., Kharchenko, N. V., Schilbach, E., et al. 2008, *A&A*, 487, 557
- Prosser, C. F. 1992, *AJ*, 103, 488
- Queloz, D., Allain, S., Mermilliod, J.-C., Bouvier, J., & Mayor, M. 1998, *A&A*, 335, 183
- Riedel, A. R., Blunt, S. C., Lambrides, E. L., et al. 2017, *AJ*, 153, 95
- Rucinski, S. M., Pribulla, T., Mochnacki, S. W., et al. 2008, *AJ*, 136, 586
- Samus, N. N., Durlevich, O. V., Kazarovets, E. V., et al. 2012, GCVS database, Version 2012Jan, CDS B/gcvs
- Savanov, I. S. 2011, *Astron. Rep.*, 55, 801
- Sestito, P. & Randich S. 2005, *A&A*, 442, 615
- Siess, L., Dufour, E., & Forestini, M. 2000, *A&A*, 358, 593
- Soderblom, D. R., Oey, M. S., Johnson, D. R. H., & Stone, R. P. S. 1990, *AJ*, 99, 595
- Soderblom, D. R., Stauffer, J. R., Hudon, J. D., & Jones, B. F. 1993a, *ApJS*, 85, 315
- Soderblom, D. R., Pilachowski, C. A., Fedel, S. B., & Jones, B. F. 1993b, *AJ*, 105, 2299

- Soderblom, D. R., Jones, B. F., Balachandran, S., et al.  
1993c, AJ, 106, 1059
- Soubiran C., Le Campion J.-F., Cayrel de Strobel G., & Caillo A. 2010, A&A515, A111
- Stauffer, J. R., Hartmann, L. W., Prosser, C. F., et al.  
1997, ApJ, 479, 776
- Sterzik, M. F., Alcalá, J. M., Neuhaeuser, R., & Schmitt, J. H. M. M. 1995, A&A, 297, 418
- Skrutskie, M. F., Cutri, R. M., Stiening, R., et al. 2006,  
AJ, 131, 1163
- Torres, C. A. O., Quast, G. R., da Silva, L., et al. 2006,  
A&A, 460, 695
- Tachihara, K., Neuhauser, R., Kun, M., & Fukui, Y. 2005,  
A&A, 437, 919
- Udry, S., Mayor, M., & Queloz, D. 1999, Precise Stellar  
Radial Velocities, IAU Colloq. 170, ed. J. B. Hearnshaw,  
& C. D. Scarfe, ASP Conf. Ser., 185, 367
- Uyama, T., Hashimoto, J., Kuzuhara, M., et al. 2017, AJ,  
153, 106
- van Leeuwen, F. 2007, A&A, 474, 653
- Voges, W., Aschenbach, B., Boller, T., et al. 1999, A&A,  
349, 389
- Watson, C. L., Henden, A. A., & Price, A. 2015, AAVSO  
International Variable Star Index VSX - CDS/ADC  
Collection of Electronic Catalogues
- White, R. J., & Basri, G. 2003, ApJ, 582, 1109
- White, R. J., Gabor, J. M., & Hillenbrand, L. A. 2007,  
AJ, 133, 2524
- Wright, E. L. Eisenhardt, P. R. M., Mainzer, A.K., et al.  
2010, AJ, 140, 1868
- Zacharias, N., Monet, D. G., Levine, S. E., et al. 2004,  
*American Astron. Soc. Meeting*, 205, #4815; *Bulletin  
of the American Astronomical Society*, Vol. 36, p.1418
- Zickgraf, F.-J., Engels, D., Hagen, H.-J., Reimers, D., &  
Voges, W. 2003, A&A, 406, 535
- Zickgraf, F.-J., Krautter, J. Reffert, S., et al. 2005, A&A,  
433, 151
- Zinnecker, H. 2008, in ESO: Star Formation Across the  
Milky Way Galaxy
- Zuckerman, B., Webb, R. A., Schwartz, M., & Becklin, E.  
E. 2001, ApJ, 549, L233
- Zuckerman, B., Song, I., & Bessell, M. S. 2004, ApJ, 613,  
L65
- Zuckerman, B., Vican, L., Song, I., & Schneider, A. 2013,  
ApJ, 778, 5

## Appendix A: The data

The data resulting from our analysis are listed in the following tables and are available in electronic format at the CDS.

**Table 3.** Very young stars and PMS candidates selected from the lithium content.

#	Name	RasTyc	$\alpha$ (2000) h m s	$\delta$ (2000) ° ' "	$C_{\text{rate}}^{\#}$ (ct/s)	Sp. Type	$T_{\text{eff}}$ (K)	$\log g$ (dex)	[Fe/H] (dex)	$A(\text{Li})$	$\log(R'_{H\alpha})$
#1	BD+78 853 <sup>†</sup>	0000+7940	00 00 41.14	+79 40 39.9	0.106	G2V	5738	4.19	-0.03	3.28	-4.43
#2	TYC 4496-780-1 <sup>†,‡</sup>	0013+7702	00 13 40.52	+77 02 10.9	0.102	G0V	5924	4.14	-0.03	3.31	-3.33
#3	TYC 4500-1478-1 <sup>†</sup>	0038+7903	00 38 06.03	+79 03 20.7	0.133	K1V	5160	4.30	-0.06	3.24	-3.87
#4	BD+78 19 <sup>*,*</sup>	0039+7905	00 39 40.13	+79 05 30.8	0.077	G5V	5444	4.14	-0.11	3.05	-4.57
#5	TYC 3266-1767-1	0046+4808	00 46 53.09	+48 08 45.2	0.278	K2V	5067	4.21	-0.09	3.58	-4.02
#6	BD+49 646	0222+5033	02 22 33.82	+50 33 37.8	0.491	K2V	5094	4.27	-0.12	2.84	-3.90
#7	TYC 3695-2260-1	0230+5656	02 30 44.81	+56 56 13.0	0.051	G1V	5874	4.31	-0.03	3.46	-4.47
#8	TYC 2338-35-1	0252+3728	02 52 24.71	+37 28 52.0	0.048	G1.5V	5784	4.35	0.02	4.02	-4.44
#9	TYC 4321-507-1	0300+7225	03 00 14.67	+72 25 41.4	0.084	K2V	5079	4.59	-0.01	2.94	-4.00
#10	Cl Melotte 20 94	0311+4810	03 11 16.82	+48 10 36.9	0.092	G1.5V	5856	4.35	0.02	3.39	-4.24
#11	TYC 3710-406-1	0316+5638	03 16 28.11	+56 38 58.1	0.084	K1V	5208	4.50	-0.05	2.81	-4.18
#12	TYC 3715-195-1	0323+5843	03 23 07.08	+58 43 07.4	0.148	K1V	5212	4.48	-0.07	2.97	-3.92
#13	Cl Melotte 20 935	0331+4859	03 31 28.98	+48 59 28.6	0.081	G1.5V	5816	4.30	-0.10	3.24	-4.05
#14	TYC 2876-1944-1	0359+4404	03 59 16.70	+44 04 17.1	0.264	K1V	5235	4.50	-0.06	3.36	-3.62
#15	TYC 3375-720-1	0616+4516	06 16 46.95	+45 16 03.1	0.097	G2V	5739	4.21	0.11	3.47	-3.83
#16	TYC 3764-338-1	0621+5415	06 21 56.92	+54 15 49.0	0.426	G2V	5719	4.14	-0.08	2.98	-4.15
#17	HD 234808 <sup>*</sup>	1908+5018	19 08 14.03	+50 18 49.6	0.045	G8III-IV	5223	3.39	-0.37	3.69	-4.20
#18	KIC 8429280 <sup>•</sup>	1925+4429	19 25 01.98	+44 29 50.7	0.254	K2V	5055	4.41	-0.02	2.96	-3.96
#19	BD-03 4778	2004-0239	20 04 49.35	-02 39 19.7	0.175	K1V	5183	4.39	-0.02	3.33	-4.26
#20	HD 332091	2016+3106	20 16 57.83	+31 06 55.6	0.167	K1V	5087	4.57	0.01	2.88	-3.72
#21	TYC 2694-1627-1	2036+3456	20 36 16.87	+34 56 46.1	0.037	G1V	5832	4.33	-0.01	3.30	-4.33
#22	TYC 2178-1225-1	2039+2644	20 39 40.81	+26 44 48.4	0.227	K1V	5149	4.30	-0.08	2.80	-4.19
#23	BD+68 1182	2106+6906	21 06 21.74	+69 06 41.0	0.114	G1.5V	5828	4.31	-0.01	3.39	-4.31
#24	TYC 3589-3858-1	2120+4636	21 20 55.42	+46 36 12.4	0.142	G1.5V	5699	4.36	0.04	3.07	-4.29
#25	BD+76 857a	2223+7741	22 23 18.87	+77 41 57.7	0.114	G1.5V	5745	4.29	-0.04	3.60	-4.28
#26	TYC 1154-1546-1	2233+1040	22 33 00.37	+10 40 34.3	0.053 <sup>°</sup>	G1.5V	5544	4.39	0.03	3.65	-3.44
#27	HD 214995 <sup>**</sup>	2241+1430	22 41 57.40	+14 30 59.2	0.094	K0III	4678	2.77	-0.04	3.61	-6.11
#28	BD+17 4799	2244+1754	22 44 41.49	+17 54 19.0	0.835	K1V	5161	4.41	-0.02	2.91	-4.14
#29	TYC 3992-349-1	2246+5749	22 46 13.19	+57 49 58.0	0.034	G2V	5752	4.32	-0.05	3.33	-4.31
#30	TYC 2751-9-1	2307+3150	23 07 24.83	+31 50 14.1	0.462	K4V	4774	4.58	0.05	2.48	-4.15
#31	V395 Cep	2320+7414	23 20 52.07	+74 14 07.1	0.035	K0IV	5093	3.58	-0.02	3.68	-3.27
#32	TYC 584-343-1	2321+0721	23 21 56.36	+07 21 33.0	0.067	K0V	5207	4.24	0.01	3.20	-4.25
#33	TYC 4606-740-1 <sup>○</sup>	2351+7739	23 51 17.29	+77 39 35.3	0.169	K1V	5146	4.52	-0.07	3.51	-3.84
a	TYC 2282-1396-1 <sup>⊕</sup>	0106+3306	01 06 18.71	+33 06 01.9	0.161	G4V	5606	4.31	-0.14	3.11	-4.16
b	BD+42 636	0249+4255	02 49 54.69	+42 55 27.1	0.036	G1.5V	5825	4.24	-0.02	3.07	-4.52
c	TYC 3325-98-1	0344+5043	03 44 34.50	+50 43 47.5	0.074	K0V	5349	4.40	-0.06	3.01	-3.99
d	TYC 2949-780-1	0646+4147	06 46 46.74	+41 47 12.2	0.043	G2V	5696	4.16	0.13	3.29	-4.60
e	TYC 2087-1742-1	1731+2815	17 31 03.33	+28 15 06.1	0.305	K1V	5169	4.47	-0.02	2.91	-3.98
f	KIC 7985370 <sup>⊗</sup>	1956+4345	19 56 59.73	+43 45 08.2	0.036	G1.5V	5815	4.24	-0.05	3.05	-4.50
g	BD+35 4198	2038+3546	20 38 17.71	+35 46 33.3	0.058	G1.5V	5895	4.23	0.01	3.00	-4.86
h	BD+39 4490	2114+3941	21 14 55.24	+39 41 11.9	0.099	G1.5V	5930	4.27	-0.02	3.01	-4.75
i	TYC 3198-1809-1	2203+3809	22 03 49.83	+38 09 42.9	0.033	G5IV-V	5678	4.28	0.04	3.06	-4.95
j	TYC 576-1220-1	2308+0000	23 08 50.46	+00 00 52.8	0.104	G2V	5620	4.38	-0.00	3.25	-3.91
k	TYC 4283-219-1	2324+6215	23 24 40.37	+62 15 51.1	0.037	F9V	6011	3.97	-0.21	3.12	-4.84

<sup>#</sup> X-ray count rate from the second ROSAT all-sky survey source catalog (2RXS, Boller et al. 2016).<sup>†</sup> PMS star in Cepheus discovered by Guillout et al. (2010).<sup>‡</sup> Close visual pair ( $\rho = 1.^{\prime\prime}41$ ,  $\Delta V \simeq 2.2$  mag, Fabricius et al. 2002). Parameters of the brighter component.<sup>\*</sup> SB2 system composed of two nearly identical stars. Parameters derived from spectra taken close to the conjunctions.<sup>•</sup> Very young star in the *Kepler* field discovered by Frasca et al. (2011).<sup>◦</sup> X-ray count rate from the ROSAT All-Sky Bright Source Catalog (1RXS, Voges et al. 1999).<sup>○</sup> Close visual pair ( $\rho = 0.^{\prime\prime}82$ ,  $\Delta V \simeq 0.15$  mag, Fabricius et al. 2002).<sup>⊕</sup> Close visual pair ( $\rho = 0.^{\prime\prime}85$ ,  $\Delta V \simeq 0.29$  mag, Fabricius et al. 2002).<sup>⊗</sup> Very young star in the *Kepler* field discovered by Fröhlich et al. (2012).<sup>\*</sup> Discarded as PMS candidate on the basis of spectral classification and the position in the HR diagram. Likely lithium-rich giant.<sup>\*\*</sup> Discarded as PMS candidate on the basis of spectral classification and the very low H $\alpha$  flux. Lithium-rich giant.

**Table 4.** Lithium-rich giant candidates.

Name	RasTyc	Sp. Type	$T_{\text{eff}}$ (K)	$\log g$ (dex)	[Fe/H] (dex)	$A(\text{Li})$	$\log(R'_{H\alpha})$	$v \sin i$ (km s $^{-1}$ )
TYC 3676-2444-1	0106+5729	G8III	5158	3.40	-0.05	1.46	-4.22	9.1
TYC 4319-714-1*	0222+7204	K0III-IV	4866	3.01	-0.09	1.69	-4.06	22.3
TYC 4364-1262-1*,†	0712+7021	K1IV	5012	2.96	-0.03	1.83	-3.97	10.3
BD+65 601	0755+6509	K0IV	5085	3.44	-0.07	2.12	-4.35	5.0
TYC 3501-626-1*,◊	1702+4713	K0IV	5031	3.38	-0.05	1.95	-3.55	15.0
BD+06 3372a*	1714+0623	G9III	4839	2.94	-0.10	1.47	-3.96	13.0
BD+02 3384*	1741+0228	G9III	4840	3.12	-0.12	1.56	-4.23	29.3
HD 234808	1908+5018	G8III-IV	5223	3.39	-0.37	3.69	-4.20	8.1
BD-04 5118*	2025-0429	K0III-IV	4943	3.22	-0.05	1.47	-3.63	9.0
BD+48 3149•	2030+4852	K1III	4667	2.60	-0.06	1.41	-5.20	54.1
HD 205173*	2132+3604	K0IV	5057	3.20	0.02	1.72	-5.01	4.1
HD 214995	2241+1430	K0III	4678	2.77	-0.04	3.61	-6.11	5.3
HD 220338*,†,•	2323-0635	K1III-IV	4755	2.87	-0.10	1.43	-3.66	26.8
TYC 3638-993-1	2348+4615	G8III	4961	2.92	-0.03	1.46	...	3.4

\* Rotationally variable star (Watson et al. 2015; Kiraga &amp; Stepień 2013).

† SB1.

◊ Small-amplitude secondary peak in the CCF. Likely SB2 with a faint component.

• Likely still undergoing the lithium dilution process.

**Table 5.** Comparison with SACY parameters for single stars and SB1 systems.

RasTyc	Sp. Type/ $T_{\text{eff}}$ /(K)		$v \sin i$ (km s $^{-1}$ )		$W_{\text{Li}}$ (mÅ)		RV (km s $^{-1}$ )		Notes
	SACY	Present	SACY	Present	SACY	Present	SACY	Present	
0051-1306	G2V	G1V	...	4.5	50	27	3.4	5.10	
0242+3837	4917	5071	6.0	6.4	146	132	-3.46	-3.53	
1959-0432	5630	5752	9.0	9.4	140	126	-19.41	-18.69	
2004-0239	5083	5183	8.0	9.0	290	298	-16.46	-15.92	
2118-0631	K1IV	K1V	...	20.9	40	48	-23.3	22.82	SB1
2155-0947	K0V	G1.5V	...	44.4	0	39	-20.0	-34.35	SB1
2157-0753	K2IV	K1V	...	28.2	0	17	6.7	14.05	SB1
2202-0406	K2V	K1V	...	8.0	200	179	0.3	5.07	SB1
2204+0236	K5V	K5V	...	10.8	0	18	-29.1	-26.36	
2236+0010	K0IV	G8IV-V	...	31.9	0	26	-3.3	7.95	SB1
2256+0235	K1IV	G1.5V	...	33.2	140	106	-9.4	-39.66	SB1
2308+0000	G8V	G2V	39.0	42.8	250	216	7.4	5.30	
2309-0225	K4Ve	K4V	13.3	12.1	200	195	-13.7	-12.16	
2321+0721	K0V	K0V	14.6	14.3	300	277	6.6	6.05	
2323-0635	G9IIIe	K1III-IV	26.4	26.8	105	87	13.4	4.06	SB1
2324-0733	G5V	G5IV-V	4.0	2.5	133	136	4.0	4.00	
2340-0402	G1V	G1V	33.6	36.2	150	128	17.7	15.73	SB1
2340-0228	G2V	G3V	31.0	29.6	0	0	66.3	-20.27	SB1
2352-1143	G1V	G1V	27.8	19.4	115	87	2.6	0.49	SB1

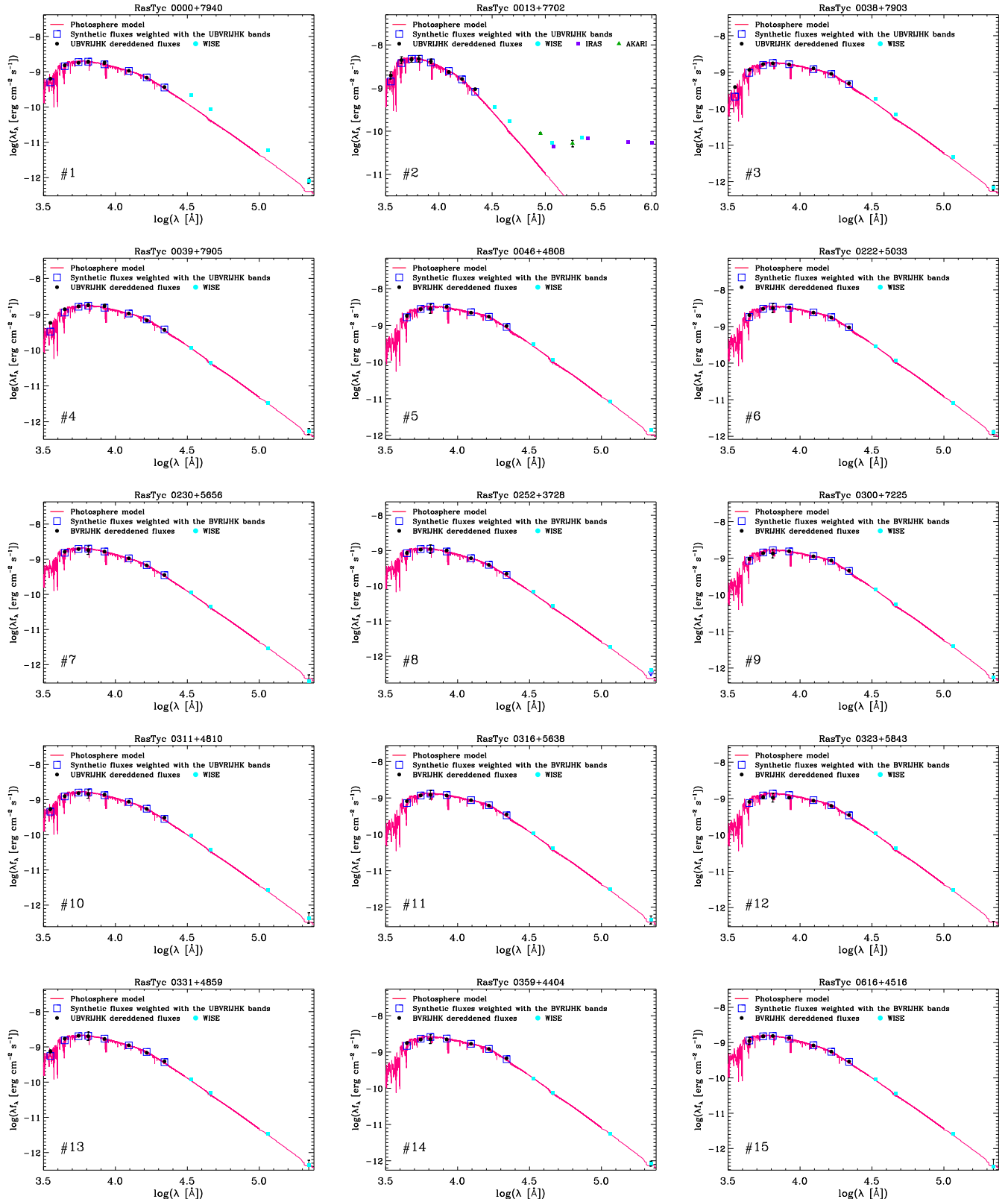


**Fig. 9.** Spectral energy distributions (dots) of the *PMS-like* sources and the two lithium-rich giants discussed in the paper. In each panel, the best fitting low-resolution NextGen spectrum (Hauschildt et al. 1999) is displayed by a continuous line. Mid-infrared fluxes are displayed with different as indicated in the legends of the plots.

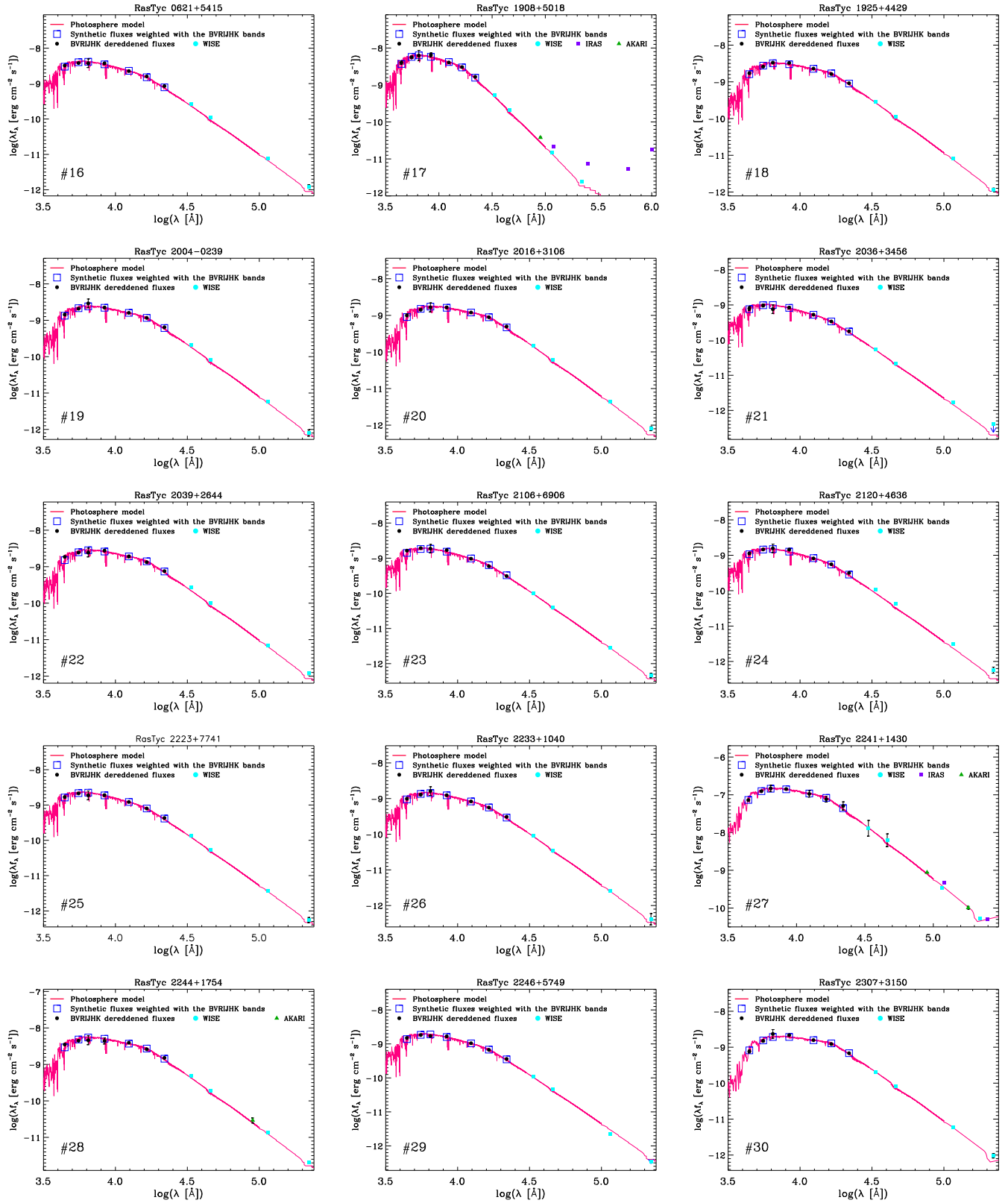


Fig. 9. continued.

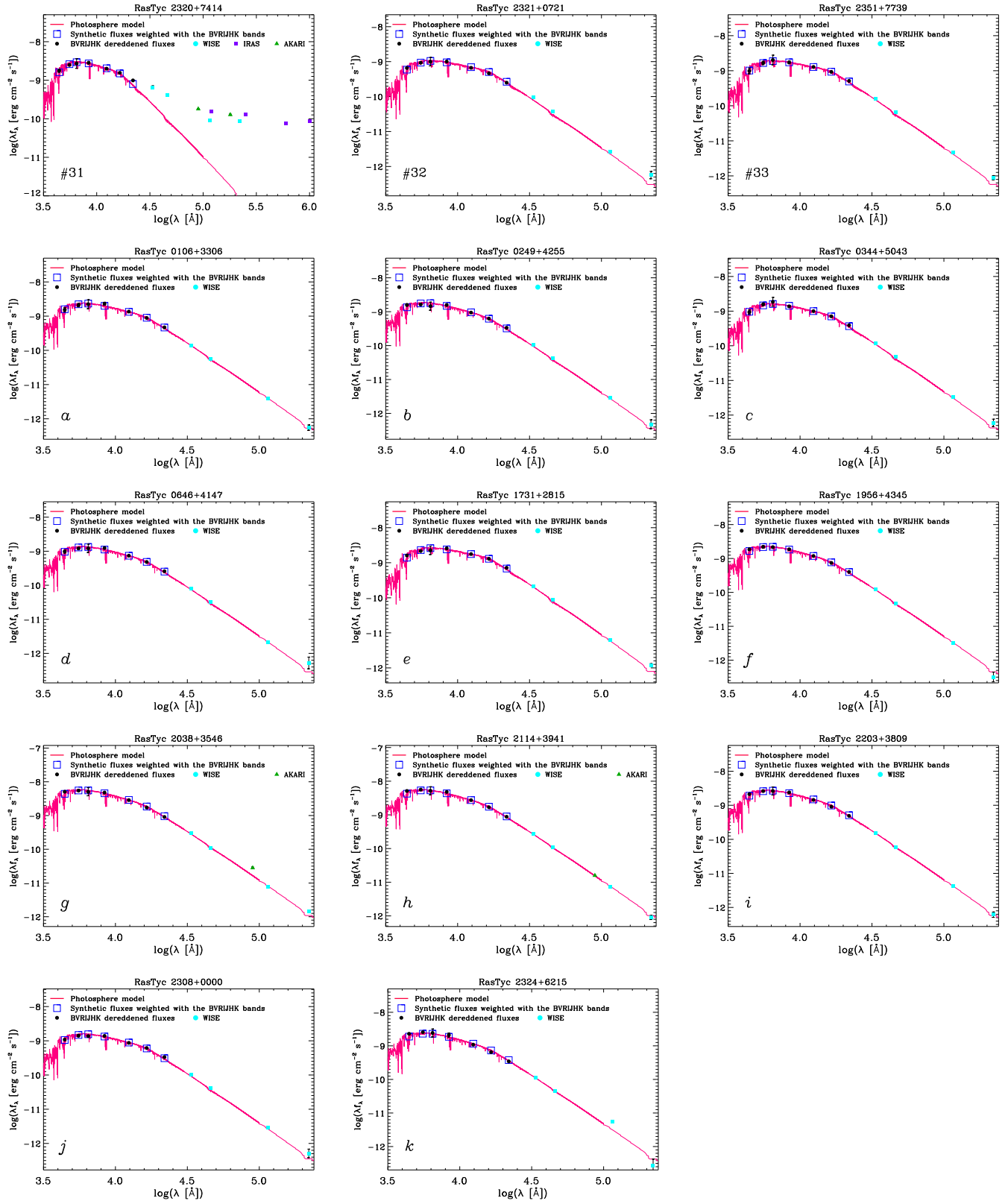
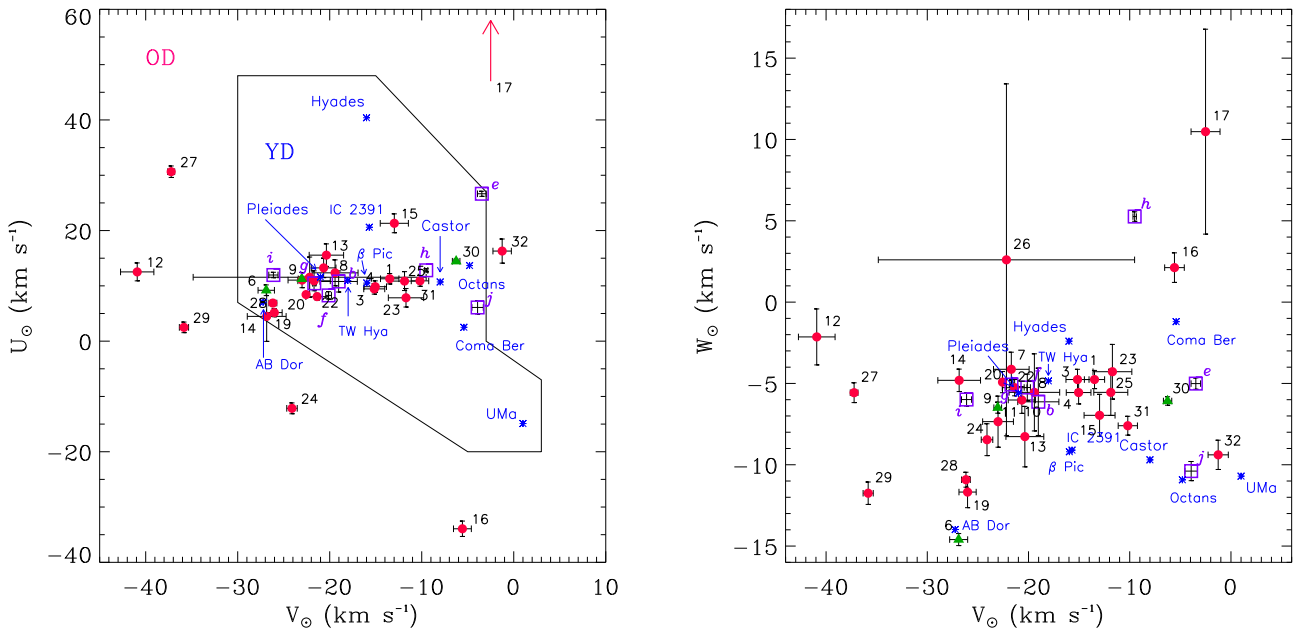


Fig. 9. continued.



**Fig. 10.** ( $V_{\odot}, U_{\odot}$ ) (left panel) and ( $V_{\odot}, W_{\odot}$ ) (right panel) diagrams for the *PMS-like* sources and the two lithium-rich giants discussed in the paper. The symbols are as in Fig. 5 and the labels are as in Table 3. The average velocity components (blue asterisks) of some young SKGs and the locus of the young-disc (YD) population (Eggen 1996) are also marked in the ( $V_{\odot}, U_{\odot}$ ) plane. The position of the source #17 ( $V_{\odot} = -2.5 \text{ km s}^{-1}$ ,  $U_{\odot} = 83.5 \text{ km s}^{-1}$ ) is out of the scale of the plot, as indicated by the red arrow.

**Table A.1.** Radial (RV) and rotational ( $v \sin i$ ) velocities for the single stars and SB1 binaries.

RasTyc Name	Name	$\alpha$ (2000) h m s	$\delta$ (2000) $^{\circ} \text{ } '$ ''	$V^a$ (mag)	$B-V^a$ (mag)	HJD (2450000+)	RV (km s $^{-1}$ )	$\sigma_{RV}$ (km s $^{-1}$ )	$v \sin i^b$ (km s $^{-1}$ )	$\sigma_{v \sin i}$ (km s $^{-1}$ )	$v \sin i^c$ (km s $^{-1}$ )	$\sigma_{v \sin i}$ (km s $^{-1}$ )	Instr. <sup>d</sup>
RasTyc0000+7940	BD+78 853	00 00 41.14	+79 40 39.9	10.27	0.704	2224.2896	-6.97	1.10	27.7	4.1	28.9	0.9	AU
RasTyc0000+7940	BD+78 853	00 00 41.14	+79 40 39.8	10.27	0.704	2234.4033	-7.46	2.93	50.3	1.6	...	...	AU
RasTyc0000+7940	BD+78 853	00 00 41.14	+79 40 39.8	10.27	0.704	5109.4942	-7.39	0.52	33.5	0.7	32.1	1.1	FR
RasTyc0000+7940	BD+78 853	00 00 41.14	+79 40 39.8	10.27	0.704	5110.5890	-7.64	0.49	33.5	1.1	32.4	0.9	FR
RasTyc0001+5212	BD+51 3761	00 01 42.66	+52 12 51.0	9.30	0.756	4347.6393	4.97	1.15	5.9	1.7	6.4	0.7	SA
RasTyc0004-0951	HD 225263	00 04 46.96	-09 51 53.4	10.37	0.831	2152.5741	-10.26	0.15	6.9	0.4	6.9	0.7	EL
RasTyc0008+5347	HD 330	00 08 04.62	+53 47 47.0	8.16	0.588	1801.5242	-41.96	0.15	3.2	0.2	2.8	0.8	EL
RasTyc0013+3946	BD+38 16	00 13 58.01	+39 46 02.3	9.55	0.711	2581.2959	-6.42	1.57	2.2	26.4	5.5	0.5	AU
RasTyc0013+3946	BD+38 16	00 13 58.01	+39 46 02.3	9.55	0.711	2584.3191	-7.65	1.53	< 5	...	5.7	0.6	AU
RasTyc0016+4104	NLTT 836	00 16 44.88	+41 04 08.6	9.48	1.111	2566.4812	1.35	1.45	4.3	10.4	4.9	1.4	AU
RasTyc0016+4104	NLTT 836	00 16 44.88	+41 04 08.6	9.48	1.111	2574.3135	1.65	1.53	< 5	...	0.5	0.5	AU
RasTyc0023+7503	TYC 4492-314-1	00 23 41.24	+75 03 16.9	10.24	1.122	4346.6353	-9.14	0.62	6.4	4.5	5.8	1.2	SA
RasTyc0032+7806	HD 2770	00 32 42.87	+78 06 47.4	9.58	0.722	2574.3489	-5.44	1.57	< 5	...	5.4	0.6	AU
RasTyc0032+7806	HD 2770	00 32 42.87	+78 06 47.4	9.58	0.722	2575.4397	-6.89	1.45	< 5	...	5.2	0.9	AU
RasTyc0033+5315°	TYC 3654-1907-1	00 33 55.90	+53 15 41.5	9.94	0.727	4347.6497	-9.04	1.05	2.7	1.6	2.6	0.8	SA
RasTyc0033+6126	TYC 4015-206-1	00 33 57.58	+61 26 33.3	9.89	0.803	2218.2630	44.34	2.77	...	...	130.0	15.0	AU
RasTyc0033+6126	TYC 4015-206-1	00 33 57.58	+61 26 33.3	9.89	0.803	2220.2727	40.63	4.58	...	...	111.0	10.0	AU
RasTyc0038+7903	TYC 4500-1478-1	00 38 06.03	+79 03 20.7	10.27	0.898	2988.2654	-8.75	1.31	8.9	6.5	10.0	1.1	AU
RasTyc0038+7903	TYC 4500-1478-1	00 38 06.03	+79 03 20.7	10.27	0.898	5076.5818	-9.44	0.24	14.7	1.5	12.6	2.7	FR
RasTyc0038+7903	TYC 4500-1478-1	00 38 06.03	+79 03 20.7	10.27	0.898	5111.5493	-9.13	0.23	14.5	2.1	12.3	2.7	FR
RasTyc0040+4343	V498 And	00 40 20.90	+43 43 25.4	9.91	1.000	4348.5851	-6.23	0.41	7.3	2.5	8.9	0.6	SA
RasTyc0041+3425	QT And	00 41 17.30	+34 25 17.2	9.97	0.909	2980.2471	4.71	1.51	22.9	2.8	23.9	1.8	AU
RasTyc0041+3425	QT And	00 41 17.30	+34 25 17.2	9.97	0.909	2982.3232	6.95	1.38	19.2	3.0	20.1	1.1	AU
RasTyc0045+7943	BD+78 22	00 45 22.95	+79 43 49.6	9.93	0.615	2988.3999	-7.03	1.50	21.6	2.3	22.1	1.1	AU
RasTyc0046+4808	TYC 3266-1767-1	00 46 53.09	+48 08 45.2	10.07	1.002	2984.2532	-4.64	1.42	15.4	3.7	15.0	0.6	AU
RasTyc0046+4808	TYC 3266-1767-1	00 46 53.09	+48 08 45.2	10.07	1.002	2985.2773	-4.54	1.41	18.0	2.4	19.7	0.8	AU
RasTyc0050+4651	TYC 3262-1820-1	00 50 38.30	+46 51 57.5	9.70	0.562	2579.3101	6.03	1.41	8.0	4.8	7.9	0.9	AU
RasTyc0050+4651	TYC 3262-1820-1	00 50 38.30	+46 51 57.5	9.70	0.562	2580.3601	6.59	1.37	7.4	6.8	7.5	1.0	AU
RasTyc0051+5425	TYC 3659-1102-1	00 51 03.32	+54 25 18.6	10.42	0.669	4346.6527	-24.15	1.40	35.9	2.9	43.3	6.7	SA
RasTyc0051+5425	TYC 3659-1102-1	00 51 03.32	+54 25 18.6	10.42	0.669	4346.6527	-24.15	1.40	35.9	2.9	43.3	6.7	SA
RasTyc0051+1306	HD 4940	00 51 17.10	-13 06 52.5	8.74	0.596	1801.6179	5.10	0.15	4.4	0.2	4.5	1.4	EL
RasTyc0100+5411	HD 232342	01 00 11.71	+54 11 01.7	9.54	0.590	2567.3870	0.24	1.37	16.5	2.8	15.8	1.4	AU
RasTyc0100+5411	HD 232342	01 00 11.71	+54 11 01.7	9.54	0.590	2574.3877	0.62	1.38	14.9	3.3	14.1	0.7	AU
RasTyc0103+5727	TYC 3676-2617-1	01 03 04.48	+57 27 17.7	10.53	1.048	4347.6641	-13.51	0.41	5.1	1.7	4.5	0.5	SA
RasTyc0106+3306 <sup>f</sup>	TYC 2282-1396-1	01 06 18.71	+33 06 01.9	10.26	1.092	2984.4043	12.60	1.41	18.8	2.4	21.8	4.2	AU
RasTyc0106+3306 <sup>f</sup>	TYC 2282-1396-1	01 06 18.71	+33 06 01.9	10.26	1.092	2986.3628	10.85	1.35	20.3	2.0	23.0	4.7	AU
RasTyc0106+5729	TYC 3676-2444-1	01 06 27.36	+57 29 44.1	10.58	1.120	4348.7071	-38.36	0.42	8.2	1.7	9.1	0.6	SA
RasTyc0116+3938	TYC 2804-13-1	01 16 50.67	+39 38 18.9	9.87	0.984	2259.3667	-3.44	1.57	< 5	...	5.0	1.3	AU
RasTyc0116+3938	TYC 2804-13-1	01 16 50.67	+39 38 18.9	9.87	0.984	2260.4512	-2.80	1.37	6.9	5.6	6.2	0.6	AU
RasTyc0137+3900	TYC 2814-1888-1	01 37 27.16	+39 00 08.6	10.42	0.684	2990.3098	-58.12	1.42	45.4	2.3	43.0	3.7	AU
RasTyc0140+4212	BD+41 324	01 40 28.78	+42 12 01.6	10.37	0.856	2982.3887	-28.05	1.37	18.1	3.2	18.3	0.6	AU
RasTyc0140+4212	BD+41 324	01 40 28.78	+42 12 01.6	10.37	0.856	2985.3267	-15.88	1.41	19.7	1.9	21.7	1.2	AU
RasTyc0140+4952	BD+49 435	01 40 51.62	+49 52 31.2	9.82	0.743	4348.6148	-23.25	0.53	12.2	1.8	11.7	0.6	SA
RasTyc0144+6508	TYC 4040-810-1	01 44 22.37	+65 08 47.2	9.80	0.904	4346.6770	-18.05	0.47	15.7	2.1	16.0	1.0	SA
RasTyc0156+4354	G 133-53	01 56 38.45	+43 54 46.8	9.64	0.904	2239.3672	-73.31	1.53	3.9	12.4	5.8	0.6	AU
RasTyc0156+4354	G 133-53	01 56 38.45	+43 54 46.8	9.64	0.904	2245.3728	-44.31	1.53	< 5	...	4.3	1.1	AU
RasTyc0158+3601	BD+35 380	01 58 26.62	+36 01 19.6	9.52	0.660	2668.2727	-7.56	1.53	4.0	12.6	8.6	0.9	AU
RasTyc0158+3601	BD+35 380	01 58 26.62	+36 01 19.6	9.52	0.660	2601.3772	-6.66	1.45	3.9	15.0	7.6	0.9	AU
RasTyc0218+4346	TYC 2842-24-1	02 18 13.49	+43 46 30.2	9.85	0.914	2235.3696	2.31	1.41	15.6	2.8	17.8	3.2	AU
RasTyc0218+4346	TYC 2842-24-1	02 18 13.49	+43 46 30.2	9.85	0.914	2245.4126	-10.00	1.31	11.0	5.3	13.3	0.5	AU
RasTyc0221+3404	BD+33 411	02 21 33.30	+34 04 45.6	9.68	0.802	2230.4668	-5.79	1.11	31.7	5.1	37.6	1.1	AU
RasTyc0221+3404	BD+33 411	02 21 33.30	+34 04 45.6	9.68	0.802	2234.4644	-23.39	2.45	52.6	1.3	37.1	1.1	AU
RasTyc0222+7204	TYC 4319-714-1	02 22 12.91	+72 04 58.0	10.16	0.958	4347.6892	19.07	0.67	19.8	2.2	22.3	0.9	SA
RasTyc0222+5033	BD+49 646	02 22 33.82	+50 33 37.8	9.63	0.850	2211.4353	-9.09	1.58	33.9	2.6	26.9	0.6	AU
RasTyc0222+5033	BD+49 646	02 22 33.82	+50 33 37.8	9.63	0.850	2212.6182	-8.73	1.30	24.4	2.3	26.2	0.9	AU
RasTyc0227+4554	TYC 3295-2024-1	02 27 40.47	+45 54 37.3	10.17	0.772	4348.6391	-12.66	0.48	8.9	2.1	7.8	0.5	SA
RasTyc0229+7206	TYC 4320-1432-1	02 29 44.65	+72 06 03.8	9.71	0.924	2218.4648	-32.17	1.45	21.4	2.4	19.7	0.6	AU
RasTyc0229+7206	TYC 4320-1432-1	02 29 44.65	+72 06 03.8	9.71	0.924	2220.5613	3.97	1.37	18.1	3.2	18.9	0.6	AU
RasTyc0230+5656	TYC 3695-2260-1	02 30 44.81	+56 56 13.0	10.12	0.613	4346.6876	-6.77	2.05	39.1	1.6	38.4	1.4	SA
RasTyc0230+5533	BD+54 561B	02 30 48.51	+55 33 07.2	9.58	0.787	2579.4356	-10.73	1.37	3.3	15.8	6.2	0.6	AU
RasTyc0230+5533	BD+54 561B	02 30 48.51	+55 33 07.2	9.58	0.787	2581.4192	-10.71	1.37	2.6	22.7	5.6	0.5	AU
RasTyc0235+3139	BD+31 455	02 35 03.79	+31 39 22.3	10.33	0.676	2987.4065	1.70	1.11	34.2	4.4	37.2	1.3	AU
RasTyc0240+6143	TYC 4047-1570-1	02 40 12.74	+61 43 59.0	10.33	0.656	4347.7025	24.09	1.45	29.1	3.3	29.1	1.8	SA
RasTyc0240+6143	TYC 4047-1570-1	02 40 12.74	+61 43 59.0	10.33	0.656	4348.6527	45.11	1.47	27.4	2.8	28.6	1.5	SA
RasTyc0242+4527	TYC 3296-219-1	02 42 20.50	+45 27 43.8	9.98	0.689	5109.6180	5.60						

**Table A.1.** continued.

RasTyc Name	Name	$\alpha$ (2000) h m s	$\delta$ (2000) $^{\circ}$ $'$ $''$	V <sup>a</sup> (mag)	B-V <sup>a</sup> (mag)	HJD (2450000+)	RV (km s <sup>-1</sup> )	$\sigma_{RV}$ (km s <sup>-1</sup> )	$v \sin i^b$ (km s <sup>-1</sup> )	$\sigma_{v \sin i}$ (km s <sup>-1</sup> )	$v \sin i^c$ (km s <sup>-1</sup> )	$\sigma_{v \sin i}$ (km s <sup>-1</sup> )	Instr. <sup>d</sup>
RasTyc0313+7417	HD 19438	03 13 27.48	+74 17 47.0	7.31	0.559	5135.5433	-51.64	1.83	69.0	1.4	73.3	3.6	FR
RasTyc0313+3832	BD+37 729	03 13 47.40	+38 32 04.9	10.00	0.741	2993.4424	18.59	1.33	2.0	28.9	6.0	1.4	AU
RasTyc0316+4724	TYC 3315-962-1	03 16 07.07	+47 24 58.7	9.87	0.759	2601.4526	34.37	1.53	< 5	...	2.0	1.5	AU
RasTyc0316+4724	TYC 3315-962-1	03 16 07.07	+47 24 58.7	9.87	0.759	2977.4292	35.20	1.57	< 5	...	3.4	2.3	AU
RasTyc0316+4724	TYC 3315-962-1	03 16 07.07	+47 24 58.7	9.87	0.759	2978.3332	33.82	1.57	< 5	...	3.0	2.2	AU
RasTyc0316+4724	TYC 3315-962-1	03 16 07.07	+47 24 58.7	9.87	0.759	2979.3315	35.24	1.53	< 5	...	3.5	2.1	AU
RasTyc0316+5638	TYC 3710-406-1	03 16 28.11	+56 38 58.1	10.58	0.752	4459.3288	-5.31	1.15	16.0	2.0	16.3	0.6	SA
RasTyc0316+6049	BD+60 656	03 16 59.73	+60 49 11.0	9.59	1.076	2669.2871	-49.64	1.50	25.6	2.2	25.3	0.9	AU
RasTyc0316+6049	BD+60 656	03 16 59.73	+60 49 11.0	9.59	1.076	2670.2769	-56.78	1.37	21.1	5.6	24.5	0.6	AU
RasTyc0319+4328	TYC 2860-1368-1	03 19 59.33	+43 28 08.1	9.50	0.559	2218.3474	1.28	1.26	5.2	5.1	8.2	1.3	AU
RasTyc0319+4328	TYC 2860-1368-1	03 19 59.33	+43 28 08.1	9.50	0.559	2220.4133	-5.38	1.45	< 5	...	6.2	1.2	AU
RasTyc0323+5843	TYC 3715-195-1	03 23 07.08	+58 43 07.4	10.56	0.633	4459.3500	-15.47	1.32	38.8	1.9	38.1	1.4	SA
RasTyc0325+3647	HD 278566	03 25 02.39	+36 47 56.8	9.62	0.756	2990.3989	5.70	1.37	8.1	5.0	9.8	1.2	AU
RasTyc0328+3114	BD+30 547	03 28 57.21	+31 14 19.2	9.96	0.729	2990.4485	12.46	1.76	30.0	2.9	33.2	1.6	AU
RasTyc0331+4859	CI Melotte 20 935	03 31 28.98	+48 59 28.6	10.08	0.643	4459.3669	3.35	2.17	66.2	3.6	67.6	4.4	SA
RasTyc0334+3846	HD 275480	03 34 38.28	+38 46 28.2	9.71	0.752	2236.5083	1.34	1.34	6.4	9.1	8.5	0.5	AU
RasTyc0334+3846	HD 275480	03 34 38.28	+38 46 28.2	9.71	0.752	2239.4775	2.03	1.31	10.7	3.7	10.3	1.4	AU
RasTyc0336+4816	TYC 3317-2589-1	03 36 40.23	+48 16 13.4	10.08	0.903	5111.6276	-25.59	0.32	7.0	4.0	5.3	4.1	FR
RasTyc0339+6639	BD+66 278	03 39 14.22	+66 39 40.3	9.46	0.687	2666.3384	-19.99	1.40	3.2	16.4	5.8	0.6	AU
RasTyc0339+6639	BD+66 278	03 39 14.22	+66 39 40.3	9.46	0.687	2601.5493	-20.08	1.37	3.9	14.5	5.7	0.6	AU
RasTyc0344+5043	TYC 3325-98-1	03 44 34.50	+50 43 47.5	10.58	0.940	4459.3830	1.80	1.81	57.4	4.5	62.6	4.0	SA
RasTyc0348+6840	TYC 4327-2618-1	03 48 00.50	+68 40 58.2	10.24	0.918	4459.3991	-14.39	0.66	4.0	1.5	5.0	0.8	SA
RasTyc0357+5051	** COU 2357	03 57 19.91	+50 51 19.2	9.72	0.878	2216.4087	-0.37	1.30	21.0	2.7	22.0	0.6	AU
RasTyc0357+5051	** COU 2357	03 57 19.91	+50 51 19.2	9.72	0.878	2217.3677	-0.74	1.55	24.1	2.9	21.8	1.3	AU
RasTyc0359+4404	TYC 2876-1944-1	03 59 16.70	+44 04 17.1	10.23	0.841	2982.4893	4.56	6.97	...	...	54.6	6.8	AU
RasTyc0359+4404	TYC 2876-1944-1	03 59 16.70	+44 04 17.1	10.23	0.841	2985.4133	-6.60	5.00	...	...	62.7	2.3	AU
RasTyc0412+7318A	BD+72 206	04 12 01.13 <sup>e</sup>	+73 18 34.2	10.15	0.728	4459.4350	-1.18	1.57	3.8	1.5	2.3	0.9	SA
RasTyc0412+7318B	2MASS J04120187+7318383	04 12 01.87 <sup>e</sup>	+73 18 38.4	...	...	4459.4561	91.39	3.77	104.1	11.5	124.9	18.7	SA
RasTyc0412+4616B	2MASS J04121487+4616128	04 12 14.87 <sup>e</sup>	+46 16 12.8	...	...	4459.4888	-2.60	0.78	4.4	1.3	6.8	2.0	SA
RasTyc0414+4218	TYC 2886-1693-1	04 14 39.01	+42 18 54.5	9.61	0.915	2239.5540	24.91	1.57	3.0	14.8	4.4	1.4	AU
RasTyc0414+4218	TYC 2886-1693-1	04 14 39.01	+42 18 54.5	9.61	0.915	2259.4980	24.92	1.53	< 5	...	1.4	1.3	AU
RasTyc0439+3407 <sup>g</sup>	CCDM J04395+3408AB	04 39 30.98	+34 07 45.0	9.65	0.786	2214.5674	8.49	1.36	< 5	...	63.7	1.9	AU
RasTyc0439+3407 <sup>g</sup>	CCDM J04395+3408AB	04 39 30.98	+34 07 45.0	9.65	0.786	2215.5818	8.57	1.41	13.3	4.3	62.6	0.5	AU
RasTyc0449+4504	TYC 3343-86-1	04 49 42.49	+45 04 54.4	10.32	0.716	4459.6622	13.29	1.61	5.1	1.7	6.4	0.9	SA
RasTyc0449+4902	TYC 3351-518-1	04 49 43.13	+49 02 55.1	9.50	1.005	2665.3494	17.96	1.38	13.8	4.1	14.3	0.7	AU
RasTyc0449+4902	TYC 3351-518-1	04 49 43.13	+49 02 55.1	9.50	1.005	2977.5364	16.67	1.37	16.5	2.3	17.2	1.6	AU
RasTyc0449+4902	TYC 3351-518-1	04 49 43.13	+49 02 55.1	9.50	1.005	2978.4243	17.74	1.37	16.4	2.3	17.2	1.6	AU
RasTyc0449+4902	TYC 3351-518-1	04 49 43.13	+49 02 55.1	9.50	1.005	2980.4653	16.36	1.37	15.4	2.5	15.4	0.7	AU
RasTyc0454+3410	HD 280272	04 54 56.37	+34 10 07.8	9.70	0.868	2664.3882	-22.99	1.53	< 5	...	5.0	0.6	AU
RasTyc0454+3410	HD 280272	04 54 56.37	+34 10 07.8	9.70	0.868	2980.5161	-22.62	1.53	< 5	...	4.5	1.2	AU
RasTyc0501+3430 <sup>h</sup>	WDS J05012+3430AB	05 01 10.83	+34 30 26.5	10.33	0.644	2993.4936	38.98	1.53	5.4	8.0	5.6	2.8	AU
RasTyc0507+4720	TYC 3349-2052-1	05 07 12.41	+47 20 37.4	9.48	0.597	2235.6299	-2.07	1.53	3.8	12.3	5.7	0.5	AU
RasTyc0507+4720	TYC 3349-2052-1	05 07 12.41	+47 20 37.4	9.48	0.597	2247.5769	-1.67	1.53	3.7	15.8	6.0	0.7	AU
RasTyc0507+4720	TYC 3349-2052-1	05 07 12.41	+47 20 37.4	9.48	0.597	2259.4272	-2.09	1.53	< 5	...	4.5	1.4	AU
RasTyc0512+4119	HD 277665	05 12 22.96	+41 19 40.3	9.58	0.901	2218.6003	5.43	1.37	7.8	6.6	7.8	0.9	AU
RasTyc0512+4119	HD 277665	05 12 22.96	+41 19 40.3	9.58	0.901	2225.7031	5.92	1.31	5.8	10.1	8.5	0.6	AU
RasTyc0512+4119	HD 277665	05 12 22.96	+41 19 40.3	9.58	0.901	2247.4729	5.32	1.33	5.9	10.0	7.8	0.5	AU
RasTyc0519+6303	TYC 4084-172-1	05 19 04.42	+63 03 34.5	9.81	0.553	2216.6101	-17.04	1.53	< 5	...	3.0	1.9	AU
RasTyc0519+6303	TYC 4084-172-1	05 19 04.42	+63 03 34.5	9.81	0.553	2217.6057	-17.83	1.45	< 5	...	4.4	1.3	AU
RasTyc0535+3946	V613 Aur	05 35 05.64	+39 46 31.9	10.20	1.085	4459.7018	-9.14	1.44	41.5	1.8	44.5	1.4	SA
RasTyc0537+5231	G 191-47	05 37 03.91	+52 31 26.1	10.13	1.101	2985.4648	-11.78	1.41	4.8	11.0	7.2	1.2	AU
RasTyc0544+4024	BD+40 1397B	05 44 26.50	+40 24 26.1	9.83	0.990	2665.4016	22.98	1.31	< 5	...	2.1	1.4	AU
RasTyc0544+4024	BD+40 1397B	05 44 26.50	+40 24 26.1	9.83	0.990	2980.6294	22.16	1.37	7.1	5.7	5.0	1.1	AU
RasTyc0609+5801	TYC 3759-804-1	06 09 00.42	+58 01 09.0	10.54	0.831	4459.7477	58.81	1.52	3.3	1.4	5.6	1.3	SA
RasTyc0612+4733	TYC 3379-358-1	06 12 30.81	+47 33 09.1	9.58	0.663	2584.6458	5.76	1.53	4.2	12.0	7.9	1.6	AU
RasTyc0612+4733	TYC 3379-358-1	06 12 30.81	+47 33 09.1	9.58	0.663	2600.6755	6.27	1.41	7.4	6.9	6.3	0.8	AU
RasTyc0616+4516	TYC 3375-720-1	06 16 46.95	+45 16 03.1	10.59	0.698	4459.7668	16.20	1.73	22.1	1.9	21.7	1.0	SA
RasTyc0620+7353	TYC 4357-209-1	06 20 07.99	+73 53 30.5	9.71	0.675	2981.5230	-7.30	1.38	8.1	6.0	7.2	1.3	AU
RasTyc0620+7353	TYC 4357-209-1	06 20 07.99	+73 53 30.5	9.71	0.675	2986.4609	-1.76	1.52	2.4	20.2	5.8	0.6	AU
RasTyc0621+5415	TYC 3764-338-1	06 21 56.92	+54 15 49.0	9.49	0.625	2216.5727	-31.02	1.31	19.9	2.4	21.8	0.8	AU
RasTyc0621+5415	TYC 3764-338-1	06 21 56.92	+54 15 49.0	9.49	0.625	2217.5481	-31.50	1.49	22.8	3.3	21.9	1.0	AU
RasTyc0624+5940	HD 44271	06 24 43.95	+59 40 10.8	7.46	0.982	3273.6428	14.96	1.57	3.7	13.2	5.1	0.9	AU
RasTyc0628+3115A	HD 257514	06 28 23.61	+31 15 51.2	9.86	0.675	2234.6238	25.33	1.34	8.2	7.1	8.1	0.8	AU
RasTyc0628+3115A	HD 257514	06 28 23.61	+31 15 51.2	9.86	0.675	2230.5986	25.68	1.30	1.7	33.8	5.5	0.6	AU
RasTyc0628+3115B	BD+31 1301p	06 28 22.99	+31 15 59.2	10.16	0.7								

**Table A.1.** continued.

RasTyc Name	Name	$\alpha$ (2000) h m s	$\delta$ (2000) $^{\circ} \ ' \ ''$	$V^a$ (mag)	$B-V^a$ (mag)	HJD (2450000+)	RV (km s $^{-1}$ )	$\sigma_{RV}$ (km s $^{-1}$ )	$v \sin i^b$ (km s $^{-1}$ )	$\sigma_{v \sin i}$ (km s $^{-1}$ )	$v \sin i^c$ (km s $^{-1}$ )	$\sigma_{v \sin i}$ (km s $^{-1}$ )	Instr. <sup>d</sup>
RasTyc0712+7021	TYC 4364-1262-1	07 12 50.04	+70 21 06.8	9.87	1.052	2981.6709	-23.67	1.30	9.4	5.3	10.3	1.1	AU
RasTyc0712+7021	TYC 4364-1262-1	07 12 50.04	+70 21 06.8	9.87	1.052	2985.5803	-31.55	1.37	9.4	4.8	10.9	0.9	AU
RasTyc0713+5106	TYC 3404-384-1	07 13 36.53	+51 06 17.3	9.74	0.634	2235.6692	20.22	1.38	27.2	3.0	26.3	0.9	AU
RasTyc0713+5106	TYC 3404-384-1	07 13 36.53	+51 06 17.3	9.74	0.634	2237.7139	20.61	1.30	20.7	2.3	22.0	2.1	AU
RasTyc0714+5307	TYC 3780-247-1	07 14 36.39	+53 07 40.4	10.03	0.575	2993.6101	11.17	1.77	...	...	32.9	2.1	AU
RasTyc0730+6343	TYC 4116-276-1	07 30 55.31	+63 43 50.1	9.93	1.009	2993.5456	-37.71	1.53	< 5	...	7.7	0.7	AU
RasTyc0734+3518	CCDM J07346+3519AB	07 34 34.76	+35 18 59.7	9.68	0.544	2239.6445	13.95	1.37	7.3	5.9	8.5	0.6	AU
RasTyc0734+3518	CCDM J07346+3519AB	07 34 34.76	+35 18 59.7	9.68	0.544	2259.6016	14.05	1.38	7.5	6.9	8.5	0.6	AU
RasTyc0755+4040	TYC 2964-272-1	07 55 04.52	+40 40 25.0	9.77	0.612	2239.6807	22.71	1.59	46.2	2.8	38.3	1.6	AU
RasTyc0755+4040	TYC 2964-272-1	07 55 04.52	+40 40 25.0	9.77	0.612	2259.6440	23.38	1.37	28.0	4.2	29.5	2.2	AU
RasTyc0755+6509	BD+65 601	07 55 54.19	+65 09 11.1	9.52	0.909	2235.7153	-42.50	1.45	3.9	12.4	7.0	1.5	AU
RasTyc0755+6509	BD+65 601	07 55 54.19	+65 09 11.1	9.52	0.909	2236.7202	-42.01	1.53	< 5	...	5.0	0.8	AU
RasTyc1505+4626	BD+47 2200	15 05 32.49	+46 26 38.6	10.58	0.930	5727.3845	28.67	1.35	65.4	8.9	63.0	3.1	SA
RasTyc1507+5515	HD 134418	15 07 27.92	+55 15 56.5	8.97	0.696	5108.2583	-11.24	0.52	39.2	1.9	39.3	1.5	FR
RasTyc1507+8629	BD+86 23	15 07 53.09	+86 29 29.4	9.78	0.651	4144.3944	-16.41	0.29	6.1	1.8	6.9	0.8	SA
RasTyc1507+0415	BD +04 2967	15 07 59.63	+04 15 21.1	9.60	0.938	2464.3857	-15.76	1.37	13.6	4.2	13.8	0.6	AU
RasTyc1507+0415	BD +04 2967	15 07 59.63	+04 15 21.1	9.60	0.938	2469.3757	-15.49	1.41	16.6	2.6	18.0	1.9	AU
RasTyc1519+3940	BD+40 2871	15 19 38.40	+39 40 05.5	9.28	0.627	4145.6007	-43.41	0.75	30.6	2.6	30.2	1.4	SA
RasTyc1521-0920	BD-08 3958	15 21 52.71	-09 20 18.3	9.23	0.837	4144.6869	-8.48	0.36	5.1	2.1	5.9	2.5	SA
RasTyc1522+4137	TYC 3055-1099-1	15 22 11.06	+41 37 08.9	10.04	0.796	4145.5535	-9.57	0.21	3.4	1.7	3.2	1.1	SA
RasTyc1522+2745	TYC 2031-874-1	15 22 35.40	+27 45 31.0	10.48	0.904	5727.4049	-41.93	0.24	2.1	1.1	0.9	0.6	SA
RasTyc1527+1801	BD+18 3026	15 27 38.20	+18 01 35.3	9.40	0.631	4144.6972	-5.89	0.31	5.3	1.7	6.4	0.7	SA
RasTyc1529+6712A	BD+67 900	15 29 24.15	+67 12 15.9	9.53	0.475	4145.5137	-12.36	0.56	16.6	1.9	18.6	0.8	SA
RasTyc1529+4836	BD+49 2392	15 29 42.46	+48 36 13.1	9.51	0.649	3572.4211	-40.67	1.53	< 5	...	5.7	1.2	AU
RasTyc1529+4836	BD+49 2392	15 29 42.46	+48 36 13.1	9.51	0.649	3576.3806	-43.51	1.46	< 5	...	9.3	0.9	AU
RasTyc1540+4027A**	V335 Boo	15 40 58.90	+40 27 00.3	10.59	0.701	5728.3908	-13.57	1.26	29.9	3.4	29.5	1.1	SA
RasTyc1540+4027B**		15 40 58.90	+40 27 00.3	...	...	5728.3908	-33.14	0.30	2.3	2.2	3.4	1.5	SA
RasTyc1541+7702	TYC 4560-1035-1	15 41 59.71	+77 02 41.8	9.54	0.644	4145.5313	-8.19	0.21	4.5	1.7	4.2	0.9	SA
RasTyc1547+5302B	TYC 3870-1361-1	15 47 09.38	+53 01 26.5	10.93	0.772	4145.5699	2.96	0.33	4.4	2.9	5.4	1.5	SA
RasTyc1549+4608A	TYC 3490-591-1	15 49 24.84	+46 08 22.2	10.90	0.807	5728.4294	41.06	0.39	15.1	1.6	15.0	0.9	SA
RasTyc1549+4608B	TYC 3490-273-1	15 49 24.32	+46 08 10.3	11.8	...	5728.4110	-4.76	0.74	13.2	3.0	12.7	0.6	SA
RasTyc1550+5250	TYC 3870-1328-1	15 50 36.72	+52 50 22.0	9.86	0.573	4148.6650	-11.58	0.29	7.9	1.9	8.6	0.8	SA
RasTyc1550+1440A	BD+15 2919	15 50 55.23	+14 40 42.8	9.10	0.474	4144.7596	-18.13	0.23	1.7	1.5	2.4	1.1	SA
RasTyc1558+0833	TYC 944-634-1	15 58 54.66	+08 33 55.3	8.95	0.788	4144.7403	-28.16	0.31	1.4	1.1	1.3	0.7	SA
RasTyc1603+8142	BD+82 477	16 03 26.61	+81 42 20.4	9.43	0.647	4144.4035	3.01	0.26	4.5	1.9	4.8	1.0	SA
RasTyc1604+0358	BD+04 3107	16 04 16.06	+03 58 09.4	9.69	0.668	4144.7321	-75.59	0.38	11.7	2.5	11.5	0.6	SA
RasTyc1617-0406	BD-03 3912	16 17 21.68	-04 06 50.0	9.78	0.860	4144.7209	0.24	0.26	3.4	2.8	6.6	0.9	SA
RasTyc1620+0707***	BD+07 3142	16 20 03.26	+07 07 29.6	9.89	0.901	2483.3706	-48.31	1.53	< 5	...	56.4	45.9	AU
RasTyc1620+0707***	BD+07 3142	16 20 03.26	+07 07 29.6	9.89	0.901	3218.3794	-70.45	1.57	< 5	...	10.5	2.0	AU
RasTyc1620+0707***	BD+07 3142	16 20 03.26	+07 07 29.6	9.89	0.901	5043.3570	-59.06	0.57	17.5	5.0	35.0	10.8	FR
RasTyc1620+4841	BD+49 2494	16 20 38.67	+48 41 13.7	9.51	0.718	4148.6529	-18.20	0.29	7.7	2.0	7.5	0.5	SA
RasTyc1623+3535	BD+35 2809	16 23 09.20	+35 35 18.3	9.28	0.589	4148.7207	-18.58	0.31	4.0	2.5	7.9	1.5	SA
RasTyc1626+3350	BD+34 2784	16 26 41.35	+33 50 42.1	9.67	0.765	4148.7298	-139.10	0.84	10.1	3.7	13.4	3.0	SA
RasTyc1626+0823	BD+08 3197	16 26 48.87	+08 23 26.0	9.09	0.725	4149.7312	-27.71	0.85	3.9	1.9	3.0	1.1	SA
RasTyc1628+7400	BD+74 668	16 28 21.48	+74 00 55.9	9.46	0.643	4145.5410	-21.71	0.38	17.7	2.6	16.9	1.0	SA
RasTyc1629+1728	BD+17 3038	16 29 29.20	+17 28 16.2	9.29	0.653	4148.7762	-17.56	0.26	6.3	1.9	6.9	0.7	SA
RasTyc1631+0849	BD+09 3217	16 31 13.87	+08 49 14.4	8.97	0.879	4149.7612	-30.82	0.88	6.5	3.3	7.7	0.8	SA
RasTyc1631+1916A	BD+19 3113A	16 31 34.45	+19 16 38.8	10.08	0.799	4150.7052	-35.30	0.32	3.1	2.1	1.0	0.8	SA
RasTyc1631+1916B	BD+19 3113B	16 31 34.09	+19 16 38.5	10.17	0.837	4150.7180	-2.94	0.41	16.5	3.1	17.0	0.9	SA
RasTyc1637+0717	BD+07 3214	16 37 35.43	+07 17 03.3	9.06	0.679	4150.6692	-29.15	0.31	6.9	1.7	8.0	0.7	SA
RasTyc1641+1520	BD+15 3037	16 41 26.95	+15 20 39.7	9.62	0.950	4148.7667	19.55	0.38	2.2	1.0	2.6	1.2	SA
RasTyc1641+0118	V2581 Oph	16 41 29.18	+01 18 48.6	9.47	0.887	4150.6602	-43.45	0.35	5.5	2.8	1.9	0.9	SA
RasTyc1641+1140	BD+11 3024	16 41 53.08	+11 40 21.1	10.10	1.065	4150.6791	7.79	0.30	7.6	2.3	8.4	0.5	SA
RasTyc1645+3000A	HD 151367	16 45 43.47	+30 00 17.2	8.69	0.356	4148.7415	14.93	0.30	7.0	2.3	13.8	1.5	SA
RasTyc1645+3000B	BD+30 2871B	16 45 44.10	+30 00 05.6	9.48	0.648	4148.7480	20.09	0.25	1.8	1.6	3.4	1.5	SA
RasTyc1649+5816	HD 238614	16 49 40.31	+58 16 08.4	9.60	0.594	5021.3887	-13.90	0.29	14.7	1.4	15.2	1.9	FR
RasTyc1649+5816	HD 238614	16 49 40.31	+58 16 08.4	9.60	0.594	5109.2836	-14.01	0.28	12.0	4.0	12.6	2.5	FR
RasTyc1652+0121	BD+01 3228	16 52 29.11	+01 21 20.1	9.69	0.585	4149.7523	1.54	0.92	6.8	2.1	7.9	0.8	SA
RasTyc1658+0547	BD+06 3324	16 58 03.46	+05 47 05.2	9.76	0.708	4150.6907	-83.68	0.38	7.6	2.8	9.3	0.6	SA
RasTyc1658+3333	TYC 2594-1053-1	16 58 20.65	+33 33 53.1	9.78	0.695	4149.7418	8.53	0.88	4.5	2.2	4.6	1.0	SA
RasTyc1702+4713°	TYC 3501-626-1	17 02 48.85	+47 13 06.5	10.08	0.856	4215.4693	-7.81	0.62	15.5	3.7	15.0	0.9	SA
RasTyc1703+2052	BD+21 3035	17 03 59.59	+20 52 49.1	9.07	0.636	4150.7590	-21.39	0.24	8.8	2.4	9.4	0.9	SA
RasTyc1705-0147	HD 154361	17 05 08.46	-01 47 09.6	9.54	1.058	2475.3704	-13.37	1.35	8.8	4.5	10.8	1.2	AU
RasTyc1706+0647	HD 154734	17 06 56.79	+06 47 49.0	9.77	1.006	2442.5188	-27.45	1.37	1.1	48.4	6.0	0.6	AU
RasTyc1706+0647	HD 154734	17 06 56.79	+06 47 49.0	9.77	1.006	2444.5149	-30.86	1.40	8.6	3.7	...	...	AU
RasTyc1714+0623</													

**Table A.1.** continued.

RasTyc Name	Name	$\alpha$ (2000) h m s	$\delta$ (2000) $^{\circ}$ ' ''	$V^a$ (mag)	$B-V^a$ (mag)	HJD (2450000+)	RV (km s $^{-1}$ )	$\sigma_{RV}$ (km s $^{-1}$ )	$v \sin i^b$ (km s $^{-1}$ )	$\sigma_{v \sin i}$ (km s $^{-1}$ )	$v \sin i^c$ (km s $^{-1}$ )	$\sigma_{v \sin i}$ (km s $^{-1}$ )	Instr. <sup>d</sup>
RasTyc1831+5418	TYC 3905-319-1	18 31 37.59	+54 18 57.9	9.96	0.842	4149.7020	-28.02	0.90	5.3	2.2	4.0	1.0	SA
RasTyc1838+0224	BD+02 3633	18 38 38.19	+02 24 12.7	9.61	0.586	4210.6953	-27.13	0.52	31.5	2.1	31.0	0.8	SA
RasTyc1842+5751	HD 173605	18 42 49.32	+57 51 54.6	7.96	0.630	2119.3499	24.73	0.15	21.6	1.1	20.8	0.8	EL
RasTyc1843+4328	KIC 7730305	18 43 58.66	+43 28 27.8	9.38	0.573	5046.5341	6.78	1.33	14.1	5.8	14.5	1.5	SA
RasTyc1843+4328	KIC 7730305	18 43 58.66	+43 28 27.8	9.38	0.573	5023.4904	5.93	0.28	17.7	1.1	16.3	3.0	FR
RasTyc1847+2930	BD+29 3349	18 47 39.96	+29 30 39.3	9.93	0.865	4249.6876	5.20	0.55	5.5	1.8	6.2	0.7	SA
RasTyc1857+6406	BD+63 1470	18 57 13.08	+64 06 21.3	9.51	1.042	4346.3490	-5.19	0.41	3.8	1.9	3.1	0.8	SA
RasTyc1857+6223	BD+62 1669	18 57 19.45	+62 23 39.5	9.52	0.827	4301.7087	-7.34	0.47	1.6	1.0	1.1	0.6	SA
RasTyc1857+0120	BD+01 3828	18 57 19.46	+01 20 33.3	9.50	0.801	2475.4119	-26.82	1.53	2.7	17.2	5.9	0.6	AU
RasTyc1857+0120	BD+01 3828	18 57 19.46	+01 20 33.3	9.50	0.801	2480.4111	-27.06	1.53	< 5	...	5.5	0.5	AU
RasTyc1908+5018	HD 234808	19 08 14.03	+50 18 49.6	9.29	0.891	4670.4747	-11.51	0.30	11.9	1.4	8.1	5.2	FR
RasTyc1918+3408	HD 181209	19 18 12.13	+34 08 10.1	8.35	1.116	2122.3822	-20.22	0.15	10.4	0.6	11.6	0.6	EL
RasTyc1919+0628	HD 181215	19 19 26.29	+06 28 42.2	9.47	0.587	5118.2997	21.24	0.19	10.0	1.0	12.7	3.2	FR
RasTyc1925+4429	KIC 8429280	19 25 01.98	+44 29 50.7	9.86	0.924	4252.4872	-33.14	0.53	38.5	2.4	37.1	2.9	SA
RasTyc1925+4429	KIC 8429280	19 25 01.98	+44 29 50.7	9.86	0.924	5055.5414	-33.10	0.44	36.5	2.5	35.1	3.0	SA
RasTyc1926+7840	TYC 4588-319-1	19 26 35.09	+78 40 04.9	9.92	0.887	4149.3394	21.31	0.68	9.0	2.3	9.4	0.8	SA
RasTyc1928+4856	KIC 11244501	19 28 10.64	+48 56 37.3	10.07	0.686	4252.4993	-20.42	3.14	102.4	4.8	107.2	5.6	SA
RasTyc1928+1232	BD+12 3917	19 28 15.43	+12 32 09.6	9.17	1.090	4249.7065	-17.82	0.51	3.5	1.6	1.1	0.5	SA
RasTyc1928+2731	HD 338348	19 28 22.32	+27 31 18.5	9.56	0.711	2483.4814	14.45	1.45	29.8	2.6	25.4	2.2	AU
RasTyc1930+4932	KIC 11560431	19 30 15.81	+49 32 08.2	10.11	0.837	4270.5128	-42.59	0.46	10.3	2.2	9.9	0.5	SA
RasTyc1930+4932	KIC 11560431	19 30 15.81	+49 32 08.2	10.11	0.837	5055.7109	-39.57	1.12	16.8	3.1	13.8	0.6	SA
RasTyc1940+2535	HD 338736	19 40 44.79	+25 35 46.9	9.59	1.008	2475.4792	2.31	1.41	8.4	6.2	7.4	1.0	AU
RasTyc1940+2535	HD 338736	19 40 44.79	+25 35 46.9	9.59	1.008	2478.4436	2.00	1.31	4.8	12.1	6.3	0.5	AU
RasTyc1949-0804	TYC 5725-63-1	19 49 35.22	-08 04 50.3	9.75	1.037	2445.5425	65.92	1.36	21.5	2.2	23.4	1.5	AU
RasTyc1949-0804	TYC 5725-63-1	19 49 35.22	-08 04 50.3	9.75	1.037	2473.5366	57.90	1.53	24.5	2.3	25.0	2.0	AU
RasTyc1956+4345	KIC 7985370	19 56 59.73	+43 45 08.2	9.96	0.637	5055.6819	-21.84	0.24	17.9	1.3	18.2	1.3	SA
RasTyc1956+4345	KIC 7985370	19 56 59.73	+43 45 08.2	9.96	0.637	5023.4390	-23.9	0.4	16.9	1.1	17.9	1.3	FR
RasTyc1956+4345	KIC 7985370	19 56 59.73	+43 45 08.2	9.96	0.637	5108.3054	-24.2	0.4	15.9	0.9	17.4	0.8	FR
RasTyc1958+5355A	HD 189572	19 58 04.00	+53 55 29.6	8.91	0.428	4347.3553	-8.59	3.37	87.2	7.2	89.0	4.3	SA
RasTyc1958+5355B	BD+53 2331a	19 58 03.39	+53 55 24.5	9.78	0.619	4347.3474	-11.02	1.75	9.6	1.3	10.4	0.5	SA
RasTyc1958+4301*	KIC 7477572	19 58 37.62	+43 01 02.5	9.54	0.579	5006.5807	14.01	1.53	33.4	4.6	37.3	9.9	FR
RasTyc1958+4301*	KIC 7477572	19 58 37.62	+43 01 02.5	9.54	0.579	5077.4854	-30.54	0.62	35.4	2.1	41.0	4.9	FR
RasTyc1958+4301*	KIC 7477572	19 58 37.62	+43 01 02.5	9.54	0.579	4346.3606	-43.24	2.25	36.5	3.0	39.1	4.0	SA
RasTyc1959-0432	HD 189285	19 59 24.10	-04 32 05.7	9.45	0.735	3579.5124	-18.69	1.34	9.4	5.3	9.4	0.5	AU
RasTyc1959-0432	HD 189285	19 59 24.10	-04 32 05.7	9.45	0.735	3580.4536	-17.87	1.37	7.6	5.4	10.6	1.7	AU
RasTyc2000+5921	TYC 3948-2133-1	20 00 31.23	+59 21 44.5	10.13	0.644	4347.3635	-15.43	1.35	2.9	1.4	2.6	1.1	SA
RasTyc2000+3256	HD 189806	20 00 45.52	+32 56 59.4	8.09	0.858	2122.3636	-25.69	0.15	3.6	0.2	3.4	0.8	EL
RasTyc2004-0239	BD-03 4778	20 04 49.35	-02 39 19.7	10.06	1.009	4270.5446	-15.92	0.44	8.5	2.1	9.0	0.6	SA
RasTyc2013+1625	HD 192362	20 13 54.27	+16 25 25.4	8.38	1.215	2120.3619	-52.38	0.15	13.8	0.7	14.2	0.6	EL
RasTyc2013+1625	HD 192362	20 13 54.27	+16 25 25.4	8.38	1.215	2123.4166	-52.50	0.15	13.1	0.7	13.4	0.6	EL
RasTyc2015+3316	HD 228564	20 15 20.54	+33 16 11.8	9.86	1.000	1762.4248	-22.50	0.15	4.3	0.2	4.0	0.8	EL
RasTyc2015+3343	HD 192787	20 15 23.79	+33 43 45.7	5.71	0.921	1761.4111	-9.07	0.15	1.4	0.1	1.3	0.7	EL
RasTyc2016+3106	HD 332091	20 16 57.83	+31 06 55.6	10.85	0.751	1796.3692	-23.83	0.15	5.2	0.3	4.0	1.0	EL
RasTyc2016+3106	HD 332091	20 16 57.83	+31 06 55.6	10.85	0.751	2147.4908	-23.85	0.15	5.2	0.3	4.1	0.9	EL
RasTyc2019+3203	HD 332148	20 19 47.52	+32 03 08.8	10.27	0.576	1763.4203	16.74	0.22	50.9	2.7	45.5	1.9	EL
RasTyc2021+3150	TYC 2672-0717-1	20 21 30.45	+31 50 32.3	11.22	0.756	2121.4478	4.34	0.80	100.6	5.4	109.5	13.5	EL
RasTyc2021+3218	V1971 Cyg	20 21 33.04	+32 18 50.7	7.85	1.015	1732.3802	-77.25	0.15	10.3	0.5	11.6	0.6	EL
RasTyc2021+0616	BD+05 4489	20 21 45.50	+06 16 13.4	9.12	0.627	4301.6780	20.90	1.77	10.3	1.7	10.3	1.5	SA
RasTyc2025-0429	BD-04 5118	20 25 04.26	-04 29 15.2	9.63	0.940	4270.5620	-55.16	0.45	6.7	1.9	9.0	0.9	SA
RasTyc2028+2510	BD+24 4140	20 28 03.50	+25 10 42.7	9.91	0.803	4301.7220	-11.27	0.42	3.9	2.2	4.0	0.7	SA
RasTyc2028+1131	TYC 1095-848-1	20 28 23.91	+11 31 11.3	9.76	0.637	2483.5217	32.42	0.98	110.0	20.0	121.3	2.4	AU
RasTyc2028-0943	BD-10 5400	20 28 42.28	-09 43 16.9	9.30	0.858	4301.5252	-6.67	3.03	88.2	4.9	87.7	6.5	SA
RasTyc2030+4852	BD+48 3149	20 30 59.56	+48 52 08.1	8.58	1.164	2121.3890	20.51	0.17	58.3	3.1	53.5	1.0	EL
RasTyc2030+4852	BD+48 3149	20 30 59.56	+48 52 08.1	8.58	1.164	2122.5300	6.17	0.17	54.4	2.9	51.5	1.1	EL
RasTyc2030+4852	BD+48 3149	20 30 59.56	+48 52 08.1	8.58	1.164	2123.3882	-8.86	0.18	56.7	3.0	54.1	0.9	EL
RasTyc2033+3128	HD 334514	20 33 24.39	+31 28 12.3	10.55	0.635	1735.4088	15.51	0.20	35.2	1.9	31.7	1.6	EL
RasTyc2034-0713	BD-07 5331	20 34 47.43	-07 13 56.7	9.59	1.094	4301.6622	-3.65	0.43	1.7	0.9	1.3	0.8	SA
RasTyc2036+3456	TYC 2694-1627-1	20 36 16.87	+34 56 46.1	10.96	0.656	1764.4230	-18.49	0.15	10.3	0.5	10.2	0.6	EL
RasTyc2037+5106	HD 235299	20 37 55.03	+51 06 23.1	9.47	0.736	3587.5122	-23.99	1.34	8.6	5.7	8.7	0.6	AU
RasTyc2037+5106	HD 235299	20 37 55.03	+51 06 23.1	9.47	0.736	3588.4963	-24.98	1.31	8.4	5.0	9.3	0.6	AU
RasTyc2038+3546	BD+35 4198	20 38 17.71	+35 46 33.3	8.97	0.567	2118.3670	-23.14	0.16	23.5	1.2	22.2	0.8	EL
RasTyc2038+3546	BD+35 4198	20 38 17.71	+35 46 33.3	8.97	0.567	4346.3782	-21.76	1.80	23.4	1.8	23.1	1.1	SA
RasTyc2039+2644	TYC 2178-1225-1	20 39 40.81	+26 44 48.4	9.87	0.720	2445.5049	-21.69	1.31	13.9	4.1	14.6	0.5	AU
RasTyc2046+2815	BU Vul	20 46 18.86	+28 15 44.2	10.16	0.667	1735.4560	-61.71	1.70	167.0	9.3	146.8	4.9	EL
RasTyc2048-0644	HD 198217	20 48 59.58	-06 44 53.4	9.54	0.799	2442.5610	-64.70	1.65	35.1	2.7	26.8	2.7	AU
RasTyc2048-0644</													

**Table A.1.** continued.

RasTyc Name	Name	$\alpha$ (2000) h m s	$\delta$ (2000) $^{\circ}$ ' ''	V <sup>a</sup> (mag)	B-V <sup>a</sup> (mag)	HJD (2450000+)	RV (km s <sup>-1</sup> )	$\sigma_{RV}$	$v \sin i^b$ (km s <sup>-1</sup> )	$\sigma_{v \sin i}$ (km s <sup>-1</sup> )	$v \sin i^c$ (km s <sup>-1</sup> )	$\sigma_{v \sin i}$ (km s <sup>-1</sup> )	Instr. <sup>d</sup>
RasTyc2100+4405	TYC 3180-1594-1	21 00 25.21	+44 05 54.7	10.52	0.877	1763.4905	35.24	0.15	4.2	0.2	4.3	0.8	EL
RasTyc2101+1008	BD+09 4700	21 01 44.80	+10 08 40.9	9.73	1.021	2474.5676	-29.21	1.38	9.3	4.7	9.0	0.5	AU
RasTyc2101+1008	BD+09 4700	21 01 44.80	+10 08 40.9	9.73	1.021	2478.4917	-29.33	1.32	9.0	6.4	7.3	0.8	AU
RasTyc2102+4553	V2436 Cyg	21 02 40.42	+45 53 03.9	7.72	0.969	1732.5386	-14.19	0.15	3.6	0.2	2.9	0.7	EL
RasTyc2103+4104	TYC 3172-643-1	21 03 16.76	+41 04 06.3	10.31	0.992	1799.3572	-23.22	0.15	9.3	0.5	9.2	0.6	EL
RasTyc2105+3949	TYC 3172-652-1	21 05 50.98	+39 49 48.1	10.74	0.765	2118.4740	0.78	0.17	24.7	1.3	23.2	1.3	EL
RasTyc2106+0217	BD+01 4422	21 06 04.29	+02 17 02.4	9.89	0.679	4301.6870	1.14	0.43	1.6	1.0	0.9	0.7	SA
RasTyc2106+6906	BD+68 1182	21 06 21.74	+69 06 41.0	10.12	0.648	4348.3773	-10.01	1.96	40.5	2.1	39.4	1.6	SA
RasTyc2107+0632	TYC 538-165-1	21 07 07.13	+06 32 32.2	9.96	0.643	4346.4128	24.62	1.89	14.8	1.6	17.5	2.4	SA
RasTyc2107+3423	TYC 2709-1412-1	21 07 30.01	+34 23 33.7	10.82	0.919	1797.4095	-4.50	0.15	12.4	0.7	12.0	0.6	EL
RasTyc2109+4029	TYC 3172-1505-1	21 09 48.50	+40 29 23.4	10.74	0.776	1798.4640	27.54	0.16	22.3	1.2	23.5	1.3	EL
RasTyc2109+4029	TYC 3172-1505-1	21 09 48.50	+40 29 23.4	10.74	0.776	2149.4831	-10.47	0.17	24.1	1.3	22.7	1.3	EL
RasTyc2114-0058	BD-01 4129	21 14 32.47	-00 58 52.8	9.10	0.688	4301.7050	-15.19	1.65	23.1	2.4	22.5	1.1	SA
RasTyc2114+3941	BD+39 4490	21 14 55.24	+39 41 11.9	8.96	0.576	1736.5920	-11.22	0.17	26.4	1.4	26.6	0.9	EL
RasTyc2115+4437	TYC 3181-1403-1	21 15 23.98	+44 37 42.8	10.77	0.860	2119.5305	23.75	0.15	11.6	0.6	11.4	0.6	EL
RasTyc2117+3153	HD 202779	21 17 21.28	+31 53 58.0	7.74	0.840	1734.4722	-5.61	0.15	7.1	0.4	7.5	0.5	EL
RasTyc2118-0631	BD-07 5533	21 18 33.53	-06 31 43.7	10.02	0.775	4270.5732	22.82	0.65	19.5	3.5	20.9	0.7	SA
RasTyc2118+2613	V457 Vul	21 18 58.13	+26 13 49.9	8.43	0.781	2120.3875	-16.81	0.15	6.3	0.3	6.6	0.8	EL
RasTyc2120+4636	TYC 3589-3858-1	21 20 55.42	+46 36 12.4	10.43	0.704	1797.4691	-23.77	0.57	107.0	5.7	109.5	3.3	EL
RasTyc2121+4020	HD 203454	21 21 01.44	+40 20 44.1	6.40	0.546	1732.4482	58.62	0.64	21.6	1.5	17.2	1.4	EL
RasTyc2121+4020	HD 203454	21 21 01.44	+40 20 44.1	6.40	0.546	1763.3702	54.81	0.15	16.9	0.9	17.4	1.5	EL
RasTyc2128+6423	HD 204734	21 28 00.96	+64 23 15.1	8.83	0.852	2123.4461	-10.72	0.15	4.1	0.2	3.8	0.7	EL
RasTyc2131+5925	HD 205113	21 31 01.20	+59 25 05.0	6.87	0.665	1801.6492	-73.95	0.15	11.8	0.6	12.1	0.7	EL
RasTyc2132+3604	HD 205173	21 32 39.29	+36 04 46.0	8.47	0.978	1764.3732	-6.76	0.15	3.9	0.2	4.1	0.6	EL
RasTyc2137+1946	HD 205762	21 37 03.18	+19 46 58.3	7.27	0.948	1733.5887	-6.00	0.15	2.1	0.1	2.5	0.6	EL
RasTyc2141+2645	HD 206374	21 41 05.97	+26 45 03.2	7.45	0.694	1761.4476	-43.08	0.15	1.0	0.1	1.3	0.8	EL
RasTyc2141+2658	TYC 2197-1430-1	21 41 16.74	+26 58 58.1	9.43	0.985	1736.5531	-19.93	0.15	10.5	0.6	11.7	0.6	EL
RasTyc2141+2658	TYC 2197-1430-1	21 41 16.74	+26 58 58.1	9.43	0.985	3574.5042	-18.96	1.37	12.4	3.7	12.7	1.2	AU
RasTyc2141+2658	TYC 2197-1430-1	21 41 16.74	+26 58 58.1	9.43	0.985	3276.4382	-8.62	1.31	11.1	4.6	11.5	0.5	AU
RasTyc2142+3814	BD+37 4406	21 42 59.83	+38 14 54.8	10.24	1.009	1797.5275	-1.21	0.15	0.6	0.2	1.8	0.6	EL
RasTyc2143+2720	BD+26 4249	21 43 31.67	+27 20 37.6	9.44	0.574	2120.4251	-13.69	0.15	3.5	0.2	2.8	0.9	EL
RasTyc2146+2446	TYC 2206-1706-1	21 46 50.43	+24 46 04.2	9.78	0.578	2119.3947	-34.34	0.15	3.5	0.2	2.4	1.2	EL
RasTyc2146+2446	TYC 2206-1706-1	21 46 50.43	+24 46 04.2	9.78	0.578	3577.4324	-35.33	1.58	< 5	...	7.5	1.4	AU
RasTyc2146+2446	TYC 2206-1706-1	21 46 50.43	+24 46 04.2	9.78	0.578	3276.5144	-33.69	1.53	< 5	...	5.6	1.0	AU
RasTyc2147+4950	TYC 3612-2224-1	21 47 48.72	+49 50 08.0	10.03	0.983	4348.3943	-5.01	0.40	5.5	1.8	6.3	1.2	SA
RasTyc2147+4950	TYC 3612-2224-1	21 47 48.72	+49 50 08.0	10.03	0.983	5076.5430	-4.76	0.23	10.1	2.6	4.6	4.0	FR
RasTyc2147+4949	BD+49 3625	21 47 54.42	+49 49 29.2	9.99	0.987	4346.4246	-3.54	0.51	5.8	2.5	6.5	1.7	SA
RasTyc2147+4949	BD+49 3625	21 47 54.42	+49 49 29.2	9.99	0.987	4348.4053	-3.45	0.38	5.0	2.0	6.2	1.1	SA
RasTyc2147+4949	BD+49 3625	21 47 54.42	+49 49 29.2	9.99	0.987	5078.5382	-3.91	0.28	13.4	2.3	5.4	4.3	FR
RasTyc2149-0350	BD-04 5541	21 49 13.15	-03 50 32.6	10.13	0.628	4270.5888	14.13	1.46	3.0	1.5	5.0	0.6	SA
RasTyc2149+3125	TYC 2718-320-1	21 49 16.02	+31 25 02.1	10.69	0.785	1796.5056	-11.80	0.15	6.7	0.4	6.3	0.7	EL
RasTyc2149+4028	TYC 3188-0129-1	21 49 26.94	+40 28 00.9	10.94	0.837	2120.5305	4.14	0.23	30.1	1.6	29.5	3.0	EL
RasTyc2152+3850	HD 208076	21 52 48.07	+38 50 08.0	7.08	0.910	2120.6243	-3.00	0.15	4.1	0.2	5.0	0.6	EL
RasTyc2153+2055	HD 208038	21 53 05.36	+20 55 50.8	8.18	0.941	1733.4691	13.52	0.15	2.8	0.2	3.3	0.8	EL
RasTyc2155-0947	BD-10 5791	21 55 07.21	-09 47 57.2	10.17	0.648	4270.6169	-34.35	2.03	46.8	2.0	44.4	2.9	SA
RasTyc2157-0753	BD-08 5773	21 57 51.37	-07 53 47.4	10.68	0.759	4348.4261	14.05	0.76	27.7	2.9	28.2	0.6	SA
RasTyc2159+0041	TYC 545-521-1	21 59 05.33	+00 41 10.2	10.39	1.090	4346.4434	67.81	2.46	34.4	2.7	35.2	4.8	SA
RasTyc2202+1520	TYC 1680-1993-1	22 02 13.96	+15 20 14.0	9.81	0.873	1795.5156	-0.95	0.15	2.8	0.2	5.0	0.7	EL
RasTyc2202+1520	TYC 1680-1993-1	22 02 13.96	+15 20 14.0	9.81	0.873	2479.5935	-0.81	1.57	< 5	...	6.0	0.6	AU
RasTyc2202+1520	TYC 1680-1993-1	22 02 13.96	+15 20 14.0	9.81	0.873	2480.5537	-0.76	1.31	2.0	2.0	29.7	4.1	AU
RasTyc2202+4831 <sup>†</sup>	BD+47 3668	22 02 26.05	+48 31 14.9	10.42	0.999	4347.4381	-29.68	6.41	145.2	14.9	148.4	5.7	SA
RasTyc2202-0406	BD-04 5601	22 02 30.14	-04 06 11.6	10.17	0.811	4348.4432	5.07	1.47	8.8	1.4	8.0	0.5	SA
RasTyc2202+3108	TYC 2719-2054-1	22 02 57.33	+31 08 46.8	9.89	0.579	1764.4834	-7.37	0.15	18.0	0.9	17.7	0.7	EL
RasTyc2202+3108	TYC 2719-2054-1	22 02 57.33	+31 08 46.8	9.89	0.579	4347.4618	-25.68	1.83	17.8	1.5	18.1	1.0	SA
RasTyc2203+3809	TYC 3198-1809-1	22 03 49.83	+38 09 42.9	9.78	0.717	4346.4700	-23.78	0.50	5.3	1.7	4.1	0.6	SA
RasTyc2204+0236	BD+01 4577	22 04 17.52	+02 36 21.0	9.53	1.133	4347.4526	-26.36	0.58	11.2	3.1	10.8	0.5	SA
RasTyc2206-0102	TYC 5224-1153-1	22 06 25.65	-01 02 43.9	11.11	0.811	4347.4803	-9.65	0.86	4.8	2.2	8.0	1.5	SA
RasTyc2206+5153	TYC 3617-844-1	22 06 34.43	+51 53 11.8	10.65	0.916	4348.4564	-77.19	0.44	12.7	1.4	12.8	0.7	SA
RasTyc2208+2208	HD 210264	22 08 50.40	+22 08 19.6	7.21	0.852	1761.4651	5.74	0.15	4.9	0.3	5.0	0.6	EL
RasTyc2210+1936	HD 210460	22 10 18.96	+19 36 59.6	6.19	0.687	1734.5320	20.41	0.15	2.6	0.2	2.9	0.9	EL
RasTyc2212+1329	HD 210750	22 12 13.38	+13 29 19.8	8.67	0.686	2122.4415	-24.91	0.15	4.4	0.2	3.7	0.7	EL
RasTyc2213+2015	TYC 1689-910-1	22 13 18.14	+20 15 35.5	10.33	0.787	2118.5306	-10.33	0.20	54.2	2.9	50.5	1.4	EL
RasTyc2213+2015*	TYC 1689-910-1	22 13 18.14	+20 15 35.5	10.33	0.787	4346.4906	-8.52	1.73	48.9	3.0	48.5	2.1	SA
RasTyc2218+6951	WW Cep	22 18 27.61	+69 51 40.0	10.69	0.889	4347.5160	-56.77	0.43	10.3	2.3	10.9	0.6	SA
RasTyc2221-0008	BD-00 4347	22 21 16.29	-00 08 35.6	9.47	0.622	4348.4745	-13.99	1.81	24.8				

**Table A.1.** continued.

RasTyc Name	Name	$\alpha$ (2000) h m s	$\delta$ (2000) $^{\circ}$ ' ''	$V^a$ (mag)	$B-V^a$ (mag)	HJD (2450000+)	RV (km s $^{-1}$ )	$\sigma_{RV}$ (km s $^{-1}$ )	$v \sin i^b$ (km s $^{-1}$ )	$\sigma_{v \sin i}$ (km s $^{-1}$ )	$v \sin i^c$ (km s $^{-1}$ )	$\sigma_{v \sin i}$ (km s $^{-1}$ )	Instr. <sup>d</sup>
RasTyc2236+0010	HD 214129	22 36 11.99	+00 10 07.6	9.86	0.667	2473.6016	-30.30	2.86	44.1	1.6	38.0	1.5	AU
RasTyc2236+0010	HD 214129	22 36 11.99	+00 10 07.6	9.86	0.667	4348.4851	7.95	0.87	31.2	0.9	31.9	0.7	SA
RasTyc2236+7032	TYC 4480-965-1	22 36 15.90	+70 32 04.1	10.61	0.961	4346.5461	14.03	0.63	10.1	1.8	11.5	0.8	SA
RasTyc2238+0217	HD 214494	22 38 29.22	+02 17 56.4	8.20	0.571	1734.5729	-9.44	0.15	17.8	0.9	18.3	0.8	EL
RasTyc2239+0406	V403 Peg	22 39 50.66	+04 06 57.1	8.49	0.915	2122.4801	24.01	0.15	2.7	0.2	3.6	0.8	EL
RasTyc2240+1432	HD 214850	22 40 52.53	+14 32 56.0	5.74	0.730	1762.6330	-10.21	0.15	1.4	0.1	1.7	0.8	EL
RasTyc2241+1430	HD 214995	22 41 57.40	+14 30 59.2	5.92	1.099	1735.5903	-28.74	0.15	4.7	0.3	5.3	0.6	EL
RasTyc2242+1900*	TYC 1705-265-1	22 42 04.91	+19 00 49.8	11.00	0.826	2121.5637	-25.54	29.18	235.9	22.0	230.0	23.6	EL
RasTyc2244+1341	HD 215363	22 44 28.34	+13 41 10.9	8.42	0.755	2122.5541	-18.55	0.15	3.0	0.2	3.0	0.7	EL
RasTyc2244+1754	BD+17 4799	22 44 41.49	+17 54 19.0	9.59	0.796	1763.5502	-16.58	0.15	9.0	0.5	8.8	0.6	EL
RasTyc2244+1754	BD+17 4799	22 44 41.49	+17 54 19.0	9.59	0.796	4348.4947	-15.28	0.40	8.3	2.0	8.4	0.5	SA
RasTyc2244+3029	TYC 2736-1564-1	22 44 46.12	+30 29 33.6	10.12	0.863	4346.6249	-37.77	0.87	12.1	2.2	13.4	3.4	SA
RasTyc2246+5749	TYC 3992-349-1	22 46 13.19	+57 49 58.0	10.09	0.603	5108.4770	-33.29	0.42	15.5	2.3	17.5	1.4	FR
RasTyc2250+4926	TYC 3629-2082-1	22 50 10.89	+49 26 14.4	10.17	0.677	4348.5044	-6.55	1.57	39.6	2.1	38.4	1.6	SA
RasTyc2251+8525	BD+84 518	22 51 28.45	+85 25 21.1	10.47	0.911	4346.5623	-15.92	0.45	5.5	1.4	5.8	0.5	SA
RasTyc2252+1730	BD+16 4830	22 52 52.75	+17 30 29.6	9.19	0.853	2121.4997	-24.10	0.15	2.7	0.2	2.7	0.8	EL
RasTyc2253+0338	BD+02 4578	22 53 41.72	+03 38 43.6	10.08	0.771	1764.5397	-2.06	0.15	8.5	0.5	8.9	0.6	EL
RasTyc2256+0235	TYC 572-382-1	22 56 49.53	+02 35 39.2	10.41	0.689	2120.5890	-39.66	0.18	36.9	1.9	33.2	1.1	EL
RasTyc2258-0018	AZ Psc	22 58 52.89	-00 18 57.5	7.43	1.015	1735.6030	-9.46	0.15	4.1	0.2	4.8	1.3	EL
RasTyc2258-0018	AZ Psc	22 58 52.89	-00 18 57.5	7.43	1.015	2209.3604	-15.45	1.41	7.1	5.8	6.5	0.6	AU
RasTyc2258-0018	AZ Psc	22 58 52.89	-00 18 57.5	7.43	1.015	2212.3514	-19.39	1.53	< 5	...	6.1	0.5	AU
RasTyc2259+4016 <sup>i</sup>	CCDM J22594+4017AB	22 59 25.44	+40 16 35.9	9.87	0.761	2474.6025	-9.02	1.57	< 5	...	0.5	0.5	AU
RasTyc2259+4016 <sup>i</sup>	CCDM J22594+4017AB	22 59 25.44	+40 16 35.9	9.87	0.761	2478.5320	-6.68	1.45	< 5	...	0.5	0.5	AU
RasTyc2301+3528	BD+34 4820	23 01 47.79	+35 28 48.7	9.65	1.068	2211.2998	-56.60	1.41	16.6	2.6	17.3	1.5	AU
RasTyc2301+3528	BD+34 4820	23 01 47.79	+35 28 48.7	9.65	1.068	2212.4641	-41.11	1.37	13.7	4.2	16.3	0.6	AU
RasTyc2302+3515	TYC 2758-1743-1	23 02 09.27	+35 15 39.5	9.96	0.891	2984.3523	5.27	1.09	25.5	4.0	28.7	0.6	AU
RasTyc2302+3515	TYC 2758-1743-1	23 02 09.27	+35 15 39.5	9.96	0.891	2986.2554	-15.82	1.38	41.0	2.5	32.3	0.5	AU
RasTyc2303+1713	TYC 1711-1440-1	23 03 23.57	+17 13 14.6	11.03	0.590	1762.5952	-19.18	0.16	11.2	0.6	10.8	2.1	EL
RasTyc2305-0149 <sup>j</sup>	TYC 5242-383-1	23 05 13.18	-01 49 25.4	10.09	0.766	1800.5940	-2.87	0.30	...	...	95.0	15.0	EL
RasTyc2307+3150	TYC 2751-9-1	23 07 24.83	+31 50 14.1	10.53	1.050	4348.5211	-0.84	0.43	5.2	1.7	4.3	1.2	SA
RasTyc2308+0207	HD 218527	23 08 40.84	+02 07 39.4	5.43	0.902	2147.6481	-8.41	0.15	3.4	0.2	4.4	1.0	EL
RasTyc2308+0000	TYC 576-1220-1	23 08 50.46	+00 00 52.8	10.24	0.929	1798.6330	5.30	0.22	46.4	2.5	42.8	5.2	EL
RasTyc2309-0225	BD-03 5579	23 09 37.09	-02 25 54.8	10.80	0.839	1797.5883	-12.16	0.15	12.7	0.7	12.1	1.1	EL
RasTyc2309+1425	HD 218687	23 09 57.17	+14 25 36.3	6.54	0.602	1734.5477	17.76	0.15	9.7	0.5	9.4	0.7	EL
RasTyc2309+1425	HD 218687	23 09 57.17	+14 25 36.3	6.54	0.602	2209.2784	-15.13	1.37	10.7	3.8	12.2	2.1	AU
RasTyc2309+1425	HD 218687	23 09 57.17	+14 25 36.3	6.54	0.602	2212.3347	-22.99	1.31	9.4	5.3	10.5	1.0	AU
RasTyc2317+0941	BD+08 5036	23 17 32.23	+09 41 36.8	9.75	1.088	1764.5881	26.53	0.15	4.8	0.3	5.0	1.0	EL
RasTyc2318+4458	TYC 3229-143-1	23 18 48.11	+44 58 15.7	9.92	0.788	5109.4908	-19.93	0.24	9.9	2.9	3.6	3.5	FR
RasTyc2320+7414	V395 Cep	23 20 52.07	+74 14 07.1	10.29	0.796	4346.5782	-5.69	1.00	39.1	1.6	40.3	1.2	SA
RasTyc2321+0211	HD 220119	23 21 11.28	+02 11 50.5	7.43	0.939	1763.6274	-0.80	0.15	4.5	0.2	5.1	1.4	EL
RasTyc2321+0211	HD 220119	23 21 11.28	+02 11 50.5	7.43	0.939	1764.6188	-0.83	0.15	4.4	0.2	4.8	0.6	EL
RasTyc2321+4510	HD 220221	23 21 44.29	+45 10 34.4	8.14	1.053	5109.4617	-13.52	0.21	12.4	0.5	1.6	0.5	FR
RasTyc2321+0721	TYC 584-343-1	23 21 56.36	+07 21 33.0	10.85	0.702	2148.5519	6.05	0.15	14.7	0.8	14.3	0.6	EL
RasTyc2323-0635	HD 220338	23 23 01.18	-06 35 43.6	9.08	1.098	1763.5958	3.02	0.15	27.5	1.5	27.6	0.8	EL
RasTyc2323-0635	HD 220338	23 23 01.18	-06 35 43.6	9.08	1.098	1796.6002	2.70	0.15	26.6	1.4	27.5	0.7	EL
RasTyc2323-0635	HD 220338	23 23 01.18	-06 35 43.6	9.08	1.098	2147.5897	4.06	0.16	26.7	1.4	26.8	0.8	EL
RasTyc2324+0733	NX Aqr	23 24 06.25	-07 33 02.7	7.62	0.686	1796.6331	4.00	0.15	2.5	0.1	2.5	1.0	EL
RasTyc2324+6215	TYC 4283-219-1	23 24 40.37	+62 15 51.1	9.82	0.582	2574.2668	-9.95	1.38	27.7	4.7	31.7	2.2	AU
RasTyc2324+6215	TYC 4283-219-1	23 24 40.37	+62 15 51.1	9.82	0.582	2575.3977	-7.60	1.41	49.4	2.7	35.6	1.3	AU
RasTyc2328+4522	TYC 3637-396-1	23 28 27.48	+45 22 40.6	10.69	0.584	4348.5375	-1.44	0.74	29.2	4.3	31.4	1.4	SA
RasTyc2331+8124	TYC 4614-981-1	23 31 29.96	+81 42 42.6	10.06	0.744	4346.5919	47.26	1.72	4.9	0.4	6.4	0.7	SA
RasTyc2340-0402	BD-04 5927	23 40 06.09	-04 02 55.1	10.01	0.565	1799.6315	15.73	0.19	37.4	2.0	36.2	3.2	EL
RasTyc2340-0228	BD-03 5686	23 40 08.35	-02 28 49.6	10.50	0.697	2147.5573	-20.27	0.18	30.0	1.6	29.6	1.3	EL
RasTyc2341-0837	HD 222522	23 41 23.80	-08 37 47.1	9.64	0.730	2118.5822	6.09	0.15	4.1	0.2	4.6	0.9	EL
RasTyc2343+5038	BD+49 4204	23 43 58.22	+50 38 01.3	9.66	0.598	2247.3245	-5.01	1.42	13.7	3.7	13.8	0.6	AU
RasTyc2343+5038	BD+49 4204	23 43 58.22	+50 38 01.3	9.66	0.598	2260.3708	-2.79	1.26	14.9	2.0	...	...	AU
RasTyc2348+4615	TYC 3638-993-1	23 48 33.85	+46 15 10.5	9.90	0.883	5121.4708	-44.65	0.23	8.1	2.6	3.4	3.2	FR
RasTyc2348+4614	TYC 3638-1539-1	23 48 35.53	+46 14 51.1	9.15	0.647	5121.4370	20.49	0.61	38.1	4.0	39.7	2.0	FR
RasTyc2351+7739	TYC 4606-740-1	23 51 17.29	+77 39 35.3	10.59	1.076	4347.6247	-9.05	0.72	24.3	3.3	25.3	3.3	SA
RasTyc2352-1143	HD 223728	23 52 10.24	-11 43 14.5	8.65	0.613	1801.5837	0.49	0.16	18.9	1.0	19.4	2.9	EL
RasTyc2353+4413	TYC 3245-1421-1	23 53 10.34	+44 13 58.0	9.67	0.720	2239.2869	-15.47	1.41	7.2	5.8	7.8	1.4	AU
RasTyc2353+4413	TYC 3245-1421-1	23 53 10.34	+44 13 58.0	9.67	0.720	2245.2769	-15.05	1.53	< 5	...	7.2	1.1	AU
RasTyc2358+5140	TYC 3651-546-1	23 58 16.09	+51 40 39.2	10.58	0.920	4346.6087	-13.71	0.86	36.6	4.7	37.1	0.9	SA

<sup>a</sup> From the TYCHO catalog (ESA 1997).<sup>b</sup>  $v \sin i$  derived from the FWHM of the CCF.<sup>c</sup>  $v \sin i$  derived with ROTFIT.<sup>d</sup> Spectrograph: SA = SARG, EL = ELODIE, AU = AURELIE, FR = FRESCO.<sup>e</sup> Coordinates from 2MASS catalog (Cutri et al. 2003).<sup>f</sup> Close visual pair ( $\$

**Table A.2.** Radial (RV) and rotational ( $v \sin i$ ) velocities for the components of SB2 binaries.

RasTyc Name	Name	$\alpha$ (2000) h m s	$\delta$ (2000) $^{\circ}$ ' ''	$V^a$ (mag)	HJD (2450000+)	$RV_1$ (km s $^{-1}$ )	$\sigma$	$RV_2$ (km s $^{-1}$ )	$\sigma$	$v \sin i_1$ (km s $^{-1}$ )	$\sigma$	$v \sin i_2$ (km s $^{-1}$ )	$\sigma$	Instr. <sup>b</sup>
RasTyc0013+7702	TYC 4496-780-1	00 13 40.52	+77 02 10.9	9.76	2226.2918	-1.30	1.57	...	...	31.7	2.3	...	...	AU
RasTyc0013+7702	TYC 4496-780-1	00 13 40.52	+77 02 10.9	9.76	2235.3276	-5.30	1.96	45.27	1.34	41.8	1.4	< 5	...	AU
RasTyc0013+7702	TYC 4496-780-1	00 13 40.52	+77 02 10.9	9.76	5108.5549	-5.78	0.70	44.73	2.74	28.2	9.9	15.6	9.0	FR
RasTyc0013+7702	TYC 4496-780-1	00 13 40.52	+77 02 10.9	9.76	5118.4417	-6.78	0.62	47.27	3.87	30.0	6.7	26.2	7.8	FR
RasTyc0020+5711	TYC 3661-1206-1	00 20 47.59	+57 11 45.1	10.06	2987.2483	-11.78	1.27	-69.15	1.52	22.0	1.4	< 5	...	AU
RasTyc0032+5558	HD 236456	00 32 09.35	+55 58 35.2	9.53	2666.2915	2.75	4.13	-23.93	2.95	< 5	...	55.8	1.2	AU
RasTyc0032+5558	HD 236456	00 32 09.35	+55 58 35.2	9.53	2601.2847	0.85	1.66	-19.42	1.39	< 5	...	43.3	0.5	AU
RasTyc0033+5315 <sup>c</sup>	TYC 3654-1907-1	00 33 55.90	+53 15 41.5	9.94	4347.6497	-9.45	0.23	36.87	9.45	3.4	2.9	14.0	8.5	SA
RasTyc0038+3325	TYC 2279-359-1	00 38 44.96	+33 25 34.5	10.27	2987.3413	6.32	1.50	...	...	28.7	2.0	...	...	AU
RasTyc0039+7905	BD+78 19	00 39 40.13	+79 05 30.8	9.60	2581.3381	-8.66	1.38	...	...	20.2	5.1	...	...	AU
RasTyc0039+7905	BD+78 19	00 39 40.13	+79 05 30.8	9.60	2584.3640	-9.68	1.37	...	...	12.0	3.5	...	...	AU
RasTyc0039+7905	BD+78 19	00 39 40.13	+79 05 30.8	9.60	5077.6191	-9.59	0.41	...	...	...	...	...	...	FR
RasTyc0039+7905	BD+78 19	00 39 40.13	+79 05 30.8	9.60	5078.6177	-23.00	0.71	4.47	0.77	6.8	5.0	11.9	5.1	FR
RasTyc0039+7905	BD+78 19	00 39 40.13	+79 05 30.8	9.60	5108.5172	7.96	0.71	-30.30	0.82	15.1	5.9	11.8	2.6	FR
RasTyc0039+7905	BD+78 19	00 39 40.13	+79 05 30.8	9.60	5110.5424	-20.37	0.72	4.26	0.70	7.3	3.4	10.4	4.1	FR
RasTyc0055+5046	TYC 3274-955-1	00 55 50.28	+50 46 12.6	9.99	2988.3284	53.25	2.01	23.46	2.81	< 5	...	61.7	1.3	AU
RasTyc0104+5533	TYC 3672-1578-1	01 04 33.02	+55 33 29.0	10.46	4348.5993	-14.77	0.52	-47.40	1.29	3.7	2.8	27.3	6.0	SA
RasTyc0110+5100	TYC 3276-1291-1	01 10 00.27	+51 00 27.8	10.19	4346.6661	-23.02	0.34	17.74	0.91	3.7	2.1	7.4	3.7	SA
RasTyc0129+3303	HN Psc	01 29 47.94	+33 03 36.1	10.65	4348.6915	43.73	17.18	-112.86	20.63	81.4	27.6	112.9	28.1	SA
RasTyc0139+7018	TYC 4314-1757-1	01 39 25.89	+70 18 50.1	10.25	4347.6776	21.65	0.31	-21.85	2.03	5.7	3.4	16.3	6.6	SA
RasTyc0146+3317	TYC 2298-964-1	01 46 33.48	+33 17 11.7	10.00	2990.2585	-17.75	6.05	9.10	2.99	< 5	...	40.1	1.7	AU
RasTyc0315+5741	TYC 3710-247-1	03 15 32.73	+57 41 23.8	10.21	4348.7382	6.75	0.67	-82.50	1.78	34.1	6.7	24.2	4.0	SA
RasTyc0326+4243	BD+42 765	03 26 38.82	+42 43 25.3	9.82	2665.3008	65.90	11.30	-226.90	18.00	...	...	...	...	AU
RasTyc0409+5558	BD+55 849	04 09 58.60	+55 58 52.6	10.44	4459.4190	-40.67	5.52	95.25	8.03	84.6	6.5	51.1	12.2	SA
RasTyc0412+4616A	TYC 3328-2470-1	04 12 14.74	+46 16 15.5	10.52	4459.4776	-97.70	2.25	104.25	3.81	52.6	9.1	46.7	10.0	SA
RasTyc0413+3832	BD+38 859	04 13 28.59	+38 32 26.6	9.67	2669.3423	-4.05	1.43	...	...	54.4	2.4	...	...	AU
RasTyc0413+3832	BD+38 859	04 13 28.59	+38 32 26.6	9.67	2673.2935	69.14	1.11	...	...	36.4	6.1	...	...	AU
RasTyc0415+3129	HD 281777	04 15 28.92	+31 29 55.8	9.68	2240.5223	-118.60	15.00	79.50	18.00	...	...	...	...	AU
RasTyc0423+5556	TYC 3723-1082-1	04 23 15.14	+55 56 53.0	9.77	2222.6230	12.92	1.52	0.98	2.02	< 5	...	43.5	0.5	AU
RasTyc0423+5556	TYC 3723-1082-1	04 23 15.14	+55 56 53.0	9.77	2230.4290	0.45	1.11	...	...	35.5	5.1	...	...	AU
RasTyc0423+5556	TYC 3723-1082-1	04 23 15.14	+55 56 53.0	9.77	2234.5657	19.18	2.60	-0.17	3.11	< 5	...	63.7	1.5	AU
RasTyc0511+3707	HD 280583	05 11 51.55	+37 07 36.4	9.51	2218.5610	-35.82	2.92	122.08	8.29	...	...	...	...	AU
RasTyc0511+3707	HD 280583	05 11 51.55	+37 07 36.4	9.51	2224.6148	24.61	6.73	-87.94	2.18	...	...	...	...	AU
RasTyc0511+3707	HD 280583	05 11 51.55	+37 07 36.4	9.51	2225.6592	-37.52	5.67	120.61	5.28	...	...	...	...	AU
RasTyc0524+5439	V607 Aur	05 24 24.58	+54 39 22.2	10.33	4459.6818	-94.15	1.58	98.77	2.38	30.2	7.4	27.9	6.4	SA
RasTyc0604+5142	TYC 3386-868-1	06 04 51.40	+51 42 00.8	9.35	4459.7215	2.34	1.50	53.24	0.61	28.7	4.5	4.9	2.5	SA
RasTyc0608+6804	TYC 4345-1307-1	06 08 04.79	+68 04 59.7	10.08	4459.7316	112.43	4.63	-93.74	3.09	32.6	5.5	37.5	6.7	SA
RasTyc0609+3229	TYC 2424-396-1	06 09 51.09	+32 29 48.7	10.05	2990.5056	14.78	1.49	-7.32	1.45	< 5	...	< 5	...	AU
RasTyc0653+3851	TYC 2942-2009-1	06 53 00.11	+38 51 52.9	9.86	2985.5321	-60.34	7.81	187.42	13.59	...	...	...	...	AU
RasTyc0702+4448	TYC 2955-479-1	07 02 45.77	+44 48 05.6	9.94	2993.6623	-26.06	1.49	-135.95	1.34	8.5	3.0	1.4	22.7	AU
RasTyc0707+4017	BD+40 1796	07 07 52.87	+40 17 07.7	10.01	4459.7978	15.21	0.53	-35.07	3.62	17.2	5.0	7.5	4.9	SA
RasTyc1502+1546	HD 133162	15 02 38.99	+15 46 29.3	9.84	2465.4009	-81.98	2.08	-49.88	4.55	62.6	1.4	< 5	...	AU
RasTyc1502+1546	HD 133162	15 02 38.99	+15 46 29.3	9.84	2467.3860	0.05	5.24	-31.73	3.05	< 5	...	71.7	1.3	AU
RasTyc1525+6142	TYC 4181-507-1	15 25 52.78	+61 42 21.5	10.89	5726.4030	-120.05	1.86	98.46	11.66	69.2	21.0	80.3	20.0	SA
RasTyc1527+6515	TYC 4187-96-1	15 27 56.19	+65 15 33.3	10.17	5726.3798	34.94	0.78	-55.55	4.05	20.9	2.8	22.4	6.7	SA
RasTyc1533+0809	BD+08 3048	15 33 45.30	+08 08 59.6	10.16	5727.4255	29.67	1.81	-82.51	1.99	37.8	6.0	28.5	4.8	SA
RasTyc1530+1440B	HIP 77628	15 50 54.36	+14 40 33.9	10.06	4144.7518	-39.01	0.35	5.31	0.90	10.0	2.3	9.4	2.9	SA
RasTyc1605+1028	BD+10 2953	16 05 02.23	+10 28 54.6	9.21	4148.6430	-50.91	0.80	-15.19	0.92	10.5	3.0	5.0	3.6	SA
RasTyc1606+0919	TYC 945-949-1	16 06 29.27	+09 19 02.5	10.06	4144.7694	-0.65	0.24	110.35	4.36	6.4	3.9	15.2	11.8	SA
RasTyc1607+0238	TYC 370-538-1	16 07 04.36	+02 38 23.8	9.53	2438.4416	-16.41	1.32	-53.21	1.52	13.5	1.6	7.1	3.4	AU
RasTyc1607+0238	TYC 370-538-1	16 07 04.36	+02 38 23.8	9.53	2466.4475	-12.68	1.45	-58.67	1.31	11.2	2.4	1.4	23.8	AU
RasTyc1620+2436	V1079 Her	16 20 13.72	+24 36 11.1	9.48	2439.4846	17.91	1.57	-45.20	1.38	18.2	1.8	19.6	1.6	AU
RasTyc1620+2436	V1079 Her	16 20 13.72	+24 36 11.1	9.48	2441.5015	41.48	1.52	-69.37	1.31	16.4	1.9	16.4	1.9	AU
RasTyc1620+2436	V1079 Her	16 20 13.72	+24 36 11.1	9.48	2443.3980	40.14	1.40	-69.29	1.30	18.8	1.8	18.8	1.8	AU
RasTyc1624+4555	BD+46 2173	16 24 10.45	+45 55 26.0	9.94	4148.6916	...	...	...	...	250 <sup>c</sup>	...	...	...	SA
RasTyc1629+3212	BD+32 2733	16 29 12.03	+32 12 29.9	9.14	4148.7118	-80.96	1.24	28.04	1.91	21.2	3.4	6.6	4.8	SA
RasTyc1639+2243	BD+23 2969	16 39 29.33	+22 43 59.6	9.99	4993.3633	-38.86	1.36	7.20	2.72	31.8	8.5	33.0	8.5	FR
RasTyc1700+2001	BD+20 3376	17 00 33.85	+20 01 33.9	9.99	4993.4370	-23.59	0.65	17.44	3.18	24.3	4.8	18.5	12.8	FR
RasTyc1702+4713 <sup>c</sup>	TYC 3501-626-1	17 02 48.85	+47 13 06.5	10.08	4215.4693	-7.85	0.21	-38.01	0.47	13.2	3.8	1.9	1.4	SA
RasTyc1703+2453	TYC 2064-1273-1	17 03 13.52	+24 53 21.1	9.83	4149.7208	30.22	0.89	-86.97	0.83	11.5	4.2	6.1	6.3	SA
RasTyc1718+2128	TYC 1548-2040-1	17 18 00.31	+21 28 09.4	9.96	4210.6407	20.21	1.50	-69.82	2.58	34.3	3.5	36.7	5.2	SA
RasTyc1736+5523	HD 238727	17 36 42.35	+55 23 02.5	10.11	5111.3185	-45.34	0.61	36.66	2.89	27.0	3.1	28.6	13.3	FR
RasTyc1744+7452	BD+74 736	17 44 49.84	+74 52 26.9	9.59	2438.4775	88.42	0.97	-106.8						

**Table A.2.** continued.

RasTyc Name	Name	$\alpha$ (2000) h m s	$\delta$ (2000) $^{\circ}$ ' ''	V <sup>a</sup> (mag)	HJD (2450000+)	RV <sub>1</sub> (km s <sup>-1</sup> )	$\sigma$	RV <sub>2</sub> (km s <sup>-1</sup> )	$\sigma$	$v \sin i_1$ (km s <sup>-1</sup> )	$\sigma$	$v \sin i_2$ (km s <sup>-1</sup> )	$\sigma$	Instr. <sup>b</sup>
RasTyc1845+2841	TYC 2120-388-1	18 45 10.88	+28 41 10.4	9.89	3578.4612	24.35	3.48	-54.93	4.62	...	...	...	...	AU
RasTyc1845+2841	TYC 2120-388-1	18 45 10.88	+28 41 10.4	9.89	3581.4358	-75.30	3.94	20.55	6.19	...	...	...	...	AU
RasTyc1852+6223	BD+62 1656	18 52 00.58	+62 23 59.9	9.31	4301.6923	-50.96	0.25	39.14	1.36	4.5	1.9	6.6	5.5	SA
RasTyc1856+0217	TYC 453-327-1	18 56 09.59	+02 17 43.9	9.95	4210.7100	-12.82	0.58	-63.21	1.51	9.3	4.1	10.2	8.2	SA
RasTyc1900+0435	BD+04 3943	19 00 46.23	+04 35 57.9	9.35	4210.7196	-1.71	0.71	-115.94	1.35	4.8	3.3	12.2	9.1	SA
RasTyc1902+1416	BD+14 3751	19 02 13.43	+14 16 53.6	10.12	4249.6741	-57.69	0.97	5.12	1.76	14.9	4.1	12.6	4.0	SA
RasTyc1905+2319	BD+23 3557	19 05 47.78	+23 19 22.0	9.59	4249.6982	-66.64	16.16	199.68	13.16	145.8	9.5	117.8	41.9	SA
RasTyc1914+6229	BD+62 1699	19 14 19.78	+62 29 57.2	9.95	4270.5264	-19.18	0.48	-71.25	1.76	4.7	3.8	29.6	8.1	SA
RasTyc1931+1143 <sup>d</sup>	HD 183957	19 31 36.98	+11 43 26.2	8.24	2120.3379	-73.93	0.15	19.73	0.15	3.8	0.2	3.9	0.5	EL
RasTyc1947+0105	HD 187003	19 47 33.32	+01 05 20.0	6.78	1797.3101	-21.11	0.15	38.75	0.15	5.1	0.3	4.9	0.6	EL
RasTyc1958+4301*	KIC 7477572	19 58 37.62	+43 01 02.5	9.54	4346.3606	-36.59	2.20	-68.66	1.41	24.5	5.5	13.8	6.3	SA
RasTyc2018+5636	V2477 Cyg	20 18 58.95	+56 36 19.0	9.94	4348.3539	56.32	13.91	-222.12	7.94	167.0	26.3	105.1	33.5	SA
RasTyc2025+3631	TYC 2697-941-1	20 25 09.60	+36 31 15.4	10.36	2120.4759	6.60	0.15	-42.75	0.16	7.3	0.4	1.2	0.5	EL
RasTyc2029+1227	TYC 1095-349-1	20 29 32.84	+12 27 31.1	9.74	3581.4871	-93.25	1.29	34.93	2.47	17.0	1.5	14.8	1.7	AU
RasTyc2029+1227	TYC 1095-349-1	20 29 32.84	+12 27 31.1	9.74	3582.5264	-3.01	1.34	-64.48	1.64	18.4	1.5	10.4	2.2	AU
RasTyc2031+3332	V2425 Cyg	20 31 07.72	+33 32 33.6	8.34	2147.4005	-31.25	0.15	-16.88	0.15	7.2	0.4	5.6	0.6	EL
RasTyc2044+2916	HD 335070	20 44 58.09	+29 16 21.4	10.80	2147.4449	96.48	0.69	-107.43	1.03	84.4	4.6	82.9	4.6	EL
RasTyc2044+2916	HD 335070	20 44 58.09	+29 16 21.4	10.80	1798.4077	-11.95	0.16	...	...	80.3 <sup>c</sup>	6.7	...	...	EL
RasTyc2051+4547	BD+45 3306	20 51 31.46	+45 47 14.3	9.86	4347.3761	-79.84	0.60	...	...	7.8	1.9	...	...	SA
RasTyc2051+4547	BD+45 3306	20 51 31.46	+45 47 14.3	9.86	5077.5466	-28.37	0.28	-95.06	2.60	16.6	2.2	23.8	8.0	FR
RasTyc2054-0808	BD-08 5514	20 54 27.81	-08 08 33.2	9.61	4301.6708	67.75	3.56	-103.92	2.47	50.9	5.4	30.7	6.8	SA
RasTyc2058+3510	CG Cyg	20 58 13.45	+35 10 29.6	10.07	1796.4274	-50.0	4.0	89.0	5.0	119.0	6.3	84.3	4.4	EL
RasTyc2058+6317	BD+62 1880	20 58 16.40	+63 17 38.8	9.75	4346.3885	37.19	0.77	-8.25	1.29	11.4	4.7	19.0	5.1	SA
RasTyc2102+2748	ER Vul	21 02 25.85	+27 48 26.4	7.36	1733.4096	93.1	7.3	-152.4	6.9	105.8	5.7	102.3	6.1	EL
RasTyc2103+3413	BD+33 4140	21 03 48.71	+34 13 13.4	10.08	1761.3788	6.32	0.17	-28.80	0.17	32.4	1.7	21.9	1.2	EL
RasTyc2103+3413	BD+33 4140	21 03 48.71	+34 13 13.4	10.08	4347.3874	5.54	1.15	-32.11	0.58	28.5	6.3	12.0	5.9	SA
RasTyc2103+3413	BD+33 4140	21 03 48.71	+34 13 13.4	10.08	5078.4865	-5.55	0.84	...	...	44.9	2.1	...	...	FR
RasTyc2109+6253	BD+62 1902	21 09 07.65	+62 53 19.5	9.88	4347.3966	-144.31	11.77	140.70	17.11	143.4	10.6	111.1	20.9	SA
RasTyc2110+3323	TYC 2706-22-1	21 10 56.16	+33 23 13.1	10.20	1736.5037	54.31	0.15	-64.53	0.16	13.9	0.7	4.7	0.6	EL
RasTyc2117+4330	TYC 3181-914-1	21 17 35.44	+43 30 52.3	10.50	1762.5273	-21.98	0.82	35.67	0.94	9.2	1.3	0.0	1.6	EL
RasTyc2129+3355	TYC 2712-2338-1	21 29 02.69	+33 55 55.6	10.85	2150.4887	53.81	49.89	-237.26	47.03	244.2	12.9	157.2	8.3	EL
RasTyc2131+2320	LO Peg	21 31 01.63	+23 20 08.6	9.24	1733.4379	-2.08	0.22	-57.79	0.23	48.2	2.5	39.3	2.1	EL
RasTyc2134+5632	HD 239702	21 34 34.34	+56 32 48.0	9.72	2443.5735	-42.16	1.88	-64.11	2.10	45.5	0.7	< 5	...	AU
RasTyc2134+5632	HD 239702	21 34 34.34	+56 32 48.0	9.72	2462.5950	1.07	1.49	-22.53	1.80	< 5	...	60.8	1.7	AU
RasTyc2140+2748	BD+27 4129	21 40 05.41	+27 48 29.5	10.60	2119.4738	19.36	0.15	-41.06	0.18	16.3	0.9	3.2	0.5	EL
RasTyc2151+0956	BD+09 4914	21 51 24.88	+09 56 22.2	10.03	4347.4248	23.10	0.34	-19.91	2.58	8.8	2.1	7.2	5.3	SA
RasTyc2156+0515	TYC 553-33-1	21 56 27.19	+05 15 56.7	9.74	2479.4976	-87.68	1.29	64.39	1.31	13.5	1.6	2.0	14.1	AU
RasTyc2156+0515	TYC 553-33-1	21 56 27.19	+05 15 56.7	9.74	2482.5432	-82.59	1.29	61.33	1.31	14.5	1.7	14.6	1.7	AU
RasTyc2159+1602 <sup>d</sup>	OT Peg	21 59 40.16	+16 02 18.5	9.77	1735.5212	-15.44	0.15	-48.01	0.17	9.0	0.5	9.4	0.5	EL
RasTyc2159+1602 <sup>d</sup>	OT Peg	21 59 40.16	+16 02 18.5	9.77	2478.5796	-28.32	1.38	...	...	10.4	2.7	...	...	AU
RasTyc2159+1602 <sup>d</sup>	OT Peg	21 59 40.16	+16 02 18.5	9.77	2483.5872	8.15	1.45	...	...	6.0	3.7	...	...	AU
RasTyc2159+0302	BD+02 4456	21 59 59.90	+03 02 25.0	9.77	2479.5481	42.44	1.29	-68.37	1.56	13.5	1.6	13.5	1.6	AU
RasTyc2159+0302	BD+02 4456	21 59 59.90	+03 02 25.0	9.77	2482.5803	49.28	1.32	-75.89	1.34	14.5	1.7	14.6	1.7	AU
RasTyc2202+4831 <sup>t</sup>	BD+47 3668	22 02 57.33	+31 08 46.8	9.89	4347.4381	-81.47	21.50	42.89	16.94	78.1	26.1	79.6	23.1	SA
RasTyc2206+1005A	HD 209845	22 06 10.58	+10 05 36.5	7.11	2150.4603	32.72	0.17	-25.09	0.32	28.0	1.5	27.0	1.5	EL
RasTyc2206+1005A	HD 209845	22 06 10.58	+10 05 36.5	7.11	2475.5757	14.44	1.11	-45.00	1.77	20.9	4.9	...	...	AU
RasTyc2206+1005A	HD 209845	22 06 10.58	+10 05 36.5	7.11	2476.5798	2.00	1.38	...	...	24.8	1.9	...	...	AU
RasTyc2212+3754	TYC 3199-3329-1	22 12 14.56	+37 54 56.4	10.63	4347.5005	-74.09	1.15	53.33	2.19	9.5	4.8	24.2	6.9	SA
RasTyc2213+2015*	TYC 1689-910-1	22 13 18.14	+20 15 35.5	10.33	4346.4906	9.66	1.72	-29.87	1.86	25.5	6.7	22.7	4.5	SA
RasTyc2213+8445	BD+84 507	22 13 19.94	+84 45 36.9	9.65	2482.4724	26.20	1.38	-11.49	1.38	30.1	0.8	19.8	...	AU
RasTyc2213+8445	BD+84 507	22 13 19.94	+84 45 36.9	9.65	3216.5720	32.55	1.50	-12.12	1.52	25.8	1.9	23.7	1.6	AU
RasTyc2214+3356 <sup>d</sup>	BD+33 4462	22 14 28.27	+33 56 29.6	8.97	1733.5008	-65.18	0.16	20.47	0.23	9.2	0.5	30.1	1.6	EL
RasTyc2222+2814B	BD+27 4302p	22 22 29.06	+28 14 38.6	9.95	1733.5518	24.38	0.16	-32.71	0.19	22.8	1.2	18.5	1.0	EL
RasTyc2222+2814B	BD+27 4302p	22 22 29.06	+28 14 38.6	9.95	4347.5607	70.51	0.93	-80.05	2.47	21.8	3.7	13.5	4.3	SA
RasTyc2222+3021	KX Peg	22 22 32.57	+30 21 27.0	7.55	1734.5085	26.52	0.15	-22.53	0.19	9.0	0.5	30.2	1.6	EL
RasTyc2224+1653	HD 212525	22 24 37.33	+16 53 48.8	8.30	2119.6232	-42.52	0.15	-8.52	0.15	5.1	0.3	4.8	0.6	EL
RasTyc2224+0637	BD+05 5019	22 24 58.42	+06 37 01.4	9.57	1761.5927	-100.39	0.36	111.99	0.56	52.1	2.8	18.5	1.3	EL
RasTyc2224+0637	BD+05 5019	22 24 58.42	+06 37 01.4	9.57	5110.4077	-68.60	0.94	74.11	3.38	49.5	8.9	35.6	6.7	FR
RasTyc2226-0050	BD-01 4295	22 26 53.26	-00 50 39.2	10.36	4347.5390	3.97	0.28	33.41	0.79	7.2	3.0	5.3	3.9	SA
RasTyc2233+5001	BD+49 3885	22 33 02.45	+50 01 10.9	9.84	3262.4890	-1.35	1.51	...	...	16.7	3.0	...	...	AU
RasTyc2233+5001	BD+49 3885	22 33 02.45	+50 01 10.9	9.84	3264.4143	-4.03	1.33	...	...	12.7	3.8	...	...	AU
RasTyc2233+1639	BD+15 4671	22 33 28.44	+16 39 01.7	9.43	1761.5433	56.29	0.41	-82.78	0.43	62.7	3.4	55.2	3.0	EL
RasTyc2233+1639	BD+15 4671	22 33 28.44	+16 39 01.7	9.43	5109.4380	-9.74	0.73	...	...</					

**Table A.2.** continued.

RasTyc Name	Name	$\alpha$ (2000) h m s	$\delta$ (2000) $^{\circ} \text{ } '$ ''	$V^a$ (mag)	HJD (2450000+)	$RV_1$ (km s $^{-1}$ )	$\sigma$	$RV_2$ (km s $^{-1}$ )	$\sigma$	$v \sin i_1$ (km s $^{-1}$ )	$\sigma$	$v \sin i_2$ (km s $^{-1}$ )	$\sigma$	Instr. <sup>b</sup>
RasTyc2322+6113	TYC 4279-1821-1	23 22 40.03	+61 13 33.3	9.90	2230.3281	33.13	1.49	-53.17	1.53	11.8	2.4	1.8	17.5	AU
RasTyc2322+6113	TYC 4279-1821-1	23 22 40.03	+61 13 33.3	9.90	2234.3389	-19.19	1.59	4.75	1.80	10.6	2.2	8.2	2.7	AU
RasTyc2330+0126	TYC 585-897-1	23 30 07.59	+01 26 04.4	10.53	1799.5573	13.30	0.24	-60.23	0.42	48.1	2.5	29.3	1.7	EL
RasTyc2339-0310	BD-03 5681	23 39 17.55	-03 10 38.7	10.66	1797.6419	-41.19	0.15	32.02	0.17	9.0	0.5	4.2	0.6	EL
RasTyc2348+5744	V651 Cas	23 48 33.48	+57 44 56.7	10.21	2984.3020	5.61	2.49	-59.20	5.87	40.0	3.0	46.2	4.2	AU
RasTyc2348+5744	V651 Cas	23 48 33.48	+57 44 56.7	10.21	2986.3049	-8.43	4.55	-58.90	6.43	45.5	4.0	41.2	3.5	AU
RasTyc2351-0636 <sup>c</sup>	HD 223688	23 51 46.78	-06 36 47.0	8.73	2121.6117	15.85	0.30	26.18	0.30	2.6	0.7	2.6	0.7	EL
RasTyc2351-0636	HD 223688	23 51 46.78	-06 36 47.0	8.73	2209.4329	-1.67	1.38	...	...	22.0 <sup>e</sup>	4.0	...	...	AU
RasTyc2351-0636	HD 223688	23 51 46.78	-06 36 47.0	8.73	2212.3741	15.98	1.45	...	...	5.7 <sup>c</sup>	0.8	...	...	AU
RasTyc2351-0636	HD 223688	23 51 46.78	-06 36 47.0	8.73	2214.3555	15.31	1.57	...	...	8.1 <sup>c</sup>	1.8	...	...	AU
RasTyc2354+3645	TYC 2780-2053-1	23 54 39.11	+36 45 16.1	10.18	4348.5692	17.13	0.34	-215.12	14.58	164.7	15.6	100.5	24.3	SA

<sup>a</sup> From the TYCHO catalog (ESA 1997).<sup>b</sup> Spectrograph: SA = SARG, EL = ELODIE, AU = AURELIE, FR = FRESCO.<sup>c</sup> Blended components; combined  $v \sin i$ .<sup>d</sup> The full set of RV data and orbital solution are reported in Frasca et al. (2006). Unpublished AURELIE data have been used here.<sup>\*</sup> Double-peaked CCF. Possible SB2 with blended lines.<sup>†</sup> Asymmetric CCF. Possible SB2 with blended lines.<sup>◊</sup> Small-amplitude secondary peak in the CCF. Likely SB2 with a faint component.<sup>•</sup> A small-amplitude third peak in the CCF at  $RV \simeq -1.0 \text{ km s}^{-1}$ . SB3?**Table A.3.** Radial (RV) and rotational ( $v \sin i$ ) velocities for the components of SB3 binaries.

RasTyc Name	Name	$\alpha$ (2000) h m s	$\delta$ (2000) $^{\circ} \text{ } '$ ''	HJD (2450000+)	$RV_1$ (km s $^{-1}$ )	$RV_2$ (km s $^{-1}$ )	$RV_3$ (km s $^{-1}$ )	$v \sin i_1$ (km s $^{-1}$ )	$v \sin i_2$ (km s $^{-1}$ )	$v \sin i_3$ (km s $^{-1}$ )
<b>SARG</b>										
RasTyc1831+2515	TYC 2110-348-1	18 31 01.05	+25 15 31.5	4210.7296	-44.89 $\pm$ 0.83	71.33 $\pm$ 2.10	15.42 $\pm$ 0.22	11.2 $\pm$ 5.6	17.6 $\pm$ 5.8	2.0 $\pm$ 2.3
RasTyc2052+4258 <sup>a</sup>	BD+42 3895	20 52 57.27	+42 58 25.7	1797.3516	-20.38 $\pm$ 0.15	-52.74 $\pm$ 0.17	9.98 $\pm$ 0.16	0.0 $\pm$ 0.2	9.6 $\pm$ 0.5	6.5 $\pm$ 0.4
RasTyc2259-0431	TYC 5238-1223-1	22 59 02.13	-04 31 35.3	4347.6046	8.68 $\pm$ 0.29	-32.54 $\pm$ 0.76	-11.60 $\pm$ 0.83	2.7 $\pm$ 2.0	6.6 $\pm$ 2.6	4.2 $\pm$ 1.6
<b>ELODIE</b>										
RasTyc2052+4258 <sup>a</sup>	BD+42 3895	20 52 57.27	+42 58 25.7	1797.3516	-20.38 $\pm$ 0.15	-52.74 $\pm$ 0.17	9.98 $\pm$ 0.16	0.0 $\pm$ 0.2	9.6 $\pm$ 0.5	6.5 $\pm$ 0.4
RasTyc2206+1005B	BD+09 4984B	22 06 11.82	+10 05 28.7	1795.5746	-40.00 $\pm$ 0.54	65.75 $\pm$ 0.48	...	52.2 $\pm$ 2.9	42.2 $\pm$ 2.3	...
RasTyc2206+1005B	BD+09 4984B	22 06 11.82	+10 05 28.7	2148.6228	-26.40 $\pm$ 0.40	18.67 $\pm$ 0.28	57.95 $\pm$ 0.64	28.9 $\pm$ 1.6	30.0 $\pm$ 1.6	28.9 $\pm$ 1.8
RasTyc2206+1005B	BD+09 4984B	22 06 11.82	+10 05 28.7	2149.4504	-29.63 $\pm$ 0.64	34.71 $\pm$ 0.77	74.12 $\pm$ 0.81	38.6 $\pm$ 2.2	43.7 $\pm$ 2.6	29.3 $\pm$ 2.0
RasTyc2206+1005B	BD+09 4984B	22 06 11.82	+10 05 28.7	2150.4430	-25.35 $\pm$ 0.35	16.05 $\pm$ 0.25	60.28 $\pm$ 0.34	29.4 $\pm$ 1.6	30.7 $\pm$ 1.6	28.9 $\pm$ 1.6
RasTyc2233+0506	TYC 573-566-1	22 33 39.30	+05 06 20.0	1799.4782	-143.86 $\pm$ 0.88	37.90 $\pm$ 0.17	87.47 $\pm$ 1.06	62.9 $\pm$ 3.6	16.5 $\pm$ 0.9	44.5 $\pm$ 2.8
RasTyc2309-0049 <sup>b</sup>	BD-01 4397	23 09 47.09	-00 49 34.4	2149.5545	-86.39 $\pm$ 0.24	-12.92 $\pm$ 0.15	62.51 $\pm$ 0.23	14.0 $\pm$ 0.8	3.1 $\pm$ 0.2	13.2 $\pm$ 0.7
<b>AURELIE</b>										
RasTyc0157+3310	BD+32 354	01 57 52.61	+33 10 19.6	2216.3262	-53.38 $\pm$ 1.45	-97.21 $\pm$ 3.91	1.33 $\pm$ 4.09	7.1 $\pm$ 1.6	17.8 $\pm$ 2.5	14.4 $\pm$ 2.6
RasTyc0157+3310	BD+32 354	01 57 52.61	+33 10 19.6	2217.3308	-52.78 $\pm$ 1.83	-100.53 $\pm$ 3.82	-3.76 $\pm$ 4.50	7.3 $\pm$ 1.4	18.8 $\pm$ 2.3	15.6 $\pm$ 2.3
RasTyc0749+5346	TYC 3783-646-1	07 49 21.54	+53 46 07.1	2986.5720	-62.75 $\pm$ 1.80	69.08 $\pm$ 1.50	16.37 $\pm$ 0.76	29.1 $\pm$ 1.8	31.0 $\pm$ 1.2	7.4 $\pm$ 1.5
RasTyc1932+5433	HD 234928	19 32 34.66	+54 33 06.4	3580.5229	56.33 $\pm$ 1.53	-38.31 $\pm$ 1.61	17.81 $\pm$ 1.31	20.1 $\pm$ 1.3	...	10.4 $\pm$ 2.2
RasTyc1932+5433	HD 234928	19 32 34.66	+54 33 06.4	3583.4944	88.24 $\pm$ 1.14	-74.74 $\pm$ 1.83	17.93 $\pm$ 1.33	20.3 $\pm$ 1.6	12.5 $\pm$ 2.0	9.5 $\pm$ 2.0
RasTyc1932+5433	HD 234928	19 32 34.66	+54 33 06.4	5002.5686	30.21 $\pm$ 0.81	...	...	30.4 $\pm$ 1.7	...	...
RasTyc2034+8253 <sup>c</sup>	BD+82 622	20 34 27.27	+82 53 35.2	2475.5159	20.57 $\pm$ 1.27	-43.24 $\pm$ 1.41	-10.96 $\pm$ 1.26	< 5	< 5	< 5
RasTyc2034+8253 <sup>c</sup>	BD+82 622	20 34 27.27	+82 53 35.2	2482.3916	-50.12 $\pm$ 1.42	29.29 $\pm$ 1.28	-9.99 $\pm$ 1.39	< 5	< 5	< 5
<b>FRESCO</b>										
RasTyc0221+7811	BD+77 80	02 21 52.44	+78 11 16.6	5108.6061	-50.73 $\pm$ 1.14	50.55 $\pm$ 1.81	0.59 $\pm$ 0.48	19.4 $\pm$ 4.0	23.7 $\pm$ 10.0	13.7 $\pm$ 1.5
RasTyc1631+5755	HD 238571	16 31 05.95	+57 55 50.9	5110.2851	-71.92 $\pm$ 1.87	35.68 $\pm$ 2.62	-19.20 $\pm$ 0.33	19.3 $\pm$ 5.6	30.0 $\pm$ 8.7	12.1 $\pm$ 3.8

<sup>a</sup> The tertiary component is much brighter than the inner binary and was also analyzed as a single star.<sup>b</sup> Close visual pair (sep  $\simeq 1.^{\prime\prime}5$ ,  $\Delta V \simeq 0.6$  mag, Hog et al. 2000).<sup>c</sup> The full set of RV data and orbital solution are reported in Klutsch et al. (2008).

**Table A.4.** Spectral types, atmospheric parameters, and equivalent widths of Li I and H $\alpha$  lines for the single stars (S) and SB1 binaries.

RasTyc Name	$\alpha$ (2000) h m s	$\delta$ (2000) $^{\circ} / '$	Sp. Type	$T_{\text{eff}}$ (K)	$\sigma_{T_{\text{eff}}}$	$\log g$	$\sigma_{\log g}$	[Fe/H]	$\sigma_{[\text{Fe}/\text{H}]}$	$W_{\text{Li}}$ (mÅ)	$\sigma_{W_{\text{Li}}}$	$W_{\text{H}\alpha}^{em} \bullet$ (mÅ)	$\sigma_{W_{\text{H}\alpha}^{em}}$	Bin <sup>a</sup>	Instr. <sup>b</sup>
RasTyc0000+7940	00 00 41.14	+79 40 39.9	G2V	5738	140	4.19	0.20	-0.03	0.09	202	40	310	50	S	AU+FR
RasTyc0001+5212	00 01 42.66	+52 12 51.0	K1V	5300	103	4.39	0.17	-0.03	0.11	64	20	130	37	S	SA
RasTyc0004-0951	00 04 46.96	-09 51 53.4	K1V	5141	63	4.53	0.14	-0.01	0.11	41	46	5	41	S	EL
RasTyc0008+5347	00 08 04.62	+53 47 47.0	F8V	5944	85	4.18	0.12	-0.12	0.11	69	6	1	6	S	EL
RasTyc0013+7702 <sup>c</sup>	00 13 40.52	+77 02 10.9	G0V	5924	243	4.14	0.22	-0.03	0.09	175	10	3900	90	SB2?	AU
RasTyc0013+3946	00 13 58.01	+39 46 02.3	G3V	5707	140	4.31	0.15	-0.07	0.12	40	7	89	9	S	AU
RasTyc0016+4104	00 16 44.88	+41 04 08.6	K3V	5010	197	4.17	0.39	0.03	0.14	2	5	272	38	S	AU
RasTyc0023+7503	00 23 41.24	+75 03 16.9	K2V	5091	347	4.52	0.27	-0.06	0.15	147	176	112	289	S	SA
RasTyc0032+7806	00 32 42.87	+78 06 47.4	G3V	5715	145	4.29	0.15	-0.02	0.11	21	7	93	14	S	AU
RasTyc0033+5315 <sup>c</sup>	00 33 55.90	+53 15 41.5	G6V	5716	70	4.32	0.11	-0.07	0.11	55	23	223	55	SB2?	SA
RasTyc0033+6126	00 33 57.58	+61 26 33.3	K0V	5209	97	4.53	0.15	0.05	0.13	1	24	1160	117	S	AU
RasTyc0038+7903	00 38 06.03	+79 03 20.7	K1V	5160	119	4.30	0.19	-0.06	0.08	290	20	1125	157	S	AU+FR
RasTyc0039+7905*	00 39 40.13	+79 05 30.8	G5V	5444	265	4.14	0.28	-0.11	0.11	216	17	221	19	SB2	AU
RasTyc0040+4343	00 40 20.90	+43 43 25.4	K2V	5095	74	4.27	0.18	-0.04	0.10	38	15	1303	108	S	SA
RasTyc0041+3425	00 41 17.30	+34 25 17.2	K1V	5174	68	4.57	0.08	-0.01	0.07	123	25	3153	160	S	AU
RasTyc0045+7943	00 45 22.95	+79 43 49.6	G3V	5705	140	4.16	0.23	-0.32	0.09	135	20	...	...	S	AU
RasTyc0046+4808	00 46 53.09	+48 08 45.2	K2V	5067	159	4.21	0.45	-0.09	0.07	355	14	809	42	S	AU
RasTyc0050+4651	00 50 38.39	+46 51 57.5	G2V	5900	152	4.30	0.11	0.05	0.07	80	10	68	12	S	AU
RasTyc0051+5425	00 51 03.32	+54 25 18.6	K0IV	5191	288	4.47	0.34	0.01	0.16	117	102	856	210	S	SA
RasTyc0051-1306	00 51 17.10	-13 06 52.5	G1V	5870	67	4.29	0.11	-0.02	0.11	27	21	51	40	S	EL
RasTyc0100+5411	01 00 11.71	+54 11 01.7	G1V	5832	80	4.29	0.11	0.03	0.06	47	11	76	13	S	AU
RasTyc0103+5727	01 03 04.48	+57 27 17.7	K3V	4909	73	4.58	0.16	0.09	0.11	17	15	175	40	S	SA
RasTyc0106+3306	01 06 18.71	+33 06 01.9	G4V	5606	134	4.31	0.11	-0.14	0.12	199	29	569	64	S	AU
RasTyc0106+5729	01 06 27.36	+57 29 44.1	G8III	5158	97	3.40	0.16	-0.05	0.11	36	16	510	97	S	SA
RasTyc0116+3938	01 16 50.67	+39 38 18.9	K1V	5148	80	4.02	0.45	-0.10	0.06	7	7	319	29	S	AU
RasTyc0137+3900	01 37 27.16	+39 00 08.6	G8IV	5241	84	3.55	0.87	-0.26	0.26	...	...	1177	69	S	AU
RasTyc0140+4212	01 40 28.78	+42 12 01.6	K2V	5060	204	4.23	0.49	-0.09	0.10	8	14	1505	83	SB1	AU
RasTyc0140+4952	01 40 51.62	+49 52 31.2	G5IV	5508	137	4.27	0.19	-0.05	0.12	168	40	553	118	S	SA
RasTyc0144+6508	01 44 22.37	+65 08 47.2	G5III	5454	139	3.89	0.21	0.08	0.11	43	34	866	172	S	SA
RasTyc0156+4354	01 56 38.45	+43 54 46.8	K2V	5129	139	4.28	0.33	-0.15	0.11	3	3	249	19	SB1	AU
RasTyc0158+3601	01 58 26.62	+36 01 19.6	G5V	5760	145	4.26	0.15	-0.14	0.18	90	8	124	17	S	AU
RasTyc0218+4346	02 18 13.49	+43 46 30.2	K2V	5124	91	4.02	0.48	-0.10	0.08	89	11	1225	61	SB1	AU
RasTyc0221+3404	02 21 33.30	+34 04 45.6	K0IV	5184	85	3.82	0.49	0.06	0.18	1	8	517	61	SB1	AU
RasTyc0222+7204	02 22 12.91	+72 04 58.0	K0III-IV	4866	128	3.01	0.28	-0.09	0.12	105	29	763	122	S	SA
RasTyc0222+5033	02 22 33.82	+50 33 37.8	K2V	5094	78	4.27	0.40	-0.12	0.09	248	17	1060	42	S	AU
RasTyc0227+4554	02 27 40.47	+45 54 37.3	G2V	5663	74	4.34	0.11	-0.02	0.11	116	22	481	137	S	SA
RasTyc0229+7206	02 29 44.65	+72 06 03.8	K0IV	5156	93	4.03	0.47	-0.06	0.10	27	16	409	20	SB1	AU
RasTyc0230+5656	02 30 44.81	+56 56 13.0	G1V	5874	97	4.31	0.14	-0.03	0.14	208	83	281	76	S	SA
RasTyc0230+5533	02 30 48.51	+55 33 07.2	K1V	5107	81	4.41	0.16	-0.10	0.07	156	11	266	18	S	AU
RasTyc0235+3139	02 35 03.79	+31 39 22.3	G5V	5584	196	4.21	0.21	-0.20	0.20	172	31	...	...	S	AU
RasTyc0240+6143	02 40 12.74	+61 43 59.0	K1V	5276	114	4.28	0.22	0.04	0.11	36	19	522-742	93	SB1	SA
RasTyc0242+4527	02 42 20.50	+45 27 43.8	K0V	5389	257	4.28	0.23	0.02	0.14	145	30	104	26	S	FR
RasTyc0242+3837	02 42 20.89	+38 37 22.2	K2V	5071	148	4.21	0.44	-0.07	0.08	132	11	607	22	S	AU
RasTyc0249+4255	02 49 54.69	+42 55 27.1	G1.5V	5825	107	4.24	0.12	-0.02	0.12	157	37	251	65	S	SA
RasTyc0252+3616	02 52 17.56	+36 16 48.5	K1IV	4679	174	3.66	0.51	-0.08	0.14	174	86	3179	237	S	SA
RasTyc0252+3728	02 52 24.71	+37 28 52.0	G1.5V	5784	157	4.35	0.15	0.02	0.14	293	187	305	108	S	SA
RasTyc0256+7253	02 56 11.33	+72 53 10.4	G1V	5804	175	4.30	0.12	-0.15	0.18	92	46	...	...	S	FR
RasTyc0256+6033	02 56 58.03	+60 33 52.7	K2V	5072	57	4.59	0.13	-0.02	0.10	32	19	189	70	S	SA
RasTyc0300+7225	03 00 14.67	+72 25 41.4	K2V	5079	59	4.59	0.13	-0.01	0.10	264	22	845	105	S	SA
RasTyc0302+4421	03 02 46.57	+44 21 03.1	K1V	5214	127	4.10	0.40	-0.08	0.06	0	8	238	13	S	AU
RasTyc0311+4810	03 11 16.82	+48 10 36.9	G1.5V	5856	110	4.35	0.14	0.02	0.15	201	72	483	136	S	SA
RasTyc0313+7417	03 13 27.48	+74 17 47.0	G0IV	6025	189	4.00	0.21	0.02	0.12	38	92	...	...	S	FR
RasTyc0313+3832	03 13 47.40	+38 32 04.9	K0V	5560	258	4.32	0.10	0.11	0.10	142	9	...	...	S	AU
RasTyc0316+4724	03 16 07.07	+47 24 58.7	G4V	5665	147	4.38	0.07	0.07	0.23	0	8	110	22	S	AU
RasTyc0316+5638	03 16 28.11	+56 38 58.1	K1V	5208	74	4.50	0.12	-0.05	0.11	223	31	550	83	S	SA
RasTyc0316+6049	03 16 59.73	+60 49 10.0	K1III	4553	186	2.33	0.58	-0.08	0.13	39	23	155	14	SB1	AU
RasTyc0319+4328	03 19 59.33	+43 28 08.1	F8V	5931	159	3.95	0.08	-0.26	0.15	2	8	162	22	SB1	AU
RasTyc0323+5843	03 23 07.08	+58 43 07.4	K1V	5212	130	4.48	0.20	-0.07	0.14	244	47	1009	135	S	SA
RasTyc0325+3647	03 25 02.39	+36 47 56.8	K0V	5375	212	4.33	0.17	-0.15	0.12	...	...	161	18	S	AU
RasTyc0328+3114	03 28 57.21	+31 14 19.2	G4V	5762	101	4.20	0.20	-0.04	0.26	...	...	234	24	S	AU
RasTyc0331+4859	03 31 28.98	+48 59 28.6	G1.5V	5816	236	4.30	0.19	-0.10	0.18	185	63	738	120	S	SA
RasTyc0334+3846	03 34 38.28	+38 46 28.2	G5V	5355	226	4.17	0.27	-0.08	0.10	118	14	81	14	S	AU
RasTyc0336+4816	03 36 40.23	+48 16 13.4	G3V	5641	187	4.14	0.32	-0.23	0.17	24	47	44	59	S	FR
RasTyc0339+6639	03 39 14.22	+66 39 40.3	K2V	5093	77	4.43	0.18	-0.10	0.07	64	7	376	22	S	AU
RasTyc0344+5043	03 44 34.50	+50 43 47.5	K0V	5349	211	4.40	0.22	-0.06	0.16	227	71	849	143	S	SA
RasTyc0348+6840	03 48 00.50	+68 40 58.2	K1V	5200	78	4.31	0.25	-0.09	0.11	29	18	323	95	S	SA
RasTyc0357+5051	03 57 19.91	+50 51 19.2	K2V	5104	76	4.25	0.43	-0.13	0.06	207	12	914	31	S	AU
RasTyc0359+4404	03 59 16.70	+44 04 17.1</													

**Table A.4.** continued.

RasTyc Name	$\alpha$ (2000) h m s	$\delta$ (2000) $^{\circ}$ $'$ $''$	Sp. Type	$T_{\text{eff}}$ (K)	$\sigma_{T_{\text{eff}}}$	$\log g$	$\sigma_{\log g}$	[Fe/H]	$\sigma_{[\text{Fe}/H]}$	$W_{\text{Li}}$ (mÅ)	$\sigma_{W_{\text{Li}}}$	$W_{\text{H}\alpha}^{em}$ • (mÅ)	$\sigma_{W_{\text{H}\alpha}^{em}}$	Bin <sup>a</sup>	Instr. <sup>b</sup>
RasTyc0501+3430 <sup>d</sup>	05 01 10.83	+34 30 26.5	...	...	...	...	...	...	...	...	...	...	...	S?	AU
RasTyc0507+4720	05 07 12.41	+47 20 37.4	G2IV	5893	112	4.22	0.14	0.12	0.09	33	9	...	...	S	AU
RasTyc0512+4119	05 12 22.96	+41 19 40.3	K1V	5107	70	4.43	0.26	-0.11	0.06	144	11	599	30	S	AU
RasTyc0519+6303	05 19 04.44	+63 03 34.5	G3V	5767	146	4.19	0.19	-0.13	0.18	17	7	1	6	S	AU
RasTyc0535+3946	05 35 05.64	+39 46 31.9	K0IV	5134	104	3.69	0.29	0.03	0.13	109	48	545	168	S	SA
RasTyc0537+5231	05 37 03.91	+52 31 26.1	K7V	4504	317	4.43	0.20	-0.04	0.07	...	...	807	39	S	AU
RasTyc0544+4024	05 44 26.50	+40 24 26.1	K1V	5206	155	4.33	0.22	-0.09	0.06	5	10	5	10	S	AU
RasTyc0609+5801	06 09 00.42	+58 01 09.0	G0V	5746	105	4.19	0.12	-0.45	0.13	2	13	348	86	S	SA
RasTyc0612+4733	06 12 30.81	+47 33 09.1	G1V	5726	153	4.37	0.04	-0.05	0.10	38	6	136	12	S	AU
RasTyc0616+4516	06 16 46.95	+45 16 03.1	G2V	5739	107	4.21	0.18	0.11	0.11	229	38	1235	220	S	SA
RasTyc0620+7353	06 20 07.99	+73 53 30.5	G5V	5587	184	4.19	0.21	-0.12	0.12	38	7	105	16	SB1	AU
RasTyc0621+5415	06 21 56.92	+54 15 49.0	G2V	5719	127	4.14	0.22	-0.08	0.13	160	12	583	22	S	AU
RasTyc0624+5940	06 24 43.95	+59 40 10.8	G8III	4994	158	2.93	0.42	0.05	0.07	...	...	1	4	S	AU
RasTyc0628+3115A	06 28 23.61	+31 15 51.2	K1V	5217	165	4.44	0.09	-0.14	0.10	126	11	224	20	S	AU
RasTyc0628+3115B	06 28 22.99	+31 15 59.2	K1V	5231	180	4.44	0.09	-0.15	0.10	126	13	142	15	S	AU
RasTyc0634+3404	06 34 34.67	+34 04 33.0	G9IV	5420	325	3.95	0.43	0.02	0.13	3	5	1829	128	S	AU
RasTyc0638+3153	06 38 12.12	+31 53 11.8	F9IV-V	5864	257	4.23	0.15	-0.05	0.17	26	11	62	11	S	AU
RasTyc0646+3124	06 46 25.20	+31 24 46.0	G8IV	5223	65	3.50	0.53	-0.15	0.22	3	8	247	137	SB1	AU
RasTyc0646+4147	06 46 46.74	+41 47 12.2	G2V	5696	84	4.16	0.13	0.13	0.11	210	30	211	65	S	SA
RasTyc0652+5720	06 52 29.28	+57 20 46.8	K0IV	5125	146	4.03	0.71	-0.11	0.11	103	14	1151	66	SB1	AU
RasTyc0712+7021	07 12 50.04	+70 21 06.8	K1IV	5012	227	2.96	0.49	-0.03	0.08	99	14	931	40	SB1	AU
RasTyc0713+5106	07 13 36.53	+51 06 17.3	G4V	5877	181	4.20	0.17	-0.11	0.20	3	11	322	23	S	AU
RasTyc0714+5307	07 14 36.39	+53 07 40.4	F7IV	6057	186	4.04	0.18	-0.14	0.17	50	11	...	...	S	AU
RasTyc0730+6343	07 30 55.31	+63 43 50.1	K1III	4672	177	2.68	0.74	-0.07	0.13	74	9	...	...	S	AU
RasTyc0734+3518	07 34 34.76	+35 18 59.7	G5V	5850	98	4.30	0.10	0.01	0.09	46	11	121	17	S	AU
RasTyc0755+4040	07 55 04.52	+40 40 25.0	F9IV-V	6034	193	4.00	0.11	-0.14	0.18	5	6	181	21	S	AU
RasTyc0755+6509	07 55 54.19	+65 09 11.1	K0IV	5085	166	3.44	0.85	-0.07	0.15	132	11	379	21	S	AU
RasTyc1505+4626	15 05 32.49	+46 26 38.6	K3V	4950	158	4.55	0.37	0.04	0.12	0	32	1340	141	S	SA
RasTyc1507+5515	15 07 27.92	+55 15 56.5	G2V	5710	134	4.27	0.12	0.01	0.13	28	26	110	49	S	FR
RasTyc1507+8629	15 07 53.09	+86 29 29.4	G2V	5787	82	4.34	0.11	0.01	0.11	79	20	90	29	S	SA
RasTyc1507+0415	15 07 59.63	+04 15 21.1	K2V	5072	152	4.22	0.47	-0.10	0.09	146	12	1231	81	S	AU
RasTyc1519+3940	15 19 38.40	+39 40 05.5	G0IV	5853	94	4.12	0.16	0.12	0.11	13	43	68	37	S	SA
RasTyc1521-0920	15 21 52.71	-09 20 18.3	K1V	5276	96	4.40	0.16	0.01	0.11	57	18	45	19	S	SA
RasTyc1522+4137	15 22 11.06	+41 37 08.9	G5IV-V	5636	71	4.28	0.12	0.03	0.11	37	22	99	44	S	SA
RasTyc1522+2745	15 22 35.40	+27 45 31.0	G9IV	5196	56	4.00	0.25	0.14	0.10	17	17	34	22	S	SA
RasTyc1527+1801	15 27 38.20	+18 01 35.3	G2V	5765	71	4.31	0.11	0.04	0.10	72	17	70	24	S	SA
RasTyc1529+6712A	15 29 24.15	+67 12 15.9	F8V	5998	100	4.04	0.15	0.03	0.12	3	19	8	16	S	SA
RasTyc1529+4836	15 29 42.46	+48 36 13.1	G3V	5782	237	4.08	0.13	-0.25	0.17	52	10	0	5	S	AU
RasTyc1540+4027A	15 40 58.90	+40 27 00.3	G8IV	5563	180	4.07	0.20	-0.04	0.14	42	21	659	96	S	SA
RasTyc1540+4027B	15 40 58.90	+40 27 00.3	K1V	5263	93	4.17	0.22	-0.03	0.11	44	58	42	57	S	SA
RasTyc1541+7702	15 41 59.71	+77 02 41.8	G5IV	5722	83	4.09	0.12	-0.06	0.11	118	20	131	40	S	SA
RasTyc1547+5302B	15 47 09.38	+53 01 26.5	K1V	5178	75	4.43	0.15	0.07	0.10	9	14	2	41	S	SA
RasTyc1549+4608A	15 49 24.84	+46 08 22.2	K1V	5158	75	4.44	0.22	-0.11	0.11	32	15	1183	152	S	SA
RasTyc1549+4608B	15 49 24.32	+46 08 10.3	K7V	4381	157	4.58	0.10	-0.14	0.11	0	46	21	62	S	SA
RasTyc1550+5250	15 50 36.72	+52 50 22.0	G1.5V	5738	94	4.16	0.15	-0.13	0.12	102	42	179	124	S	SA
RasTyc1550+1440A	15 50 55.23	+14 40 42.8	F8V	6008	98	4.15	0.12	-0.20	0.12	2	6	-31	31	S	SA
RasTyc1558+0833	15 58 54.66	+08 33 55.3	K1V	5325	85	4.33	0.15	0.03	0.11	3	12	23	14	S	SA
RasTyc1603+8142	16 03 26.61	+81 42 20.4	G2V	5845	65	4.32	0.10	0.09	0.10	38	18	159	38	S	SA
RasTyc1604+0358	16 04 16.06	+03 58 09.4	G1.5V	5728	99	4.29	0.11	0.06	0.12	6	14	409	68	S	SA
RasTyc1617-0406	16 17 21.68	-04 06 50.0	F9IV-V	6005	121	3.99	0.13	-0.25	0.12	30	10	397	81	S	SA
RasTyc1620+0707	16 20 03.26	+07 07 29.6	G9V	5340	253	4.34	0.29	-0.40	0.36	32	155	673	173	SB1	FR
RasTyc1620+4841	16 20 38.67	+48 41 13.7	G2V	5705	124	4.34	0.12	0.06	0.11	129	32	60	24	S	SA
RasTyc1623+3535	16 23 09.20	+35 35 18.3	F8V	5875	326	4.24	0.22	-0.12	0.16	62	57	104	115	S	SA
RasTyc1626+3350	16 26 41.35	+33 50 42.1	G1V	6019	124	3.99	0.19	-0.80	0.19	15	32	644	298	S	SA
RasTyc1626+0823	16 26 48.87	+08 23 26.0	G1.5V	5687	106	4.28	0.13	0.08	0.10	120	25	169	72	S	SA
RasTyc1628+7400	16 28 21.48	+74 00 55.9	G2V	5737	103	4.38	0.12	0.01	0.12	155	25	474	85	S	SA
RasTyc1629+1728	16 29 29.20	+17 28 16.2	G1V	5820	75	4.30	0.11	-0.01	0.11	98	22	100	39	S	SA
RasTyc1631+0849	16 31 13.87	+08 49 14.4	K1V	5118	60	4.54	0.18	0.03	0.10	6	15	69	26	S	SA
RasTyc1631+1916A	16 31 34.45	+19 16 38.8	G9.5IV	5350	100	4.19	0.14	0.01	0.11	16	31	-13	21	S	SA
RasTyc1631+1916B	16 31 34.09	+19 16 38.5	K0IV	5307	92	4.29	0.18	-0.01	0.12	12	19	527	67	S	SA
RasTyc1637+0717	16 37 35.43	+07 17 03.3	G2V	5747	87	4.36	0.11	-0.01	0.11	117	24	166	38	S	SA
RasTyc1641+1520	16 41 26.95	+15 20 39.7	K0IV	5013	89	3.31	0.20	-0.04	0.11	11	17	0	29	S	SA
RasTyc1641+0118	16 41 29.18	+01 18 48.6	G8V	5125	63	4.30	0.24	0.14	0.10	3	12	70	28	S	SA
RasTyc1641+1140	16 41 53.08	+11 40 21.1	K0III-IV	4921	119	3.02	0.34	-0.14	0.11	30	15	1318	96	S	SA
RasTyc1645+3000A	16 45 43.47	+30 00 17.2	F5IV-V	6315	233	3.98	0.13	-0.23	0.11	37	45	61	162	S	SA
RasTyc1645+3000B	16 45 44.10	+30 00 05.6	F8V	5862	66	4.24	0.12	0.01	0.11	68	38	61	35	S	SA
RasTyc1649+5816	16 49 40.31	+58 16 08.4	G2V	5800	146	4.28	0.15	0.03	0.10	134	52	195	62	S	FR
RasTyc1652+0121	16 52 29.11	+01 21 20.1	G0.5IV	5924	75	4.27	0.11	0.07	0.11	81	26	116	41	S	SA</

**Table A.4.** continued.

RasTyc Name	$\alpha$ (2000) h m s	$\delta$ (2000) $^{\circ}$ $'$ $''$	Sp. Type	$T_{\text{eff}}$ (K)	$\sigma_{T_{\text{eff}}}$	$\log g$	$\sigma_{\log g}$	[Fe/H] (dex)	$\sigma_{[\text{Fe}/H]}$ (dex)	$W_{\text{Li}}$ (mÅ)	$\sigma_{W_{\text{Li}}}$	$W_{\text{H}\alpha}^{em} \bullet$ (mÅ)	$\sigma_{W_{\text{H}\alpha}^{em}}$	Bin <sup>a</sup>	Instr. <sup>b</sup>
RasTyc1728-0128	17 28 09.38	-01 28 52.0	K1V	5083	93	4.49	0.19	0.00	0.11	13	11	1343	151	S	SA
RasTyc1731+2815	17 31 03.33	+28 15 06.1	K1V	5169	71	4.47	0.19	-0.02	0.11	243	22	875	79	S	SA
RasTyc1740+0554	17 40 57.39	+05 54 46.5	K0V	5393	223	4.24	0.35	0.09	0.17	185	39	25	24	S	FR
RasTyc1741+0228	17 41 46.17	+02 28 56.2	G9III	4840	93	3.12	0.21	-0.12	0.11	90	22	514	50	S	SA
RasTyc1743+6606	17 43 01.88	+66 06 43.1	F8V	5936	109	4.15	0.13	-0.22	0.12	7	15	193	40	S	SA
RasTyc1758+0155	17 58 55.52	+01 55 06.3	K0V	5142	61	4.55	0.16	-0.01	0.10	15	24	439	68	S	SA
RasTyc1802+3356	18 02 38.80	+33 56 34.5	G3V	5705	90	4.04	0.15	-0.29	0.13	14	7	272	21	S	AU
RasTyc1808-0858 <sup>†</sup>	18 08 01.34	-08 58 57.5	K1V	5173	123	4.37	0.15	-0.06	0.12	189	29	225	38	SB2?	SA
RasTyc1816+2848	18 16 31.34	+28 48 11.2	G3V	5704	123	4.16	0.22	-0.19	0.17	130	15	151	17	SB1?	AU
RasTyc1831+5418	18 31 37.59	+54 18 57.9	G2.5V	5676	79	4.26	0.13	0.05	0.12	9	21	556	121	S	SA
RasTyc1838+0224	18 38 38.19	+02 24 12.7	F9IV-V	6011	108	4.15	0.13	0.00	0.12	112	28	138	38	S	SA
RasTyc1842+5751	18 42 49.32	+57 51 54.6	G0.5IV	5843	74	4.30	0.12	0.07	0.10	8	13	116	26	S	EL
RasTyc1843+4328	18 43 58.66	+43 28 27.8	G1.5V	5964	110	4.20	0.13	0.02	0.12	49	12	109	31	S	SA
RasTyc1847+2930	18 47 39.96	+29 30 39.3	K1V	5220	59	4.31	0.14	0.02	0.10	4	9	236	31	S	SA
RasTyc1857+6406	18 57 13.08	+64 06 21.3	K3V	4834	95	4.59	0.16	0.04	0.10	32	22	59	30	S	SA
RasTyc1857+6223	18 57 19.45	+62 23 39.5	G8III	5020	87	3.14	0.17	0.03	0.10	7	8	-3	13	S	SA
RasTyc1857+0120	18 57 19.46	+01 20 33.3	G5V	5420	290	4.29	0.22	-0.03	0.07	186	12	222	13	S	AU
RasTyc1908+5018	19 08 14.03	+50 18 49.6	G8III-IV	5223	226	3.39	0.76	-0.37	0.23	339	67	529	113	S	FR
RasTyc1918+3408	19 18 12.13	+34 08 10.1	K1III	4658	69	2.67	0.16	-0.10	0.11	22	9	160	25	S	EL
RasTyc1919+0628	19 19 26.29	+06 28 42.2	F8V	5986	195	4.12	0.25	-0.08	0.19	93	47	226	78	S	FR
RasTyc1925+4429	19 25 01.98	+44 29 50.7	K2V	5055	135	4.41	0.25	-0.02	0.10	270	20	922	107	S	SA
RasTyc1926+7840	19 26 35.09	+78 40 04.9	K1V	5205	72	4.23	0.20	0.03	0.11	21	19	319	61	S	SA
RasTyc1928+4856	19 28 10.64	+48 56 37.3	K0V	5197	254	4.47	0.29	-0.03	0.14	9	45	550	118	S	SA
RasTyc1928+1232	19 28 15.43	+12 32 09.6	K3V	4805	93	4.57	0.11	0.07	0.10	3	14	24	14	S	SA
RasTyc1928+2731	19 28 22.32	+27 31 18.5	G2V	5745	127	4.20	0.20	0.14	0.14	...	...	246	17	S	AU
RasTyc1930+4932	19 30 15.81	+49 32 08.2	K1V	5180	64	3.80	0.25	-0.01	0.11	18	17	185-330	71	SB1	SA
RasTyc1940+2535	19 40 44.79	+25 34 46.9	K3V	5051	215	4.37	0.13	-0.06	0.07	67	7	340	30	S	AU
RasTyc1949-0804	19 49 35.22	-08 04 50.3	G8III	5233	451	3.67	0.83	-0.06	0.28	48	13	1229	38	SB1	AU
RasTyc1956+4345	19 56 59.73	+43 45 08.2	G1.5V	5815	95	4.24	0.12	-0.05	0.10	155	20	264	30	S?	SA
RasTyc1958+5355A	19 58 04.00	+53 55 29.6	F5.5IV-V	6296	174	4.03	0.12	-0.10	0.14	11	16	-13	35	S	SA
RasTyc1958+5355B	19 58 03.39	+53 55 24.5	F8V	5899	91	4.18	0.12	-0.10	0.12	86	22	48	28	S	SA
RasTyc1958+4301*	19 58 37.62	+43 01 02.5	F9IV-V	5919	203	4.06	0.16	-0.21	0.17	64	34	197	92	SB2?	SA
RasTyc1959-0432	19 59 24.10	-04 32 05.7	G5V	5752	116	4.17	0.18	0.06	0.10	126	8	147	17	S	AU
RasTyc2000+5921	20 00 31.23	+59 21 44.5	G0V	5653	77	4.28	0.12	-0.49	0.12	22	20	37	38	S	SA
RasTyc2000+3256	20 00 45.52	+32 56 59.4	K0V	5212	65	4.40	0.13	0.02	0.10	48	12	95	22	S	EL
RasTyc2004+0239	20 04 49.35	-02 39 19.7	K1V	5183	63	4.39	0.17	-0.02	0.11	298	38	457	76	S	SA
RasTyc2013+1625	20 13 54.27	+16 25 25.4	K1III	4555	73	2.55	0.14	-0.11	0.11	55	10	486-517	50	S	EL
RasTyc2015+3316	20 15 20.54	+33 16 11.8	K3V	4921	69	4.57	0.14	0.10	0.10	6	19	126	31	S	EL
RasTyc2015+3343	20 15 23.79	+33 43 45.7	G8III	5086	85	3.15	0.16	0.01	0.10	4	5	3	8	S	EL
RasTyc2016+3106	20 16 57.83	+31 06 55.6	K1V	5087	60	4.57	0.14	0.03	0.11	254	24	1168-1585	163	S	EL
RasTyc2019+3203	20 19 47.52	+32 03 08.8	F8V	6036	132	4.06	0.14	0.10	0.12	20	29	315	60	S	EL
RasTyc2021+3150	20 21 30.45	+31 50 32.3	G1.5V	5714	219	4.35	0.18	-0.02	0.15	23	29	1983	225	S	EL
RasTyc2021+3218	20 21 33.04	+32 18 50.7	G8III	4885	64	3.01	0.17	-0.07	0.10	43	9	370	56	S	EL
RasTyc2021+0616	20 21 45.50	+06 16 13.4	G5IV	5426	233	3.95	0.23	-0.03	0.13	66	19	285	33	S	SA
RasTyc2025-0429	20 25 04.26	-04 29 15.2	K0III-IV	4943	114	3.22	0.34	-0.05	0.12	61	19	2008	212	S	SA
RasTyc2028+2510	20 28 03.50	+25 10 42.7	K1V	5314	88	4.21	0.19	0.02	0.12	34	15	73	27	S	SA
RasTyc2028+1131	20 28 23.91	+11 31 11.3	G2V	5436	187	4.41	0.14	-0.16	0.25	...	...	496	88	SB?	AU
RasTyc2028-0943	20 28 42.28	-09 43 16.9	G5III	5373	268	3.70	0.40	0.07	0.14	34	47	3293	313	S	SA
RasTyc2030+4852	20 30 59.56	+48 52 08.1	K1III	4667	87	2.60	0.19	-0.06	0.12	103	21	57-229	98	SB1	EL
RasTyc2033+3128	20 33 24.39	+31 28 12.3	G2V	5439	196	4.37	0.16	-0.06	0.14	81	28	1188	135	S	EL
RasTyc2034-0713	20 34 47.43	-07 13 56.7	K0III	4751	60	2.78	0.13	-0.06	0.11	16	11	4	24	S	SA
RasTyc2036+3456	20 36 16.87	+34 56 46.1	G1V	5832	78	4.33	0.11	-0.01	0.11	192	16	390	37	S	EL
RasTyc2037+5106	20 37 55.03	+51 06 23.1	G5V	5471	318	4.20	0.30	-0.07	0.11	133	11	179	15	S	AU
RasTyc2038+3546	20 38 17.71	+35 46 33.3	G1.5V	5895	82	4.23	0.11	0.01	0.11	134	16	117	26	S	EL
RasTyc2039+2644	20 39 40.81	+26 44 48.4	K1V	5149	116	4.30	0.27	-0.08	0.08	232	11	541	22	S	AU
RasTyc2046+2815	20 46 18.86	+28 15 44.2	G1.5V	5765	205	4.26	0.16	0.14	0.13	41	51	211	185	SB2	EL
RasTyc2048-0644	20 48 59.58	-06 44 53.4	G8IV	5118	171	3.66	0.62	-0.24	0.26	69	11	1295	44	SB1?	AU
RasTyc2052+2705	20 52 07.73	+27 05 49.7	G5III	5267	81	3.34	0.19	0.08	0.11	0	4	15	13	S	EL
RasTyc2052+4258 <sup>‡</sup>	20 52 57.27	+42 58 25.7	K1V	5162	78	4.55	0.12	-0.09	0.11	10	15	670	104	SB	SA
RasTyc2052+4407	20 52 58.28	+44 07 20.1	F5IV-V	6227	249	3.99	0.13	-0.01	0.13	22	11	164	26	S	EL
RasTyc2053+2629	20 53 04.20	+26 29 32.1	G0.5IV	5964	86	4.08	0.12	0.12	0.11	10	27	19	24	S	EL
RasTyc2053+3641	20 53 35.39	+36 41 49.7	G1V	5877	68	4.30	0.11	-0.09	0.11	98	15	90	25	S	EL
RasTyc2053+4423	20 53 53.63	+44 23 11.1	G5III	5427	229	3.73	0.31	0.14	0.15	0	11	1241-1308	158	S?	EL
RasTyc2055+5348	20 55 42.25	+53 48 21.4	G8III	4990	76	3.03	0.15	0.00	0.11	20	7	19	10	S	EL
RasTyc2057+2624	20 57 39.50	+26 24 17.4	G1V	5868	59	4.29	0.10	0.02	0.10	48	9	24	8	S	EL
RasTyc2058+4403	20 58 55.63	+44 03 37.5	K0.5III	4743	53	2.84	0.11	-0.02	0.10	26	8	30	13	S	EL
RasTyc2059+4447	20 59 11.79	+44 47 25.6	K0III-IV	5209	79	3.57	0.15	0.01	0.10	33	10	50	11	S	EL
RasTyc2100+4405	21 00 25.21														

**Table A.4.** continued.

RasTyc Name	$\alpha$ (2000) h m s	$\delta$ (2000) $^{\circ}$ ' ''	Sp. Type	$T_{\text{eff}}$ (K)	$\sigma_{T_{\text{eff}}}$	$\log g$	$\sigma_{\log g}$	[Fe/H]	$\sigma_{[\text{Fe}/H]}$	$W_{\text{Li}}$ (mÅ)	$\sigma_{W_{\text{Li}}}$	$W_{\text{H}\alpha}^{em} \bullet$ (mÅ)	$\sigma_{W_{\text{H}\alpha}^{em}}$	Bin <sup>a</sup>	Instr. <sup>b</sup>
RasTyc2109+4029	21 09 48.50	+40 29 23.4	G1.5V	5707	115	4.33	0.13	-0.04	0.12	85	22	1181–1340	182	SB1	EL
RasTyc2114-0058	21 14 32.47	-00 58 52.8	G1.5V	5714	212	4.09	0.20	-0.11	0.14	94	29	1794	201	S	SA
RasTyc2114+3941	21 14 55.24	+39 41 11.9	G1.5V	5930	90	4.27	0.12	-0.02	0.12	131	27	149	34	S	EL
RasTyc2115+4437	21 15 23.98	+44 37 42.8	K0IV	5072	84	3.69	0.26	-0.01	0.11	73	19	547	41	S	EL
RasTyc2117+3153	21 17 21.28	+31 53 58.0	G5IV	5283	61	3.63	0.14	0.07	0.10	87	14	91	18	S	EL
RasTyc2118-0631	21 18 33.53	-06 31 43.7	K1V	5149	83	4.34	0.23	0.10	0.11	48	23	553	69	SB1 <sup>d</sup>	SA
RasTyc2118+2613	21 18 58.13	+26 13 49.9	K0V	5404	93	4.34	0.12	0.03	0.10	40	6	86	11	S	EL
RasTyc2120+4636	21 20 55.42	+46 36 12.4	G1.5V	5699	192	4.36	0.16	0.04	0.14	176	49	426	117	S	EL
RasTyc2121+4020	21 21 01.44	+40 20 44.1	F8IV	6050	111	4.01	0.12	-0.25	0.13	78	12	115–126	24	SB1	EL
RasTyc2128+6423	21 28 00.96	+64 23 15.1	K1V	5220	64	4.44	0.12	0.01	0.10	11	6	83	14	S	EL
RasTyc2131+5925	21 31 01.20	+59 25 05.0	G2.5V	5760	74	4.20	0.11	0.09	0.10	50	21	56	21	S	EL
RasTyc2132+3604	21 32 39.29	+36 04 46.0	K0IV	5057	80	3.20	0.17	0.02	0.11	75	9	83	11	S	EL
RasTyc2137+1946	21 37 03.18	+19 46 58.3	G8III	4930	64	3.08	0.13	0.02	0.10	23	9	26	13	S	EL
RasTyc2141+2645	21 41 05.97	+26 45 03.2	G5IV-V	5668	60	4.27	0.10	0.00	0.10	3	3	31	16	S	EL
RasTyc2141+2658	21 41 16.74	+26 58 58.1	K0III	4850	82	3.00	0.16	-0.03	0.11	37	17	387–495	92	SB1	EL
RasTyc2142+3814	21 42 59.83	+38 14 54.8	G8III	4892	66	2.97	0.13	0.01	0.10	24	16	7	21	S	EL
RasTyc2143+2720	21 43 31.67	+27 20 37.6	F8V	6065	69	4.03	0.11	-0.30	0.11	35	6	48	15	S	EL
RasTyc2146+2446	21 46 50.43	+24 46 04.2	G2V	6039	84	3.95	0.12	-0.26	0.11	11	11	63–91	21	S	EL
RasTyc2147+4950	21 47 48.72	+49 50 08.0	K2V	5061	70	4.60	0.14	-0.02	0.11	85	22	533	67	S	SA
RasTyc2147+4949	21 47 54.42	+49 49 29.2	K2V	5080	85	4.58	0.20	-0.04	0.11	53	14	135–297	65	S	SA
RasTyc2149-0350	21 49 13.15	-03 50 32.6	G2V	5723	90	4.09	0.16	-0.02	0.14	109	27	102	49	S	SA
RasTyc2149+3125	21 49 16.02	+31 25 02.1	K1V	5141	59	4.49	0.13	0.02	0.10	12	20	738	95	S	EL
RasTyc2149+4028	21 49 26.94	+40 28 00.9	F8V	5858	162	3.99	0.13	-0.44	0.14	15	18	705	129	S	EL
RasTyc2152+3850	21 52 48.07	+38 50 08.0	K0III-IV	5036	75	3.26	0.18	-0.04	0.10	22	5	54	8	S	EL
RasTyc2153+2055	21 53 05.36	+20 55 50.8	K1V	5107	53	4.57	0.12	-0.03	0.10	17	6	83	18	S	EL
RasTyc2155-0947	21 55 07.21	-09 47 57.2	G1.5V	5663	169	4.27	0.19	-0.07	0.13	39	32	597	121	SB1 <sup>d</sup>	SA
RasTyc2157-0753	21 57 51.37	-07 53 47.4	K1V	5110	72	4.55	0.18	0.02	0.11	17	33	1016	189	SB1 <sup>d</sup>	SA
RasTyc2159+0041	21 59 05.33	+00 41 10.2	G2.5V	5693	186	4.33	0.16	0.04	0.14	45	52	1052	216	S	SA
RasTyc2202+1520	22 02 13.96	+15 20 14.0	K0V	5148	57	4.54	0.12	-0.07	0.10	37	11	266–363	75	S	EL
RasTyc2202+4831 <sup>t</sup>	22 02 26.05	+48 31 14.9	K3V	4804	322	4.58	0.40	-0.02	0.14	3	64	1455	261	S?	SA
RasTyc2202-0406	22 02 30.14	-04 06 11.6	K1V	5119	54	4.56	0.15	-0.04	0.10	179	23	349	69	SB1 <sup>d</sup>	SA
RasTyc2202+3108	22 02 57.33	+31 08 46.8	G1V	5921	92	4.31	0.12	0.02	0.11	40	29	126–186	42	SB1	SA
RasTyc2203+3809	22 03 49.83	+38 09 42.9	G5IV-V	5678	71	4.28	0.12	0.04	0.11	178	29	93	35	S	SA
RasTyc2204+0236	22 04 17.52	+02 36 21.0	K5V	4654	111	4.60	0.13	0.01	0.10	18	18	50	22	S	SA
RasTyc2206-0102	22 06 25.65	-01 02 43.9	G0V	5632	96	4.28	0.13	-0.33	0.16	32	32	1236	220	S	SA
RasTyc2206+5153	22 06 34.43	+51 53 11.8	K1V	5204	79	4.31	0.17	-0.00	0.11	140	31	908	164	S	SA
RasTyc2208+2208	22 08 50.40	+22 08 19.6	G5III	5397	70	3.40	0.20	-0.07	0.11	4	3	20	9	S	EL
RasTyc2210+1936	22 10 18.96	+19 36 59.6	G1V	5737	78	4.25	0.13	-0.04	0.12	12	10	40	15	S	EL
RasTyc2212+1329	22 12 13.38	+13 29 19.8	G2.5V	5665	75	4.28	0.12	0.10	0.10	78	12	58	20	S	EL
RasTyc2213+2015*	22 13 18.14	+20 15 35.5	G9.5IV	5197	198	4.12	0.40	-0.00	0.14	104	68	390–705	88	SB2?	SA
RasTyc2218+6951	22 18 27.61	+69 51 40.0	G9.5IV	5322	113	4.28	0.16	0.01	0.11	22	24	411	62	SB	SA
RasTyc2221-0008	22 21 16.29	-00 08 35.6	G1.5V	5811	76	4.17	0.14	0.09	0.11	4	21	408	92	S	SA
RasTyc2222+2922	22 22 28.77	+29 22 13.0	K1V	5171	216	4.46	0.38	-0.13	0.20	0	26	1014–1327	164	S?	EL
RasTyc2222+2814A	22 22 30.10	+28 14 24.9	F6IV	6257	153	3.91	0.11	-0.17	0.12	58	72	12	62	S	SA
RasTyc2223+7741	22 23 18.87	+77 41 57.7	G1.5V	5745	114	4.29	0.13	-0.04	0.13	245	50	440	110	S	SA
RasTyc2224+2016	22 24 23.35	+20 16 34.5	G5IV-V	5377	103	3.80	0.21	-0.01	0.11	8	11	77	13	S	EL
RasTyc2225+4607	22 25 12.03	+46 07 01.7	G1.5V	5751	103	4.26	0.19	0.09	0.09	76	78	358	159	S	FR
RasTyc2226+1814	22 26 34.99	+18 14 00.4	F8V	5991	147	4.01	0.14	-0.18	0.14	98	27	310	56	S	EL
RasTyc2227+1509	22 27 12.27	+15 09 15.3	G1V	5825	68	4.34	0.10	-0.04	0.11	90	13	83	14	S	EL
RasTyc2227+2649	22 27 27.08	+26 49 05.3	F8V	6348	83	4.03	0.11	-0.27	0.12	31	14	32	24	S	EL
RasTyc2233+1040	22 33 00.37	+10 40 34.3	G1.5V	5544	350	4.39	0.30	0.03	0.15	282	102	2974	445	S	EL
RasTyc2236+0010	22 36 11.99	+00 10 07.6	G8IV-V	5252	99	4.09	0.24	0.07	0.12	26	34	667	85	SB1	SA
RasTyc2236+7032	22 36 15.90	+70 32 04.1	K0IV	5080	87	3.78	0.31	-0.04	0.11	75	23	1551	128	S	SA
RasTyc2238+0217	22 38 29.22	+02 17 56.4	G1V	5839	82	4.32	0.11	-0.10	0.12	88	19	117	23	S	EL
RasTyc2239+0406	22 39 50.66	+04 06 57.1	K2V	5040	83	4.59	0.11	-0.06	0.11	16	5	208	38	S	EL
RasTyc2240+1432	22 40 52.53	+14 32 56.0	G5IV-V	5651	61	4.23	0.11	-0.01	0.10	13	5	11	6	S	EL
RasTyc2241+1430	22 41 57.40	+14 30 59.2	K0III	4678	54	2.77	0.11	-0.04	0.10	362	13	7	11	S	EL
RasTyc2242+1900*	22 42 04.91	+19 00 49.8	K2V	5112	195	4.54	0.39	0.02	0.14	36	50	568	129	SB2?	EL
RasTyc2244+1341	22 44 28.34	+13 41 10.9	K0V	5349	67	4.23	0.13	0.08	0.10	1	4	29	9	S	EL
RasTyc2244+1754	22 44 41.49	+17 54 19.0	K1V	5161	58	4.41	0.16	-0.02	0.11	245	18	601–720	64	SB1	EL/SA
RasTyc2244+3029	22 44 46.12	+30 29 33.6	G8IV	5471	172	4.31	0.23	-0.08	0.14	73	62	294	196	S	SA
RasTyc2246+5749	22 46 13.19	+57 49 58.0	G2V	5752	145	4.32	0.10	-0.05	0.11	207	41	410	110	S	FR
RasTyc2250+4926	22 50 10.89	+49 26 14.4	G5V	5552	164	4.36	0.16	-0.03	0.13	38	42	677	123	S	SA
RasTyc2251+8525	22 51 28.45	+85 25 21.1	K1V	5177	71	4.46	0.14	-0.04	0.10	176	22	304	41	S	SA
RasTyc2252+1730	22 52 52.75	+17 30 29.6	K1V	5156	59	4.53	0.11	-0.05	0.10	4	12	219	28	S	EL
RasTyc2253+0338	22 53 41.72	+03 38 43.6	G2V	5575	89	4.29	0.13	0.04	0.11	65	15	120	28	S	EL
RasTyc2256+0235	22 56 49.53	+02 35 39.2	G1.5V	5665	133	4.00	0.15	0.12	0.11	106	23	809	115	SB1 <sup>d</sup>	EL
RasTyc2258-0018</															

## Appendix B: Notes on the very young stars and PMS-like candidates

We briefly summarise the known properties of the very young stars and *PMS-like* candidates listed in Table 3 from the Simbad and Vizier databases and the literature.

- #1 RasTyc 0000+7940 (=BD+78 853) was discovered by Guillout et al. (2010) as a WTTS in the surroundings of the Cepheus flare region (e.g., Tachihara et al. 2005, and references therein). Guillout et al. (2010), on the basis of the different  $v \sin i$  values measured in the two AURELIE spectra, suspected that it was an SB2, but they warned that the different  $v \sin i$  may also be the result of a different CCF shape in the two spectral domains. In several spectra subsequently acquired with FRESCO we measured always the same RV, within the errors, and no significant  $v \sin i$  variation (see Table A.1). Therefore, we considered this star as a single one. The position on the HR diagram with the Siess et al. (2000) isochrones suggests an age of  $\approx 20$  Myr (Fig. 7).
- #2 RasTyc 0013+7702 (=TYC 4496-780-1) was discovered by Guillout et al. (2010) as a CTTS star, with a broad double-peaked emission, in the surroundings of the Cepheus flare region. They noticed two peaks with a very different height in the CCF that are centered at about 5 and 45 km s $^{-1}$  which suggests an SB2 system with components of very different luminosity. Other spectra subsequently taken with FRESCO confirm the binary nature of this source (see Table A.2). We have assumed that the atmospheric parameters derived with ROTFIT are basically those of the primary component and the effect of the secondary star is negligible, due to its faintness. RasTyc 0013+7702 is also a close visual binary ( $\rho = 1.^{\prime\prime}41$ ,  $\Delta V \simeq 2.2$  mag, Fabricius et al. 2002). The companion was also detected in the  $H$  band by the SEEDS survey (Uyama et al. 2017).
- #3 RasTyc 0038+7903 (=TYC 4500-1478-1) was discovered as a PMS star by Tachihara et al. (2005), who reported a K1 spectral type. It is one of the four co-moving PMS stars in the Cepheus flare region investigated by Guillout et al. (2010). It is a single star, based on the spectrum appearance and the constant RV. Its position on the HR diagram suggests an age of  $\approx 10$  Myr (Fig. 7).
- #4 RasTyc 0039+7905 (=BD+78 19) is the fourth PMS discovered by Guillout et al. (2010) in the surroundings of the Cepheus flare region. They suggested that BD+78 19 may be a binary system of mass ratio  $\approx 1$ . Indeed, further observations made by us revealed two CCF peaks of the same intensity with a separation of about 25 km s $^{-1}$  in two epochs (see Table A.2). The atmospheric parameters listed in Tables 3 and A.4 were derived from the analysis of the spectra taken at the conjunctions and can be considered as typical for both components. The position on the HR diagram suggests an age of  $\approx 10$  Myr (Fig. 7). However, considering the

system composed of two nearly equal stars, the luminosity of each component should be a factor of two less, bringing them closer to the 20 Myr isochrone.

- #5 RasTyc 0046+4808 (=TYC 3266-1767-1) is one the stars with the highest  $W_{\text{Li}}$  in our sample. No specific reference is found in the Simbad database. This object is listed in the catalog of the International Deep Planet Survey (Galicher et al. 2016) as a K3.5-type star with an age between 5 and 30 Myr. The classification is in fairly good agreement with our own (K2). No distance is reported in the Gaia DR1 catalog, which prevented us from estimating its age from the position on the HR diagram and studying its kinematical properties.
- #6 RasTyc 0222+5033 (=BD+49 646) was proposed as the optical counterpart of the X-ray source RX J0222.5+5033 by Motch et al. (1998) and classified as an active-corona source on the basis of the ROSAT hardness ratios. The star is located just below the Pleiades upper envelope in the  $(B - V)_0 - W_{\text{Li}}$  diagram (see Fig. 5). The space velocity components are fully compatible with the AB Dor moving group.
- #7 RasTyc 0230+5656 (=TYC 3695-2260-1). From its sky location Kharchenko et al. (2004) give a possible membership to the h and  $\chi$  Per open clusters. However its magnitude and colors are totally inconsistent with the color-magnitude of these clusters, as well as the Gaia distance of 165 pc, which is much smaller than that of these clusters ( $\sim 2.3$  kpc). The position on the HR diagram suggests an age of  $\approx 20$  Myr (Fig. 7) and its space velocity components are fairly compatible with the Pleiades SKG or the TW Hya association.
- #8 RasTyc 0252+3728 (=TYC 2338-35-1) is given as a G5 IV T Tau-type star in Simbad. It is listed in the Washington Visual Double Star (WDS) catalog (Mason et al. 2001) as a close physical visual binary with a separation of 0.^{\prime}6 and components of 9.34 and 10.77 mag in the  $K$  band; a third component of 13.4 mag separated by 4.^{\prime}9 is reported in the same catalog, but it is not given as a physical component. Li & Hu (1998) report an  $W_{\text{H}\alpha}^{\text{em}} = 0.50$  Å and  $W_{\text{Li}} = 220$  mÅ. Li (2004) classifies the system as a WTTS candidate with proper motions consistent with the Pleiades. From their survey with adaptive optics of young solar analogs Metchev & Hillenbrand (2009) estimated an age of about 200 Myr and a mass  $M = 1.1 M_{\odot}$  by adopting a distance of 170 pc. From high resolution spectroscopy White et al. (2007) found an  $W_{\text{H}\alpha}^{\text{em}} = 2.29$  Å and  $W_{\text{Li}} = 166$  mÅ. Moreover they report  $\text{RV} = 0.78 \pm 2.20$  km s $^{-1}$  and  $v \sin i = 29.59 \pm 1.55$  km s $^{-1}$ , in very good agreement with our determinations. We found a larger lithium EW ( $W_{\text{Li}} = 293 \pm 187$  mÅ) but with a large error, due to the low S/N of our spectrum. We confirm that the space velocity components are compatible with the Pleiades SKG.
- #9 RasTyc 0300+7225 (=TYC 4321-507-1) This star is located just below the Pleiades upper envelope in the  $(B - V)_0 - W_{\text{Li}}$  diagram (see Fig. 5). The position in the

**Table A.4.** continued.

RasTyc Name	$\alpha$ (2000) h m s	$\delta$ (2000) $^{\circ} \text{ } '$	Sp. Type	$T_{\text{eff}}$ (K)	$\sigma_{T_{\text{eff}}}$	$\log g$	$\sigma_{\log g}$	[Fe/H]	$\sigma_{[\text{Fe}/\text{H}]}$	$W_{\text{Li}}$ (mÅ)	$\sigma_{W_{\text{Li}}}$	$W_{\text{H}\alpha}^{em}$ • (mÅ)	$\sigma_{W_{\text{H}\alpha}^{em}}$	Bin <sup>a</sup>	Instr. <sup>b</sup>
RasTyc2308+0207	23 08 40.84	+02 07 39.4	G8III	5273	106	3.42	0.18	-0.08	0.11	8	5	26	9	S	EL
RasTyc2308+0000	23 08 50.46	+00 00 52.8	G2V	5620	211	4.38	0.23	-0.00	0.16	216	43	1009	189	S	EL
RasTyc2309-0225	23 09 37.09	-02 25 54.8	K4V	4557	74	4.60	0.10	0.01	0.11	195	26	1411	94	S	EL
RasTyc2309+1425	23 09 57.17	+14 25 36.3	G1V	5855	63	4.29	0.11	-0.10	0.11	2	7	96–127	23	SB1	EL
RasTyc2317+0941	23 17 32.23	+09 41 36.8	K4V	4738	107	4.58	0.10	0.03	0.11	10	7	62	21	S	EL
RasTyc2318+4458	23 18 48.11	+44 58 15.7	K0V	5237	123	4.34	0.26	0.01	0.15	189	52	88	46	S	FR
RasTyc2320+7414	23 20 52.07	+74 14 07.1	K0IV	5093	100	3.58	0.40	-0.02	0.12	365	44	4523	237	S	SA
RasTyc2321+0211	23 21 11.28	+02 11 50.5	K0III-IV	4974	72	3.10	0.14	-0.01	0.11	10	8	19–25	11	S	EL
RasTyc2321+4510	23 21 44.29	+45 10 34.4	K3V	4855	153	4.50	0.22	0.09	0.17	3	45	16	24	S	FR
RasTyc2321+0721	23 21 56.36	+07 21 33.0	K0V	5207	81	4.24	0.16	0.01	0.11	277	25	464	53	S	EL
RasTyc2323-0635	23 23 01.18	-06 35 43.6	K1III-IV	4755	104	2.87	0.26	-0.10	0.11	87	15	1345–2852	157	SB1	EL
RasTyc2324-0733	23 24 06.25	-07 33 02.7	G5IV-V	5677	57	4.29	0.10	-0.00	0.10	136	10	68	23	S	EL
RasTyc2324+6215	23 24 40.37	+62 15 51.1	F9V	6011	199	3.97	0.10	-0.21	0.17	136	20	123	23	S	AU
RasTyc2328+4522	23 28 27.48	+45 22 40.6	K0V	5428	136	4.21	0.17	0.05	0.11	50	41	684	149	S	SA
RasTyc2331+8124	23 31 29.96	+81 24 42.6	K1V	5239	80	4.08	0.20	0.00	0.11	18	22	245	38	S	SA
RasTyc2340-0402	23 40 06.09	-04 02 55.1	G1V	5853	108	4.26	0.14	-0.15	0.14	128	29	288	42	SB1 <sup>d</sup>	EL
RasTyc2340-0228	23 40 08.35	-02 28 49.6	G3V	5762	76	4.22	0.12	0.00	0.11	0	22	413	79	SB1 <sup>d</sup>	EL
RasTyc2341-0837	23 41 23.80	-08 37 47.1	K1V	5202	103	4.43	0.13	-0.05	0.11	22	15	100	21	S	EL
RasTyc2343+5038	23 43 58.22	+50 38 01.3	G5V	5731	106	4.34	0.08	-0.15	0.19	106	11	...	...	S	AU
RasTyc2348+4615	23 48 33.85	+46 15 10.5	G8III	4961	259	2.92	0.37	-0.03	0.18	58	111	...	...	S	FR
RasTyc2348+4614	23 48 35.53	+46 14 51.1	G0IV	5937	218	3.92	0.27	-0.00	0.15	...	...	43	96	S	FR
RasTyc2351+7739	23 51 17.29	+77 39 35.3	K1V	5146	78	4.52	0.17	-0.07	0.11	330	76	1197	156	S	SA
RasTyc2352-1143	23 52 10.24	-11 43 14.5	G1V	5822	109	4.30	0.13	-0.03	0.12	87	27	198	44	SB1 <sup>d</sup>	EL
RasTyc2353+4413	23 53 10.34	+44 13 58.0	G5V	5508	244	4.23	0.18	-0.04	0.09	184	9	165	14	S	AU
RasTyc2358+5140	23 58 16.09	+51 40 39.2	K1V	5158	75	4.52	0.18	-0.00	0.11	90	42	867	108	S	SA

• The full range of  $W_{\text{H}\alpha}^{em}$  values is reported for the stars observed in different epochs.

<sup>a</sup> S=single or only one RV measure; SB1=single-lined spectroscopic binary; SB2=double-lined.

<sup>b</sup> Spectrograph: SA = SARG, EL = ELODIE, AU = AURELIE, FR = FRESCO.

<sup>c</sup> Small-amplitude secondary peak in the CCF. Likely SB2 with a faint component. See Table A.2.

<sup>d</sup> RV variation with respect to SACY (Torres et al. 2006).

\* Double-peaked CCF. Possible SB2 with blended lines. See Table A.2.

\*\* Possible SB2. Broad- + narrow-line components at the same wavelength. Close visual pair with  $\rho = 0.^{\prime\prime}4$  (ESA 1997).

† Asymmetric CCF. Possible SB2 with blended lines. See Table A.2.

‡ Close visual binary. Composite spectrum. Unreliable parameters.

HR diagram is close to the ZAMS. The space velocity components are compatible with the Pleiades SKG.

#10 RasTyc 0311+4810 (=Cl Melotte 20 94) is given as

a rotationally variable F9V star in Simbad. Prosser (1992) classifies it as a photometric member of the  $\alpha$  Per cluster ( $d = 185$  pc, age=72 Myr). From kinematic parameters and a distance of 190 pc assumed for the center of the  $\alpha$  Per cluster, Makarov (2006) estimates for this stars an  $RV=2.65$  km s $^{-1}$  and a distance  $d=156$  pc, which are in reasonable agreement with our RV and the TGAS distance of  $133 \pm 5$  pc.

#11 RasTyc 0316+5638 (=TYC 3710-406-1) is listed in the TYCHO reference catalog Hoogerwerf (2000), which reports this star as a member of the  $\alpha$  Per OB association. The position on the sky along with the strong lithium line, the strongly filled in H $\alpha$  line, and its kinematics suggest that this star is related to the  $\alpha$  Per association.

#12 RasTyc 0323+5843 (=TYC 3715-195-1). In the WISE catalog (Wright et al. 2010) a weak probable variability in the W1 (3.35  $\mu$ m) band is reported. The H $\alpha$  line, in our SARG spectrum, is totally filled in by core emission that reaches the local continuum. Its position on the HR diagram suggests an age of  $\approx 15$  Myr (Fig. 7). However, its space velocity components are far from

the known young SKGs. It also lies outside of the locus of the young-disc (YD) population (see Fig. 10). With only one spectrum, we cannot exclude that this source is an SB1 system observed far from the conjunction.

#13 RasTyc 0331+4859 (=Cl Melotte 20 935) is a F9.5V star, in the  $\alpha$  Per cluster. From high-resolution spectroscopy Prosser (1992) found  $RV = -2.7$  km s $^{-1}$  and  $v \sin i = 78$  km s $^{-1}$  and defined the star as a member of  $\alpha$  Per cluster. In their analysis of rotation in young OCs Marilli et al. (1997) found  $V = 10.05$  mag,  $B-V = 0.62$  mag, a rotation period  $P_{\text{rot}} = 0.275$  d and a variation amplitude of 0.05 mag in the  $V$  band. From high-dispersion spectra of young nearby stars White et al. (2007) report an absorption H $\alpha$  feature with an equivalent width of 3.02 Å, a lithium absorption with  $W_{\text{Li}} = 110$  mÅ,  $RV = -1.8$  km s $^{-1}$ , and  $v \sin i = 64.44$  km s $^{-1}$ . On our SARG spectrum we measured nearly the same  $v \sin i$  (66.2 km s $^{-1}$ ), a slightly higher radial velocity ( $RV = 3.35 \pm 2.17$  km s $^{-1}$ ), and revealed an H $\alpha$  strongly filled in by core emission.

#14 RasTyc 0359+4404 (=TYC 2876-1944-1) is given as a rotationally variable star in Simbad. The variability with a period  $P_{\text{rot}} \approx 0.456$  d and a variation amplitude in the  $V$  band of 0.18 mag has been detected by ASAS (Kiraga & Stepień 2013). We found an RV variation of

- about  $11 \text{ km s}^{-1}$  in the two AURELIE spectra, which is, however, just smaller than the sum of the two uncertainties. Therefore, we have classified this star as single, but further observations are needed to exclude binarity.
- #15 RasTyc 0616+4516 (=TYC 3375-720-1) displays a H $\alpha$  line that is strongly filled in by core emission in our SARG spectrum. Its kinematics is not far from the average of the IC 2391 supercluster.
- #16 RasTyc 0621+5415 (=TYC 3764-338-1) has an age of  $\approx 20 \text{ Myr}$  based on its position on the HR diagram (Fig. 7). However, its space velocity components are far from the known young associations and moving groups. It is also outside the locus of the young-disc population (YD, see Fig. 10).
- #17 RasTyc 1908+5018 (=HD 234808) was already included in Paper I (the only reference present in the Simbad database), but the data were not analyzed in that paper. The position of this star in the HR diagram is well above the region occupied by the PMS stars and is more consistent with a giant star (see Figs. 4 and 7). The spectral classification (G8III-IV), the  $\log g$  value of 3.39 dex and the kinematics strengthen the hypothesis of a lithium-rich giant. This star shows far-infrared excess (see Sect. 4.7 and Fig. 9). The high lithium content of this target could have been synthesized through the Cameron & Fowler (1971) mechanism. This seems to be also supported by the presence of IR excess, which could be due to dust shell possibly generated via the same mechanism (de la Reza et al. 1996). A conclusive explanation is out of the scope of this work.
- #18 RasTyc 1925+4429 (=KIC 8429280) was identified as the optical counterpart of the X-ray source RX J1925.0+4429 by Motch et al. (1998). It is an active star observed by the *Kepler* space telescope whose light curves were analyzed by Savanov (2011) and Frasca et al. (2011) reconstructing the starspot pattern and evolution. In addition to measuring the differential rotation, Frasca et al. (2011) have also measured the atmospheric parameters, RV,  $v \sin i$ ,  $W_{\text{Li}}$  and chromospheric fluxes from the analysis of SARG and FRESCO spectra. These data have been also used in the present work. Unfortunately, the Gaia DR1 TGAS parallax and proper motions are not available for this source.
- #19 RasTyc 2004-0239 (=BD-03 4778) was identified as the optical counterpart of the X-ray source 1RXS J200449.5-023915 by Haakonsen & Rutledge (2009). A lower-mass stellar companion ( $\Delta K \approx 2.2 \text{ mag}$  at about  $2''.5$ ) was discovered by Elliott et al. (2015). From high resolution spectroscopy, da Silva et al. (2009) found  $T_{\text{eff}}=5083 \text{ K}$ ,  $W_{\text{Li}} = 290 \text{ m}\text{\AA}$ , and  $v \sin i=8 \text{ km s}^{-1}$ . Desidera et al. (2015) reported a K1 V spectral type and values of  $T_{\text{eff}}=5160 \pm 30 \text{ K}$ ,  $v \sin i=8 \text{ km s}^{-1}$ , and  $W_{\text{Li}} = 280 \text{ m}\text{\AA}$ . Folsom et al. (2016), with high-resolution spectropolarimetry, determined  $T_{\text{eff}}=5130 \pm 161 \text{ K}$ ,  $\log g=4.45 \pm 0.27$ ,  $v \sin i=9.6 \text{ km s}^{-1}$ , and measured the magnetic field. These values are close to our determinations ( $T_{\text{eff}}=5183 \pm 63 \text{ K}$ ,  $W_{\text{Li}} = 298 \text{ m}\text{\AA}$ ,  $v \sin i=9 \text{ km s}^{-1}$ ). Messina et al. (2010) found it as a member of AB Dor association and measured a rotation period  $P_{\text{rot}}=4.68 \text{ d}$  and a full amplitude of the variation in the  $V$  band of about 0.10 mag. This star is located just above the Pleiades upper envelope in our  $(B-V)_0-W_{\text{Li}}$  diagram (Fig. 5), which indicates an age of  $\approx 100 \text{ Myr}$ , which is in line with the age adopted by Desidera et al. (2015) and with that of AB Dor (100–125 Myr, Luhman et al. 2005). Its position on the HR diagram is, however, closer to 300 Myr isochrone, but the isochrones at ages larger than 50 Myr are very close to each other for  $T_{\text{eff}}>5000 \text{ K}$ , so that they are not very useful to infer ages in this case. The space velocity components derived by us (Fig. 10) confirm the membership to the AB Dor association.
- #20 RasTyc 2016+3106 (=HD 332091) was identified as the optical counterpart of the X-ray source 1RXS J200449.5-023915 by Haakonsen & Rutledge (2009). A temperature about 350 K cooler than our value was found by Muñoz Bermejo et al. (2013), who analyzed the same ELODIE spectra acquired by us. We note that our temperature value,  $T_{\text{eff}}=5082 \text{ K}$  is closer to the value of 5500 K derived with the Pecaut & Mamajek (2013) calibrations from the dereddened color index  $(B-V)_0=0.715 \text{ mag}$  than the value  $T_{\text{eff}}=4704 \text{ K}$  reported by Muñoz Bermejo et al. (2013). The H $\alpha$  line is a faint emission feature in all the three ELODIE spectra with a variation of  $\approx 30\%$ . The kinematics of this star suggest membership to the Pleiades SKG.
- #21 RasTyc 2036+3456 (=TYC 2694-1627-1). A temperature about 160 K cooler than our value was found by Muñoz Bermejo et al. (2013) from the analysis of our ELODIE spectrum. The H $\alpha$  line is filled in by core emission. The kinematics of this star suggest membership to the Pleiades SKG.
- #22 RasTyc 2039+2644 (=TYC 2178-1225-1) is given as a rotationally variable star in Simbad. The variability with a period  $P_{\text{rot}} \approx 3.485 \text{ d}$  and a variation amplitude in the  $V$  band of 0.06 mag has been detected by ASAS (Kiraga & Stepień 2013). The components of the space velocity indicate a possible association to the Pleiades supercluster.
- #23 RasTyc 2106+6906 (=BD+68 1182) is a chromospherically active star with the H $\alpha$  line filled in by core emission and  $v \sin i \approx 40 \text{ km s}^{-1}$ . Both the position on the HR diagram (Fig. 7) and on the  $(B-V)_0-W_{\text{Li}}$  diagram (Fig. 5) indicate a PMS object with an age of  $\approx 20\text{--}30 \text{ Myr}$ . Its space-velocity components are close to those of the other stars in the Cepheus flare region discovered by Guillout et al. (2010). Despite the large apparent distance on the sky, both the kinematics and age suggest that RasTyc 2106+6906 could be related to this stellar group.

- #24 RasTyc 2120+4636 (=TYC 3589-3858-1) was identified as the optical counterpart of the X-ray source RX J2120.9+4636 by Motch et al. (1997), who derived a spectral type F9V on the basis of medium-resolution spectra. Our spectral classification (G1.5 V) is in fairly good agreement with the previous work. It is classified as a rotationally variable star in Simbad. The variability with a period  $P_{\text{rot}} \simeq 0.266$  d and a variation amplitude in the  $V$  band of 0.08 mag has been detected by ASAS (Kiraga & Stepien 2013). RasTyc 2120+4636 is a very fast rotating star ( $v \sin i \simeq 110 \text{ km s}^{-1}$ ) with a filled H $\alpha$  line. Its space velocity components are far from the known young SKGs. It is also outside the locus of the young-disc population (YD, see Fig. 10). With only one spectrum, we cannot exclude that this source is an SB1 system observed far from the conjunction.
- #25 RasTyc 2223+7741 (=BD+76 857a). Both the position on the HR diagram (Fig. 7) and on the  $(B - V)_0 - W_{\text{Li}}$  diagram (Fig. 5) indicate a PMS object with an age of  $\approx 20$  Myr. Its space-velocity components are close to the Castor SKG and the Cepheus flare group.
- #26 RasTyc 2233+1040 (=TYC 1154-1546-1) was identified as the optical counterpart of the X-ray source RX J2232.9+1040 by Appenzeller et al. (1998). Zickgraf et al. (2005) give an uncertain spectral type K2V:,  $T_{\text{eff}} = 4836$  K,  $v \sin i = 97 \text{ km s}^{-1}$ , and  $W_{\text{Li}} = 285 \text{ m}\text{\AA}$ , which lead to an abundance  $A(\text{Li}) = 2.76$ . With these parameters, they classify the source as a ZAMS star with a lithium abundance between the lower and upper envelope of the Pleiades. We find a very similar  $W_{\text{Li}} = 282 \text{ m}\text{\AA}$ , but a very different temperature ( $T_{\text{eff}} = 5544$  K) and projected rotation velocity ( $v \sin i = 234 \text{ km s}^{-1}$ ). As a consequence of the higher  $T_{\text{eff}}$ , we determine a much higher lithium abundance,  $A(\text{Li}) = 3.65$  and the star lies over the Pleiades upper envelope, both in Figs. 5 and 6. We note that the TYCHO  $B - V = 0.558$ , that becomes  $(B - V)_0 = 0.521$  considering the reddening, is inconsistent with both the Zickgraf et al. (2005) and our  $T_{\text{eff}}$  determinations. The color listed in the APASS catalog (Henden et al. 2016),  $B - V = 0.723$  or  $(B - V)_0 = 0.686$ , agrees much better with our  $T_{\text{eff}}$  determination and that of 5361 K by Ammons et al. (2006). This star, due the aforementioned inconsistencies, deserves future investigations.
- #27 RasTyc 2241+1430 (=HD 214995) was identified as the optical counterpart of the X-ray source RX J2241.9+1431 by Appenzeller et al. (1998). Zickgraf et al. (2005) report a K0III spectral type,  $T_{\text{eff}} = 5152$  K,  $W_{\text{Li}} = 307 \text{ m}\text{\AA}$ ,  $A(\text{Li}) = 3.36$  and classify this star as an evolved lithium-rich one. The strong lithium line ( $W_{\text{Li}} = 389 \text{ m}\text{\AA}$ ) was confirmed by Luck & Heiter (2007). It was originally included in our list of ELODIE targets, but, based on the literature following our observations and on our results, we discard RasTyc 2241+1430 as PMS candidate and confirm its nature of a lithium-rich giant. The values of  $T_{\text{eff}}$  and  $\log g$  listed in the PASTEL catalog (Soubiran et al. 2010) are in the ranges 4560–4709 K and 2.61–2.70 dex, respectively. Our determinations (Table A.4) are in very good agreement with them.
- #28 RasTyc 2244+1754 (=BD+17 4799) is given as a K2 star in Simbad. This source was selected by Jeffries (1995) as optical counterpart of an EUV source. From intermediate-resolution spectroscopy, he estimated a spectral type K0V/IV, RV spanning from 0.7 to  $5.9 \text{ km s}^{-1}$ ,  $W_{\text{Li}} \simeq 300 \text{ m}\text{\AA}$ , and was also able to obtain a spectrum of a secondary visual component of spectral type M2Ve,  $V = 12.7$  mag, and  $RV = -2.5 \text{ km s}^{-1}$ , with a separation of about 3''; from kinematical analysis the system came out to belong to the Local Association. From high resolution spectroscopy, Fekel (1997) found for the primary visual component  $RV = -20.2 \text{ km s}^{-1}$ , suggesting a SB1 behavior, and  $v \sin i = 11.4 \text{ km s}^{-1}$ . Christian & Mathioudakis (2002) give  $v \sin i = 8 \text{ km s}^{-1}$  and  $W_{\text{Li}} = 244 \text{ m}\text{\AA}$  ( $A(\text{Li}) = 2.8$ ) in excellent agreement with our values (see Table A.4). López-Santiago et al. (2010) found from high-resolution spectra an average  $RV = -16.4 \text{ km s}^{-1}$ ,  $v \sin i = 11.03 \text{ km s}^{-1}$  and  $W_{\text{Li}} = 248 \text{ m}\text{\AA}$ , confirming the membership to the Local Association. Their values of H $\alpha$  equivalent width in the subtracted spectrum,  $W_{\text{H}\alpha}^{\text{em}}$ , are in the range 0.51–0.76  $\text{\AA}$ , in good agreement with our values of 0.60–0.72  $\text{\AA}$ . The spectrum of this source is shown in Fig. 2. The two RV values measured in our spectra are  $-16.58$  and  $-15.28$  whose difference is larger than the sum of errors. For this reason and from the literature data, we consider this star as SB1. The kinematical properties are still consistent with the Local Association, but the velocity components are closer to the AB Dor association (see Fig. 10).
- #29 RasTyc 2246+5749 (=TYC 3992-349-1) has only one reference in Simbad. It has been used as a local photometric standard star by Henden et al. (1999), who provide  $BVR_CI_C$  photometry, in a study of two eclipsing variables in Cepheus. Its space velocity components are far from the known young associations. It is also outside the locus of the young-disc population (YD, see Fig. 10). With only one spectrum, we cannot exclude that this source is an SB1 system observed far from the conjunction.
- #30 RasTyc 2307+3150 (=TYC 2751-9-1) is given as a K-type variable star in Simbad. In the General Catalogue of Variable Stars (GCVS, Samus et al. 2012) a period  $P_{\text{rot}} = 7.7129$  d with an amplitude of 0.04 mag is given. The space-velocity components are fairly consistent with Octans association or Castor group.
- #31 RasTyc 2320+7414 (=V395 Cep) is given as a variable star of Orion type in Simbad. Herbig (1977) reported a radial velocity of  $-10 \text{ km s}^{-1}$  with a strong Li I line and a spectral type G5-8Ve. In the Catalog of Emission-Line Stars of the Orion Population, Herbig & Bell (1988) reported emission in the H $\alpha$  line with an equivalent width of about 8  $\text{\AA}$  and located the star in the

L1259 nebulosity. In a study of PMS stars in the Cepheus flare region, Kun et al. (2009) classified this object as a CTTS belonging to the L1261 cloud. With the exception of the two lithium-rich giants, this is the star with the highest position on the HR diagram, close to the 5-Myr isochrone of Siess et al. (2000). Our SARG spectrum displays a broad double-peaked H $\alpha$  emission profile with a central absorption, which is typical of CTTS stars.

- #32 RasTyc 2321+0721 (=TYC 584-343-1) is given as a rotationally variable star in Simbad. A rotation period  $P_{\text{rot}} \simeq 2.5$  d and an amplitude  $\Delta V \simeq 0.076$  mag are reported by Watson et al. (2015). Torres et al. (2006) quote a K0V spectral type,  $v \sin i = 14.6$  km s $^{-1}$  and  $W_{\text{Li}} \simeq 300$  mÅ. Muñoz Bermejo et al. (2013), from the analysis of our ELODIE spectrum, found  $T_{\text{eff}} = 5221$  K. Our determinations (K0V,  $T_{\text{eff}} = 5207$  K,  $v \sin i = 14.3$  km s $^{-1}$ ,  $W_{\text{Li}} = 277 \pm 25$  mÅ) are in excellent agreement with the aforementioned values from the literature. A visual companion at 5''.1, which is 2 mag fainter in the  $J$  band, has been discovered by Elliott et al. (2015). Both the position on the HR diagram (Fig. 7) and on the  $(B-V)_0 - W_{\text{Li}}$  diagram (Fig. 5) indicate a young object with an age of  $\approx 30$  Myr. Its space-velocity components are just outside the YD locus but they are not far from those of Octans association.
- #33 RasTyc 2351+7739 (=TYC 4606-740-1). In the TYCHO Double Star Catalogue (Fabricius et al. 2002) it is quoted as a close visual binary with a separation of 0''.82 and components of  $V$  magnitudes 11.34 and 11.49 mag. The position on the  $(B-V)_0 - W_{\text{Li}}$  diagram (Fig. 5) indicates a *PMS-like* object on the upper envelope of the IC 2602 cluster ( $\text{age} \approx 30$  Myr). Unfortunately, the parallax is not available, preventing us to place this object on the HR diagram and to investigate its kinematical properties.
- a RasTyc 0106+3306 (=TYC 2282-1396-1) is quoted as a close visual pair ( $\rho = 0''.85$ ,  $\Delta V \simeq 0.29$  mag, Fabricius et al. 2002). The  $B - V$  color reported in TYCHO catalog ( $B - V = 1.092$  mag) is probably unreliable, as well as the individual colors of both components ( $B - V \approx 1.0 - 1.1$  mag, Fabricius et al. 2002), which are at odds with our spectral classification. This could be due to binary nature. However, the value of  $B - V = 0.646$  mag reported by Henden et al. (2016) agrees much better with our G4V type and  $T_{\text{eff}} = 5606$  K. With this color RasTyc 0106+3306 would move on the left side in the  $(B-V)_0 - W_{\text{Li}}$  diagram (Fig. 5), overcoming the Pleiades upper envelope. The parallax is not available, preventing us to place this object on the HR diagram and to investigate its kinematical properties. Anyway, Dias et al. (2014) consider this star as a member of the cluster Platais 2 ( $\text{age} \sim 350$  Myr).
- b RasTyc 0249+4255 (=BD+42 636) is given as a G3 star of the NGC 1039 OC ( $d = 499$  pc,  $\text{age} = 180$  My) in Simbad. Kharchenko et al. (2004) found that the star

is not a member of NGC 1039. Indeed, the Gaia DR1 TGAS distance,  $d = 118.3 \pm 13.9$  pc, is inconsistent with NGC 1039. The space-velocity components are close to those of the TW Hya association.

- c RasTyc 0344+5043 (=TYC 3325-98-1) is reported as a close pair in the WDS catalog (Mason et al. 2001), with a separation of 0''.7 and components of magnitudes 10.80 and 12.80 mag. This star is well inside the inner radius of the  $\alpha$  Per cluster, but its photometry and kinematics exclude membership to the cluster (Kharchenko et al. 2004). The Gaia DR1 parallax is not available, preventing us to place this object on the HR diagram and to investigate its kinematical properties.
- d RasTyc 0646+4147 (=TYC 2949-780-1) has no specific reference in Simbad.
- e RasTyc 1731+2815 (=TYC 2087-1742-1) is quoted as a rotationally variable star in Simbad. The rotation period of about 1.26 d was measured both by SuperWASP (Norton et al. 2007) and ASAS (Kiraga 2012) observations. Dragomir et al. (2007) associated the X-ray source 1RXS J173103.4+281510 to this optical counterpart and classified it as a G/K star from low-resolution spectra. This star was observed spectroscopically by Binks et al. (2015) who found  $RV = -18.2 \pm 0.5$  km s $^{-1}$ ,  $W_{\text{Li}} = 265 \pm 36$  mÅ, and a faint H $\alpha$  absorption line with equivalent width of 0.19 Å. They estimated the age in the range 30–150 Myr, based on  $W_{\text{Li}}$ , and a lower limit of 37 Myr, on the basis of the H $\alpha$  and  $(V - I)$  color. Our values of  $RV = -19.22 \pm 0.62$  km s $^{-1}$  and  $W_{\text{Li}} = 243 \pm 22$  mÅ are not significantly different from that of (Binks et al. 2015). The H $\alpha$  line is totally filled in with emission.
- f RasTyc 1956+4345 (=KIC 7985370) was discovered as a periodic variable in the field of the *Kepler* space telescope by Pigulski et al. (2009), who found a period  $P_{\text{rot}} = 0.4249$  d and amplitudes of 0.04 mag and 0.02 mag in the  $V$  and  $I$  light curves, respectively. The *Kepler* light curves were analyzed by Fröhlich et al. (2012) who redetermined the period as 2.86 d and reconstructed the starspot distribution and evolution over 229 days with a Bayesian spot model. In addition to measuring the differential rotation, Fröhlich et al. (2012) have also measured the atmospheric parameters,  $RV$ ,  $v \sin i$ ,  $W_{\text{Li}}$ , and chromospheric fluxes from the analysis of SARG and FRESCO spectra. These data have been also used in the present work. As already discussed by Fröhlich et al. (2012), the kinematical properties of KIC 7985370 indicate it is a member of the Local Association (Pleiades SKG).
- g RasTyc 2038+3546 (=BD+35 4198) was included in the bright catalog (Paper I) but the ELODIE spectrum was not analyzed with ROTFIT. In the present paper, the analysis of the ELODIE and a new SARG spectrum provided us with revised values of atmospheric parameters,  $W_{\text{Li}}$ , and  $W_{\text{H}\alpha}^{\text{em}}$ . The value of  $T_{\text{eff}}$  we find (5895 K) is slightly larger than in Paper I and agrees better with the determination of 5954 K by

- Muñoz Bermejo et al. (2013). Based on its kinematical properties, it could be a member of the Pleiades SKG.
- h* RasTyc 2114+3941 (=BD+39 4490) was included in the RasTyc bright catalog (Paper I) but the ELODIE spectrum was not analyzed with ROTFIT. In that paper the parameters were derived from two AURELIE spectra which provided  $T_{\text{eff}} = 5731 \text{ K}$ ,  $W_{\text{Li}} = 101 \text{ m}\text{\AA}$ , and  $W_{\text{H}\alpha}^{\text{em}} = 64 \text{ m}\text{\AA}$ . The ELODIE spectrum, with its higher quality (especially in terms of the wider spectral range), provides us with a higher value of  $T_{\text{eff}} = 5930 \text{ K}$ , which agrees better with the value of 5955 K derived by Muñoz Bermejo et al. (2013). The slightly larger  $W_{\text{Li}} = 131 \pm 27 \text{ m}\text{\AA}$  measured in the ELODIE spectrum leads to a lithium abundance  $A(\text{Li}) = 3.01$ , which brings the star just above the Pleiades upper envelope in Fig. 6. We also find a higher  $W_{\text{H}\alpha}^{\text{em}} = 149 \pm 34 \text{ m}\text{\AA}$ , which is likely due to variations of the chromospheric activity. The  $U_{\odot}$  and  $V_{\odot}$  velocity components are close to Castor, but the  $W_{\odot}$  is not.
- i* RasTyc 2203+3809 (=TYC 3198-1809-1) has no specific reference in Simbad. We did not find any spectroscopic study in the literature. This object lies under the Pleiades upper envelope in the  $(B - V)_0 - W_{\text{Li}}$  diagram (Fig. 5), but it is just above it in the diagram  $T_{\text{eff}} - A(\text{Li})$  (Fig. 6).
- j* RasTyc 2308+0000 (=TYC 576-1220-1) is quoted as a PMS star in Simbad. It was associated to the X-ray source RX J2308.8+0001 by Zickgraf et al. (2003). Torres et al. (2006) quote a G8V spectral type,  $RV = 7.4 \text{ km s}^{-1}$ ,  $v \sin i = 39.0 \pm 9.0 \text{ km s}^{-1}$  and  $W_{\text{Li}} = 250 \text{ m}\text{\AA}$ . We find an earlier spectral type (G2V) and a slightly lower  $W_{\text{Li}} = 216 \pm 43 \text{ m}\text{\AA}$ . The  $v \sin i$  value of  $42.8 \pm 5.2 \text{ km s}^{-1}$  agrees with that of Torres et al. (2006), but the  $RV = 5.30 \pm 0.22 \text{ km s}^{-1}$  can be indicative of an SB1 system, even if Torres et al. (2006) do not provide the error of their RV measure. However, an RV variation is also indicated by the value of  $RV = 1.696 \pm 2.642 \text{ km s}^{-1}$  reported in the RAVE 5th data release (Kunder et al. 2017). In this catalog, values for the atmospheric parameters of  $T_{\text{eff}} = 6000 \text{ K}$ ,  $\log g = 4.00$ , and  $[\text{Fe}/\text{H}] = -0.25$  are also reported. The effective temperature of  $T_{\text{eff}} = 5533 \text{ K}$  derived by Kunder et al. (2017) with the infrared flux method is in better agreement with our determination of  $T_{\text{eff}} = 5620 \pm 211 \text{ K}$ . This star lies between the 20- and 30-Myr isochrones in the HR diagram (Fig. 7) and close to the UVW position of Octans association.
- k* RasTyc 2324+6215 (=TYC 4283-219-1) has no specific reference in Simbad, where an F8 spectral type is reported. The Gaia DR1 parallax is not available, preventing us to place this object on the HR diagram and to investigate in detail its kinematical properties.
- ‘HD 157214’ on page 4  
 ‘HD 32923’ on page 4  
 ‘HD 117176’ on page 4  
 ‘HD 10700’ on page 4  
 ‘HD 145675’ on page 4  
 ‘HD 221354’ on page 4  
 ‘HD 115404’ on page 4  
 ‘HD 182572’ on page 4  
 ‘HD 12929’ on page 4  
 ‘HD 161096’ on page 4  
 ‘BD+78 853’ on page 23  
 ‘BD+51 3761’ on page 23  
 ‘HD 225263’ on page 23  
 ‘HD 330’ on page 23  
 ‘BD+38 16’ on page 23  
 ‘BD+38 16’ on page 23  
 ‘NLTT 836’ on page 23  
 ‘NLTT 836’ on page 23  
 ‘TYC 4492-314-1’ on page 23  
 ‘HD 2770’ on page 23  
 ‘HD 2770’ on page 23  
 ‘TYC 3654-1907-1’ on page 23  
 ‘TYC 4015-206-1’ on page 23  
 ‘TYC 4015-206-1’ on page 23  
 ‘TYC 4500-1478-1’ on page 23  
 ‘TYC 4500-1478-1’ on page 23  
 ‘TYC 4500-1478-1’ on page 23  
 ‘V498 And’ on page 23  
 ‘QT And’ on page 23  
 ‘QT And’ on page 23  
 ‘BD+78 22’ on page 23  
 ‘TYC 3266-1767-1’ on page 23  
 ‘TYC 3266-1767-1’ on page 23  
 ‘TYC 3262-1820-1’ on page 23  
 ‘TYC 3262-1820-1’ on page 23  
 ‘TYC 3659-1102-1’ on page 23  
 ‘HD 4940’ on page 23  
 ‘HD 232342’ on page 23  
 ‘HD 232342’ on page 23  
 ‘TYC 3676-2617-1’ on page 23  
 ‘TYC 2282-1396-1’ on page 23  
 ‘TYC 2282-1396-1’ on page 23  
 ‘TYC 3676-2444-1’ on page 23  
 ‘TYC 2804-13-1’ on page 23  
 ‘TYC 2804-13-1’ on page 23  
 ‘TYC 2814-1888-1’ on page 23  
 ‘BD+41 324’ on page 23  
 ‘BD+41 324’ on page 23  
 ‘BD+49 435’ on page 23  
 ‘TYC 4040-810-1’ on page 23  
 ‘G 133-53’ on page 23  
 ‘G 133-53’ on page 23  
 ‘BD+35 380’ on page 23  
 ‘BD+35 380’ on page 23  
 ‘TYC 2842-24-1’ on page 23

## List of Objects

- ‘HD 187691’ on page 4  
 ‘HD 102870’ on page 4

- ‘TYC 2842-24-1’ on page 23
- ‘BD+33 411’ on page 23
- ‘BD+33 411’ on page 23
- ‘TYC 4319-714-1’ on page 23
- ‘BD+49 646’ on page 23
- ‘BD+49 646’ on page 23
- ‘TYC 3295-2024-1’ on page 23
- ‘TYC 4320-1432-1’ on page 23
- ‘TYC 4320-1432-1’ on page 23
- ‘TYC 3695-2260-1’ on page 23
- ‘BD+54 561B’ on page 23
- ‘BD+54 561B’ on page 23
- ‘BD+31 455’ on page 23
- ‘TYC 4047-1570-1’ on page 23
- ‘TYC 4047-1570-1’ on page 23
- ‘TYC 3296-219-1’ on page 23
- ‘BD+37 604B’ on page 23
- ‘BD+37 604B’ on page 23
- ‘BD+42 636’ on page 23
- ‘V875 Per’ on page 23
- ‘TYC 2338-35-1’ on page 23
- ‘HD 17785A’ on page 23
- ‘TYC 4048-1944-1’ on page 23
- ‘TYC 4321-507-1’ on page 23
- ‘TYC 2859-1123-1’ on page 23
- ‘TYC 2859-1123-1’ on page 23
- ‘Cl Melotte 20 94’ on page 23
- ‘HD 19438’ on page 24
- ‘BD+37 729’ on page 24
- ‘TYC 3315-962-1’ on page 24
- ‘TYC 3710-406-1’ on page 24
- ‘BD+60 656’ on page 24
- ‘BD+60 656’ on page 24
- ‘TYC 2860-1368-1’ on page 24
- ‘TYC 2860-1368-1’ on page 24
- ‘TYC 3715-195-1’ on page 24
- ‘HD 278566’ on page 24
- ‘BD+30 547’ on page 24
- ‘Cl Melotte 20 935’ on page 24
- ‘HD 275480’ on page 24
- ‘HD 275480’ on page 24
- ‘TYC 3317-2589-1’ on page 24
- ‘BD+66 278’ on page 24
- ‘BD+66 278’ on page 24
- ‘TYC 3325-98-1’ on page 24
- ‘TYC 4327-2618-1’ on page 24
- ‘\*\* COU 2357’ on page 24
- ‘\*\* COU 2357’ on page 24
- ‘TYC 2876-1944-1’ on page 24
- ‘TYC 2876-1944-1’ on page 24
- ‘BD+72 206’ on page 24
- ‘2MASS J04120187+7318383’ on page 24
- ‘2MASS J04121487+4616128’ on page 24
- ‘TYC 2886-1693-1’ on page 24
- ‘TYC 2886-1693-1’ on page 24
- ‘CCDM J04395+3408AB’ on page 24
- ‘CCDM J04395+3408AB’ on page 24
- ‘TYC 3343-86-1’ on page 24
- ‘TYC 3351-518-1’ on page 24
- ‘TYC 3349-2052-1’ on page 24
- ‘TYC 3349-2052-1’ on page 24
- ‘TYC 3349-2052-1’ on page 24
- ‘HD 280272’ on page 24
- ‘HD 280272’ on page 24
- ‘WDS J05012+3430AB’ on page 24
- ‘HD 277665’ on page 24
- ‘HD 277665’ on page 24
- ‘HD 277665’ on page 24
- ‘TYC 4084-172-1’ on page 24
- ‘TYC 4084-172-1’ on page 24
- ‘V613 Aur’ on page 24
- ‘G 191-47’ on page 24
- ‘BD+40 1397B’ on page 24
- ‘BD+40 1397B’ on page 24
- ‘TYC 3759-804-1’ on page 24
- ‘TYC 3379-358-1’ on page 24
- ‘TYC 3379-358-1’ on page 24
- ‘TYC 3375-720-1’ on page 24
- ‘TYC 4357-209-1’ on page 24
- ‘TYC 4357-209-1’ on page 24
- ‘TYC 3764-338-1’ on page 24
- ‘TYC 3764-338-1’ on page 24
- ‘HD 44271’ on page 24
- ‘HD 257514’ on page 24
- ‘HD 257514’ on page 24
- ‘BD+31 1301p’ on page 24
- ‘BD+31 1301p’ on page 24
- ‘HD 259536’ on page 24
- ‘HD 259536’ on page 24
- ‘HD 260708’ on page 24
- ‘HD 260708’ on page 24
- ‘HD 263268’ on page 24
- ‘HD 263268’ on page 24
- ‘TYC 2949-780-1’ on page 24
- ‘HD 237554’ on page 24
- ‘HD 237554’ on page 24
- ‘TYC 4364-1262-1’ on page 25
- ‘TYC 4364-1262-1’ on page 25
- ‘TYC 3404-384-1’ on page 25
- ‘TYC 3404-384-1’ on page 25
- ‘TYC 3780-247-1’ on page 25
- ‘TYC 4116-276-1’ on page 25
- ‘CCDM J07346+3519AB’ on page 25
- ‘CCDM J07346+3519AB’ on page 25
- ‘TYC 2964-272-1’ on page 25
- ‘TYC 2964-272-1’ on page 25
- ‘BD+65 601’ on page 25
- ‘BD+65 601’ on page 25
- ‘BD+47 2200’ on page 25
- ‘HD 134418’ on page 25

- ‘BD+86 23’ on page 25  
 ‘BD +04 2967’ on page 25  
 ‘BD +04 2967’ on page 25  
 ‘BD+40 2871’ on page 25  
 ‘BD-08 3958’ on page 25  
 ‘TYC 3055-1099-1’ on page 25  
 ‘TYC 2031-874-1’ on page 25  
 ‘BD+18 3026’ on page 25  
 ‘BD+67 900’ on page 25  
 ‘BD+49 2392’ on page 25  
 ‘BD+49 2392’ on page 25  
 ‘V335 Boo’ on page 25  
 ‘TYC 4560-1035-1’ on page 25  
 ‘TYC 3870-1361-1’ on page 25  
 ‘TYC 3490-591-1’ on page 25  
 ‘TYC 3490-273-1’ on page 25  
 ‘TYC 3870-1328-1’ on page 25  
 ‘BD+15 2919’ on page 25  
 ‘TYC 944-634-1’ on page 25  
 ‘BD+82 477’ on page 25  
 ‘BD+04 3107’ on page 25  
 ‘BD-03 3912’ on page 25  
 ‘BD+07 3142’ on page 25  
 ‘BD+07 3142’ on page 25  
 ‘BD+49 2494’ on page 25  
 ‘BD+35 2809’ on page 25  
 ‘BD+34 2784’ on page 25  
 ‘BD+08 3197’ on page 25  
 ‘BD+74 668’ on page 25  
 ‘BD+17 3038’ on page 25  
 ‘BD+09 3217’ on page 25  
 ‘BD+19 3113A’ on page 25  
 ‘BD+19 3113B’ on page 25  
 ‘BD+07 3214’ on page 25  
 ‘BD+15 3037’ on page 25  
 ‘V2581 Oph’ on page 25  
 ‘BD+11 3024’ on page 25  
 ‘HD 151367’ on page 25  
 ‘BD+30 2871B’ on page 25  
 ‘HD 238614’ on page 25  
 ‘HD 238614’ on page 25  
 ‘BD+01 3328’ on page 25  
 ‘BD+06 3324’ on page 25  
 ‘TYC 2594-1053-1’ on page 25  
 ‘TYC 3501-626-1’ on page 25  
 ‘BD+21 3035’ on page 25  
 ‘HD 154361’ on page 25  
 ‘HD 154734’ on page 25  
 ‘HD 154734’ on page 25  
 ‘BD+06 3372a’ on page 25  
 ‘HD 156517’ on page 25  
 ‘HD 156517’ on page 25  
 ‘TYC 1545-934-1’ on page 25  
 ‘BD-01 3338’ on page 25  
 ‘TYC 2087-1742-1’ on page 25  
 ‘BD+05 3448’ on page 25  
 ‘BD+02 3384’ on page 25  
 ‘BD+66 1042’ on page 25  
 ‘BD+01 3549’ on page 25  
 ‘BD+33 3013’ on page 25  
 ‘BD+33 3013’ on page 25  
 ‘BD-08 4562’ on page 25  
 ‘BD+28 2972’ on page 25  
 ‘BD+28 2972’ on page 25  
 ‘TYC 3905-319-1’ on page 26  
 ‘BD+02 3633’ on page 26  
 ‘HD 173605’ on page 26  
 ‘KIC 7730305’ on page 26  
 ‘KIC 7730305’ on page 26  
 ‘BD+29 3349’ on page 26  
 ‘BD+63 1470’ on page 26  
 ‘BD+62 1669’ on page 26  
 ‘BD+01 3828’ on page 26  
 ‘BD+01 3828’ on page 26  
 ‘HD 234808’ on page 26  
 ‘HD 181209’ on page 26  
 ‘HD 181215’ on page 26  
 ‘KIC 8429280’ on page 26  
 ‘KIC 8429280’ on page 26  
 ‘TYC 4588-319-1’ on page 26  
 ‘KIC 11244501’ on page 26  
 ‘BD+12 3917’ on page 26  
 ‘HD 338348’ on page 26  
 ‘KIC 11560431’ on page 26  
 ‘KIC 11560431’ on page 26  
 ‘HD 338736’ on page 26  
 ‘HD 338736’ on page 26  
 ‘TYC 5725-63-1’ on page 26  
 ‘TYC 5725-63-1’ on page 26  
 ‘KIC 7985370’ on page 26  
 ‘KIC 7985370’ on page 26  
 ‘KIC 7985370’ on page 26  
 ‘HD 189572’ on page 26  
 ‘BD+53 2331a’ on page 26  
 ‘KIC 7477572’ on page 26  
 ‘KIC 7477572’ on page 26  
 ‘KIC 7477572’ on page 26  
 ‘HD 189285’ on page 26  
 ‘HD 189285’ on page 26  
 ‘TYC 3948-2133-1’ on page 26  
 ‘HD 189806’ on page 26  
 ‘BD-03 4778’ on page 26  
 ‘HD 192362’ on page 26  
 ‘HD 192362’ on page 26  
 ‘HD 228564’ on page 26  
 ‘HD 192787’ on page 26  
 ‘HD 332091’ on page 26  
 ‘HD 332091’ on page 26  
 ‘HD 332091’ on page 26  
 ‘HD 332148’ on page 26  
 ‘TYC 2672-0717-1’ on page 26  
 ‘V1971 Cyg’ on page 26  
 ‘BD+05 4489’ on page 26  
 ‘BD-04 5118’ on page 26  
 ‘BD+24 4140’ on page 26

- ‘TYC 1095-848-1’ on page 26  
 ‘BD-10 5400’ on page 26  
 ‘BD+48 3149’ on page 26  
 ‘BD+48 3149’ on page 26  
 ‘BD+48 3149’ on page 26  
 ‘HD 334514’ on page 26  
 ‘BD-07 5331’ on page 26  
 ‘TYC 2694-1627-1’ on page 26  
 ‘HD 235299’ on page 26  
 ‘HD 235299’ on page 26  
 ‘BD+35 4198’ on page 26  
 ‘BD+35 4198’ on page 26  
 ‘TYC 2178-1225-1’ on page 26  
 ‘TYC 2178-1225-1’ on page 26  
 ‘BU Vul’ on page 26  
 ‘HD 198217’ on page 26  
 ‘HD 198217’ on page 26  
 ‘HD 198809’ on page 26  
 ‘BD+42 3895’ on page 26  
 ‘BD+43 3754’ on page 26  
 ‘HD 341233’ on page 26  
 ‘BD+36 4301’ on page 26  
 ‘V1794 Cyg’ on page 26  
 ‘V1794 Cyg’ on page 26  
 ‘HD 199546’ on page 26  
 ‘HD 199598’ on page 26  
 ‘HD 199956’ on page 26  
 ‘HD 200019’ on page 26  
 ‘TYC 3180-1594-1’ on page 27  
 ‘BD+09 4700’ on page 27  
 ‘BD+09 4700’ on page 27  
 ‘V2436 Cyg’ on page 27  
 ‘TYC 3172-643-1’ on page 27  
 ‘TYC 3172-652-1’ on page 27  
 ‘BD+01 4422’ on page 27  
 ‘BD+68 1182’ on page 27  
 ‘TYC 538-165-1’ on page 27  
 ‘TYC 2709-1412-1’ on page 27  
 ‘TYC 3172-1505-1’ on page 27  
 ‘TYC 3172-1505-1’ on page 27  
 ‘BD-01 4129’ on page 27  
 ‘BD+39 4490’ on page 27  
 ‘TYC 3181-1403-1’ on page 27  
 ‘HD 202779’ on page 27  
 ‘BD-07 5533’ on page 27  
 ‘V457 Vul’ on page 27  
 ‘TYC 3589-3858-1’ on page 27  
 ‘HD 203454’ on page 27  
 ‘HD 203454’ on page 27  
 ‘HD 204734’ on page 27  
 ‘HD 205113’ on page 27  
 ‘HD 205173’ on page 27  
 ‘HD 205762’ on page 27  
 ‘HD 206374’ on page 27  
 ‘TYC 2197-1430-1’ on page 27  
 ‘TYC 2197-1430-1’ on page 27  
 ‘TYC 2197-1430-1’ on page 27  
 ‘BD+37 4406’ on page 27  
 ‘BD+26 4249’ on page 27  
 ‘TYC 2206-1706-1’ on page 27  
 ‘TYC 2206-1706-1’ on page 27  
 ‘TYC 2206-1706-1’ on page 27  
 ‘TYC 3612-2224-1’ on page 27  
 ‘TYC 3612-2224-1’ on page 27  
 ‘BD+49 3625’ on page 27  
 ‘BD+49 3625’ on page 27  
 ‘BD+49 3625’ on page 27  
 ‘BD-04 5541’ on page 27  
 ‘TYC 2718-320-1’ on page 27  
 ‘TYC 3188-0129-1’ on page 27  
 ‘HD 208076’ on page 27  
 ‘HD 208038’ on page 27  
 ‘BD-10 5791’ on page 27  
 ‘BD-08 5773’ on page 27  
 ‘TYC 545-521-1’ on page 27  
 ‘TYC 1680-1993-1’ on page 27  
 ‘TYC 1680-1993-1’ on page 27  
 ‘TYC 1680-1993-1’ on page 27  
 ‘BD+47 3668’ on page 27  
 ‘BD-04 5601’ on page 27  
 ‘TYC 2719-2054-1’ on page 27  
 ‘TYC 2719-2054-1’ on page 27  
 ‘TYC 3198-1809-1’ on page 27  
 ‘BD+01 4577’ on page 27  
 ‘TYC 5224-1153-1’ on page 27  
 ‘TYC 3617-844-1’ on page 27  
 ‘HD 210264’ on page 27  
 ‘HD 210460’ on page 27  
 ‘HD 210750’ on page 27  
 ‘TYC 1689-910-1’ on page 27  
 ‘TYC 1689-910-1’ on page 27  
 ‘WW Cep’ on page 27  
 ‘BD-00 4347’ on page 27  
 ‘TYC 2230-469-1’ on page 27  
 ‘TYC 2230-469-1’ on page 27  
 ‘TYC 2230-469-1’ on page 27  
 ‘BD+27 4302s’ on page 27  
 ‘BD+27 4302s’ on page 27  
 ‘BD+76 857a’ on page 27  
 ‘BD+19 4915’ on page 27  
 ‘TYC 3607-2096-1’ on page 27  
 ‘TYC 1699-745-1’ on page 27  
 ‘HD 212873’ on page 27  
 ‘TYC 2226-2417-1’ on page 27  
 ‘TYC 1154-1546-1’ on page 27  
 ‘HD 214129’ on page 28  
 ‘HD 214129’ on page 28  
 ‘TYC 4480-965-1’ on page 28  
 ‘HD 214494’ on page 28  
 ‘V403 Peg’ on page 28  
 ‘HD 214850’ on page 28  
 ‘HD 214995’ on page 28  
 ‘TYC 1705-265-1’ on page 28  
 ‘HD 215363’ on page 28  
 ‘BD+17 4799’ on page 28  
 ‘BD+17 4799’ on page 28

- ‘TYC 2736-1564-1’ on page 28
- ‘TYC 3992-349-1’ on page 28
- ‘TYC 3629-2082-1’ on page 28
- ‘BD+84 518’ on page 28
- ‘BD+16 4830’ on page 28
- ‘BD+02 4578’ on page 28
- ‘TYC 572-382-1’ on page 28
- ‘AZ Psc’ on page 28
- ‘AZ Psc’ on page 28
- ‘AZ Psc’ on page 28
- ‘CCDM J22594+4017AB’ on page 28
- ‘CCDM J22594+4017AB’ on page 28
- ‘BD+34 4820’ on page 28
- ‘BD+34 4820’ on page 28
- ‘TYC 2758-1743-1’ on page 28
- ‘TYC 2758-1743-1’ on page 28
- ‘TYC 1711-1440-1’ on page 28
- ‘TYC 5242-383-1’ on page 28
- ‘TYC 2751-9-1’ on page 28
- ‘HD 218527’ on page 28
- ‘TYC 576-1220-1’ on page 28
- ‘BD-03 5579’ on page 28
- ‘HD 218687’ on page 28
- ‘HD 218687’ on page 28
- ‘HD 218687’ on page 28
- ‘BD+08 5036’ on page 28
- ‘TYC 3229-143-1’ on page 28
- ‘V395 Cep’ on page 28
- ‘HD 220119’ on page 28
- ‘HD 220119’ on page 28
- ‘HD 220221’ on page 28
- ‘TYC 584-343-1’ on page 28
- ‘HD 220338’ on page 28
- ‘HD 220338’ on page 28
- ‘HD 220338’ on page 28
- ‘NX Aqr’ on page 28
- ‘TYC 4283-219-1’ on page 28
- ‘TYC 4283-219-1’ on page 28
- ‘TYC 3637-396-1’ on page 28
- ‘TYC 4614-981-1’ on page 28
- ‘BD-04 5927’ on page 28
- ‘BD-03 5686’ on page 28
- ‘HD 222522’ on page 28
- ‘BD+49 4204’ on page 28
- ‘BD+49 4204’ on page 28
- ‘TYC 3638-993-1’ on page 28
- ‘TYC 3638-1539-1’ on page 28
- ‘TYC 4606-740-1’ on page 28
- ‘HD 223728’ on page 28
- ‘TYC 3245-1421-1’ on page 28
- ‘TYC 3245-1421-1’ on page 28
- ‘TYC 3651-546-1’ on page 28
- ‘TYC 4496-780-1’ on page 29
- ‘TYC 3661-1206-1’ on page 29
- ‘HD 236456’ on page 29
- ‘HD 236456’ on page 29
- ‘TYC 3654-1907-1’ on page 29
- ‘TYC 2279-359-1’ on page 29
- ‘BD+78 19’ on page 29
- ‘TYC 3274-955-1’ on page 29
- ‘TYC 3672-1578-1’ on page 29
- ‘TYC 3276-1291-1’ on page 29
- ‘HN Psc’ on page 29
- ‘TYC 4314-1757-1’ on page 29
- ‘TYC 2298-964-1’ on page 29
- ‘TYC 3710-247-1’ on page 29
- ‘BD+42 765’ on page 29
- ‘BD+55 849’ on page 29
- ‘TYC 3328-2470-1’ on page 29
- ‘BD+38 859’ on page 29
- ‘BD+38 859’ on page 29
- ‘HD 281777’ on page 29
- ‘TYC 3723-1082-1’ on page 29
- ‘TYC 3723-1082-1’ on page 29
- ‘TYC 3723-1082-1’ on page 29
- ‘HD 280583’ on page 29
- ‘HD 280583’ on page 29
- ‘HD 280583’ on page 29
- ‘V607 Aur’ on page 29
- ‘TYC 3386-868-1’ on page 29
- ‘TYC 4345-1307-1’ on page 29
- ‘TYC 2424-396-1’ on page 29
- ‘TYC 2942-2009-1’ on page 29
- ‘TYC 2955-479-1’ on page 29
- ‘BD+40 1796’ on page 29
- ‘HD 133162’ on page 29
- ‘HD 133162’ on page 29
- ‘TYC 4181-507-1’ on page 29
- ‘TYC 4187-96-1’ on page 29
- ‘BD+08 3048’ on page 29
- ‘BD+49 2412’ on page 29
- ‘BD+49 2412’ on page 29
- ‘G 137-52’ on page 29
- ‘G 137-52’ on page 29
- ‘HIP 77628’ on page 29
- ‘BD+10 2953’ on page 29
- ‘TYC 945-949-1’ on page 29
- ‘TYC 370-538-1’ on page 29
- ‘TYC 370-538-1’ on page 29
- ‘V1079 Her’ on page 29
- ‘V1079 Her’ on page 29
- ‘V1079 Her’ on page 29
- ‘BD+46 2173’ on page 29
- ‘BD+32 2733’ on page 29
- ‘BD+23 2969’ on page 29
- ‘BD+20 3376’ on page 29
- ‘TYC 3501-626-1’ on page 29
- ‘TYC 2064-1273-1’ on page 29

- ‘TYC 1548-2040-1’ on page 29
- ‘HD 238727’ on page 29
- ‘BD+74 736’ on page 29
- ‘BD+74 736’ on page 29
- ‘BD+04 3503’ on page 29
- ‘BD+04 3503’ on page 29
- ‘V1298 Her’ on page 29
- ‘BD-08 4562’ on page 29
- ‘BD+38 3104’ on page 29
- ‘BD+28 2992’ on page 29
- ‘BD+28 2992’ on page 29
- ‘AW Her’ on page 29
- ‘AW Her’ on page 29
- ‘G 141-30’ on page 29
- ‘G 141-30’ on page 29
- ‘TYC 2120-388-1’ on page 30
- ‘TYC 2120-388-1’ on page 30
- ‘BD+62 1656’ on page 30
- ‘TYC 453-327-1’ on page 30
- ‘BD+04 3943’ on page 30
- ‘BD+14 3751’ on page 30
- ‘BD+23 3557’ on page 30
- ‘BD+62 1699’ on page 30
- ‘HD 183957’ on page 30
- ‘HD 187003’ on page 30
- ‘KIC 7477572’ on page 30
- ‘V2477 Cyg’ on page 30
- ‘TYC 2697-941-1’ on page 30
- ‘TYC 1095-349-1’ on page 30
- ‘TYC 1095-349-1’ on page 30
- ‘V2425 Cyg’ on page 30
- ‘HD 335070’ on page 30
- ‘HD 335070’ on page 30
- ‘BD+45 3306’ on page 30
- ‘BD+45 3306’ on page 30
- ‘BD-08 5514’ on page 30
- ‘CG Cyg’ on page 30
- ‘BD+62 1880’ on page 30
- ‘ER Vul’ on page 30
- ‘BD+33 4140’ on page 30
- ‘BD+33 4140’ on page 30
- ‘BD+33 4140’ on page 30
- ‘BD+62 1902’ on page 30
- ‘TYC 2706-22-1’ on page 30
- ‘TYC 3181-914-1’ on page 30
- ‘TYC 2712-2338-1’ on page 30
- ‘LO Peg’ on page 30
- ‘HD 239702’ on page 30
- ‘HD 239702’ on page 30
- ‘BD+27 4129’ on page 30
- ‘BD+09 4914’ on page 30
- ‘TYC 553-33-1’ on page 30
- ‘TYC 553-33-1’ on page 30
- ‘OT Peg’ on page 30
- ‘OT Peg’ on page 30
- ‘OT Peg’ on page 30
- ‘BD+02 4456’ on page 30
- ‘BD+02 4456’ on page 30
- ‘BD+47 3668’ on page 30
- ‘HD 209845’ on page 30
- ‘HD209845’ on page 30
- ‘HD209845’ on page 30
- ‘TYC 3199-3329-1’ on page 30
- ‘TYC 1689-910-1’ on page 30
- ‘BD+84 507’ on page 30
- ‘BD+84 507’ on page 30
- ‘BD+33 4462’ on page 30
- ‘BD+27 4302p’ on page 30
- ‘BD+27 4302p’ on page 30
- ‘KX Peg’ on page 30
- ‘HD 212525’ on page 30
- ‘BD+05 5019’ on page 30
- ‘BD+05 5019’ on page 30
- ‘BD-01 4295’ on page 30
- ‘BD+49 3885’ on page 30
- ‘BD+49 3885’ on page 30
- ‘BD+15 4671’ on page 30
- ‘BD+15 4671’ on page 30
- ‘TYC 2739-689-1’ on page 30
- ‘HD 214261’ on page 30
- ‘HD 214261’ on page 30
- ‘TYC 1705-265-1’ on page 30
- ‘TYC 3625-1314-1’ on page 30
- ‘BD+13 5000’ on page 30
- ‘BD+09 5155’ on page 30
- ‘SZ Psc’ on page 30
- ‘BD+05 5154’ on page 30
- ‘TYC 4279-1821-1’ on page 31
- ‘TYC 4279-1821-1’ on page 31
- ‘TYC 585-897-1’ on page 31
- ‘BD-03 5681’ on page 31
- ‘V651 Cas’ on page 31
- ‘V651 Cas’ on page 31
- ‘HD 223688’ on page 31
- ‘TYC 2780-2053-1’ on page 31
- ‘TYC 2110-348-1’ on page 31
- ‘BD+42 3895’ on page 31
- ‘TYC 5238-1223-1’ on page 31
- ‘BD+42 3895’ on page 31
- ‘BD+09 4984B’ on page 31
- ‘TYC 573-566-1’ on page 31
- ‘BD-01 4397’ on page 31
- ‘BD+32 354’ on page 31
- ‘BD+32 354’ on page 31
- ‘TYC 3783-646-1’ on page 31
- ‘HD 234928’ on page 31
- ‘HD 234928’ on page 31
- ‘HD 234928’ on page 31
- ‘BD+82 622’ on page 31
- ‘BD+82 622’ on page 31

'BD+77 80' on page 31

'HD 238571' on page 31